The contribution of stress-induced mutagenesis to evolvability in *Escherichia coli*

A thesis presented in partial fulfilment of the requirements for the degree of

Master of Science
in
Biological Sciences

at Massey University, Albany,
New Zealand.

Courtney Armstrong

2023

ABSTRACT

The emergence of antibiotic resistance is a significant public health concern. Stress-induced mutagenesis (SIM) in bacteria has been identified as a potential mechanism contributing to antibiotic resistance evolution. SIM is a process that occurs when cells are under stress and struggling to adapt to their environment. This stress induces the production of enzymes that can increase mutation rates. In bacteria, SIM relies on two stress responses: the SOS response and the RpoS stress response, which control a regulatory switch. This switch changes the type of DNA polymerase used for replication from high-fidelity (Pol III) to error-prone (Pol IV, Pol V, Pol II) DNA polymerases. The genes that encode these error-prone DNA polymerases play a vital role in maintaining fitness and generating genetic diversity by allowing the replication of damaged DNA and bypassing various DNA lesions.

In this study, I investigated whether stress-induced mutagenesis in *Escherichia coli* contributes to evolvability, specifically the ability of a population to adapt to changing environments. I compared the evolvability of a SIM^- mutant, which lacked error-prone DNA polymerases Pol IV and Pol II, to a wild-type SIM^+ strain from a long-term evolution experiment and ancestral strains. I examined both ancestral strains and those from a long-term evolution experiment in environments with and without mitomycin C, an SOS inducer. My results showed that the presence of both stress and error-prone polymerases enhances evolvability. I observed a more significant increase in fitness and mutation rates in the SIM^+ strain compared to the SIM^- mutant or when only one or neither factor was present. I also found that the SIM^- mutant decreased the frequency of mutations and fitness in evolved populations, demonstrating that error-prone polymerases are crucial for SIM to enhance evolvability.

My study highlights the significant role of SIM and error-prone polymerases in the evolution of antibiotic resistance, providing valuable insights into the SOS response and suggesting potential avenues for developing new drugs and treatments to combat this growing threat. Limiting the impact of SIM through targeted inhibition of error-prone polymerases and reducing stress levels may improve the management and prevention of antibiotic resistance.

ACKNOWLEDGMENTS

First and foremost, I would like to express my sincere gratitude to my supervisor, Dr. Tim Cooper, for allowing me to pursue this degree under his guidance and for his unwavering support and assistance throughout this project. Secondly, I would like to extend my thanks to my fellow lab mates, Huei-Yi and Razvan, for their constant support, engaging conversations and willingness to assist whenever possible.

I would also like to take this opportunity to thank my friends and flatmates for their endless encouragement and listening ear and for reminding me to take breaks from my studies to enjoy the world outside of the university. Without their unwavering support, I would not have been able to complete this challenging journey.

Lastly, I want to express my heartfelt appreciation to my family and partner for their unrelenting support, love, and guidance throughout my academic journey. Their belief in me and words of encouragement have been invaluable. I could not have achieved this milestone without their constant love and support.

ABBREVIATIONS

ºC	Degrees Celsius
Amp	Ampicillin
Amp^R	Ampicillin resistance
DNA	Deoxyribonucleic acid
DSB	Double-strand break
dsDNA	Double-stranded DNA
CFP	Cyan fluorescent protein
Cm	Chloramphenicol
Cm^R	Chloramphenicol resistance
E. coli	*Escherichia coli*
EtBr	Ethidium bromide
GFP	Green fluorescent protein
GOI	Gene of interest
Km	Kanamycin
MMC	Mitomycin C
MMR	Mismatch repair
Nal	Nalidixic acid
NI	No inducer
Pol II	DNA polymerase II
Pol III	DNA polymerase III

Pol IV	DNA polymerase IV
Pol V	DNA polymerase V
Rif	Rifampicin
Rif^R	Rifampicin resistance
ROS	Reactive oxygen species
RNA	Ribonucleic acid
SIM	Stress-induced mutagenesis
SIM^+	Wild-type strain with SIM genes
SIM^-	Double mutant strain lacking SIM genes (Δ*dinB* and Δ*polB*)
SIMs	Stress-induced mutators
ssDNA	Single-stranded DNA
ts	Temperature-sensitive
WT	Wild-type
YFP	Yellow fluorescent protein

TABLE OF CONTENTS

LIST OF FIGURES

LIST OF TABLES

1. INTRODUCTION

Most bacteria live in changing environments. Many of these changes—for example, due to variations in temperature, pH, lack of nutrients, or chemical carcinogens—are stressors that disturb normal cell function, increasing mortality and decreasing the fitness of a population (Battesti et al., 2011; Kishony & Leibler, 2003; Tenaillon et al., 2001). Bacteria have evolved specific genes to regulate various responses that help them adapt or resist stressful conditions. These responses enable them to counteract the effects of stress, restore cellular homeostasis, and repair any DNA damage incurred due to the stress, allowing them to function at their best (Battesti et al., 2011). Despite this, such responses can potentially elevate the mutation rates of bacteria, leading to a decline in fitness due to increased production of deleterious mutations (Denamur & Matic, 2006).

Bacteria are constantly selected for resistance to stressors. Resistance occurs through cellular responses resulting from stress-induced mutagenesis (SIM) (Dellus-Gur et al., 2017; MacLean et al., 2013). SIM results in an elevated mutation rate (Bjedov et al., 2003; Lukačišinová et al., 2017; MacLean et al., 2013; Ram & Hadany, 2014; Taddei et al., 1995). A specific example is the effect of DNA-damaging antibiotics increasing the rate at which resistance is acquired (Pribis et al., 2019; Ragheb et al., 2019). Antibiotic-resistant bacteria are becoming a big issue as they can harm the health of humans, animals and plants (Cirz & Romesberg, 2006). There is potentially an arms race between the development of antibiotic drugs and bacterial resistance to them (Hede, 2014). Bacteria need new mutations to fuel the arms race, enabling them to acquire resistance through new routes or evolve resistance to new antibiotics. Therefore, understanding the mechanisms and selection of SIM and how it contributes to the evolution of resistance is of great importance. Identifying these factors has the potential in helping stop the evolution of antibiotic resistance pathogens (Mothersill & Seymour, 2013).

1.1 Mutations and resistance

Mutations drive evolution as they are the source of the genetic variation essential for organisms to adapt to changing environments and even create new species (Agashe, 2017; Lukačišinová et al., 2017; Urry et al., 2017). A simple definition of a mutation is a change in

the nucleotide sequence of an organism's genome, resulting in either harmful, beneficial or neutral effects (Brown, 2002). Mutations can arise in two ways: (1) induction by mutagens (a physical or chemical agent that alters DNA through inducing a mutation), such as UV light and chemical carcinogens, that cause structural alterations of nucleotides (Brown, 2002; Lodish et al., 2000b) and (2) spontaneous errors produced during DNA replication that are not detected by DNA polymerases that proofread the newly synthesised strand of nucleotides (Brown, 2002).

Induced mutations are increased when cells and organisms face environmental stress, such as changes in pH level, temperature, starvation, exposure to antibiotics and oxidative stress, resulting in them being maladapted to their environment (Galhardo et al., 2007). Organisms can undergo genetic changes due to exposure to diverse stress-inducing environments (Foster, 2007). These stresses lead to increased mutation rates in poorly adapted cells, leading to stress-induced mutagenesis (SIM) (Agashe, 2017; Correa et al., 2018; Ram & Hadany, 2014; Zhu et al., 2014).

1.1.1 Mutation rate and population size

The rate of adaptation in asexual populations is limited by population size, mutation rate, and the fraction of mutations that result in a benefit, which is impacted by the initial adaptation of the population and environmental variability (De Visser & Rozen, 2005). The rate of adaptation refers to how quickly an organism's fitness improves over a given period (De Visser & Rozen, 2005; Fogle et al., 2008; Wilke, 2004). The mutation rate must strike a balance between adaptability (the capacity to adapt) and adaptedness (the ability to stay adapted) (Ram & Hadany, 2014). A smaller population size means the availability of beneficial mutations limits adaptation; however, increasing the population size and mutation rate can speed up adaptation (De Visser & Rozen, 2005; Jiang et al., 2010; Vahdati et al., 2017; Wilke, 2004). Increasing population size can initially increase the rate of adaptation due to the increased availability of beneficial mutations, as more individuals in the population can act as potential sources of beneficial mutations (De Visser & Rozen, 2005). However, this increase in the rate of adaptation is limited, as the availability of beneficial mutations is finite (Wilke, 2004). The rate of adaptation initially increases as the population size grows, but it eventually begins to decline because the limited number of beneficial mutations results

in diminishing returns (De Visser & Rozen, 2005). Another phenomenon to consider is that the rate of adaptation may become disproportionate or approach a maximum, meaning that it is no longer directly proportional to population size (De Visser & Rozen, 2005; Wilke, 2004). As population size increases, so does the mutation rate, which increases the probability of clonal interference (De Visser & Rozen, 2005; Fogle et al., 2008). Clonal interference slows down the rate of adaptation in large populations by increasing the fixation time of multiple beneficial mutations, but at the same time, it can increase the fitness effect of ultimately successful mutations (De Visser & Rozen, 2005; Lanfear et al., 2014; Vahdati et al., 2017; Wilke, 2004). The net effect of these factors is that the rate of adaptation may increase initially with population size, but eventually, it will reach a maximum.

The selection of hypermutation, or an increase in the genomic mutation rate, is a surprising phenomenon considering that most mutations have a deleterious effect, decreasing fitness (Ram & Hadany, 2012). However, in maladapted populations and changing environments, mutators (alleles that induce hypermutation) can increase in frequency when they "hitchhike" with the beneficial mutations they generate, leading to a higher mutation rate than in well-adapted populations (De Visser & Rozen, 2005; Ram & Hadany, 2012; Shaw & Baer, 2011; Swings et al., 2017). Well-adapted populations may only have access to mutations with minor fitness effects as large-effect mutations are expected to be fixed first due to clonal interference (De Visser & Rozen, 2005). This increased mutation rate in adapted cells eventually decreases as deleterious mutations accumulate, restoring the population-wide mutation rate to its minimum limit (Ram & Hadany, 2012; Swings et al., 2017).

1.1.2 Resistance

Mutations bring about change in species and adaptations but also are a factor in developing antibiotic resistance and diseases such as cancer. The frequency of mutations are not occurring at a consistent rate or in a uniform manner across the genome, leading to a conflict between maintaining genetic stability and promoting adaptability (Maharjan & Ferenci, 2014). This conflict can be addressed through stress-induced mutagenesis (SIM), which involves an increase in mutation rate due to unfavourable environments (Ram & Hadany, 2014). In laboratory studies, bacteria such as *Escherichia coli* and *Pseudomonas aeruginosa* have been observed to have higher mutation rates in adverse conditions (Cirz et al., 2005;

Torres-Barceló et al., 2015). Antibiotic exposure increases mutation rates in bacteria through two mechanisms that lead to antibiotic resistance in laboratory studies. The first mechanism is selecting hypermutator phenotypes with high mutation rates due to loss-of-function mutations in systems that prevent high mutation rates (Revitt-Mills & Robinson, 2020). The second mechanism is the direct promotion of error-prone DNA repair or temporary down-regulation of mismatch repair, resulting in elevated mutation rates, known as stress-induced mutagenesis (Revitt-Mills & Robinson, 2020).

1.2 Stress-induced mutagenesis

Stress-induced mutagenesis (SIM) is a mechanism in which cells that are poorly adapted to their environment (e.g. are stressed) induce enzyme activities that result in an increase in mutation rates (MacLean et al., 2013; Poole, 2012; Shee, Gibson, et al., 2011; Shee et al., 2013). These mechanisms have been detected in bacteria, human, yeast and plant cells when stressful conditions (e.g., antibiotic stresses, exposure to UV light or starvation) activate mutation pathways that are controlled by stress responses (Dellus-Gur et al., 2017; Frisch et al., 2010; Galhardo et al., 2009; Shee et al., 2013; Shee, Ponder, et al., 2011). SIM has been best studied in bacteria, especially *E. coli*. Antibiotic resistance and cancer progression and resistance are essential processes that SIM mechanisms may influence (Frisch et al., 2010; Shee et al., 2013).

In bacteria, the primary stress responses that control SIM are the SOS response, known as the bacterial DNA-damage response, and the RpoS general or starvation stress response (Agashe, 2017; Ponder et al., 2005; Rosenberg et al., 2012; Shee, Gibson, et al., 2011; Shee et al., 2013). These stress responses control a regulatory switch resulting in a change from almost exclusive use of high-fidelity (non-mutagenic Pol III) DNA polymerases to the substantial use of error-prone DNA polymerases, including the DNA damage-induced Pol IV polymerase and two other low-fidelity polymerases, Pol V and Pol II. When in a stressful environment, these polymerases are controlled and upregulated by the RpoS transcriptional activator (Frisch et al., 2010; Moore et al., 2017; Ponder et al., 2005; Shee, Gibson, et al., 2011; Yeiser et al., 2002). These responses' mechanism is important in explaining and understanding SIM. Rosenberg et al. (2012) state that three events are needed for DSB-dependent SIM to occur in *E. coli*: (i) formation and repair of DNA DSBs, (ii) DSBs inducing

the SOS response and, (iii) activation of the Rpos general/starvation stress response by the RpoS (σ^S) transcriptional activator, generated by a second stress (Rosenberg et al., 2012). If all these events occur simultaneously, SIM ensues (Figure 1-1).

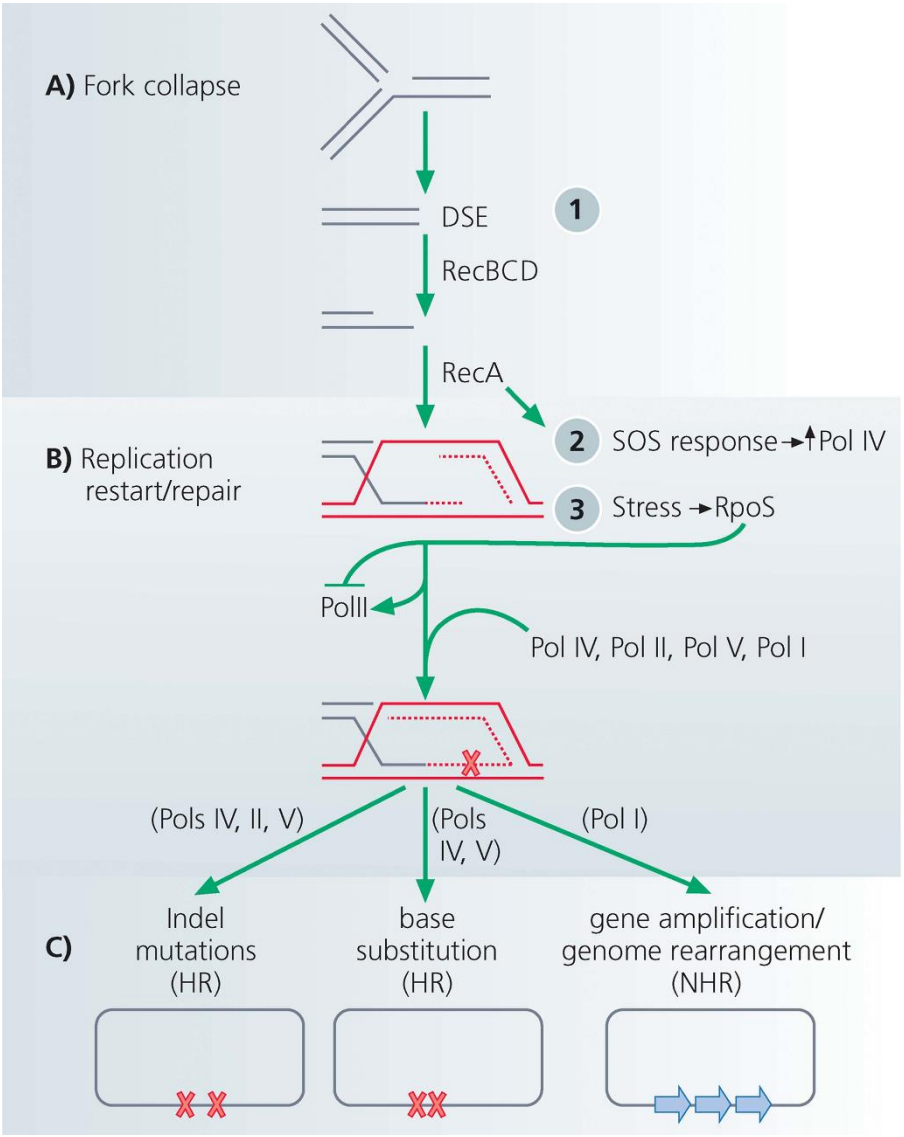

Figure 1-1: Interpretation of the SIM mechanism involving SOS response and RpoS general stress response.
First a ssDNA break occurs resulting in the induction of the SOS response (1). The SOS response is induced, upregulating the *dinB* gene, known as DNA Pol IV (2). The RpoS response is induced via the cell being exposed to stress (3). Both responses require multiple error-prone polymerases due to their ability to carry out DSB repair synthesis (Pol IV, Pol V, Pol II, Pol I). Each of these polymerases result in errors incorporated into the genome. Reproduced from Rosenberg et al. (2012) with permission from Copyright 2012 by WILEY Periodicals, Inc.

1.3 The SOS response

The SOS response system in *E. coli* is an inducible genetic network expressed when cells are exposed to DNA-damaging agents (Matic, 2013; Nohmi, 2006; Poole, 2012). Exposure to DNA-damaging agents results in mutations that overwhelm error-free DNA repair mechanisms, increasing the concentration of single-stranded DNA (ssDNA) (Foster, 2007; Galhardo et al., 2007; Lodish et al., 2000a; Matic, 2013; Saint-Ruf et al., 2007; Wagner et al., 1999; Williams & Foster, 2012). The induction of the SOS response is initiated by single-stranded DNA (ssDNA), which blocks DNA replication and acts as a signal (Nohmi, 2006). The SOS response relies on two essential proteins: RecA and LexA. RecA binds to the ssDNA region and forms a RecA-nucleofilament (RecA*) (Friedberg et al., 2005b; Matic, 2013; Nohmi, 2006; Shinagawa, 1996). In contrast, LexA is the SOS repressor, which binds to the chromosome's promoter regions of SOS-inducible genes and suppresses their expression (Nohmi, 2006).

Proteolytic cleavage of LexA is necessary to induce the SOS response (Friedberg et al., 2005b; Saint-Ruf et al., 2007). The co-protease activity of the RecA protein gets activated when it comes into contact with a high concentration of ssDNA with ATP (RecA*), which enables self-cleavage of LexA, inducing the SOS response (Culyba et al., 2015; Erill et al., 2007; Friedberg et al., 2005b; Galhardo et al., 2007; McKenzie et al., 2000; Nohmi, 2006; Shinagawa, 1996). Therefore, the cleavage of LexA results in the activation of SOS genes. The SOS response upregulates ~40 genes that have essential roles in DNA repair and DNA synthesis past DNA lesions that block replication (Foster, 2007; Galhardo et al., 2007; Matic, 2013; Saint-Ruf et al., 2007). The mechanism of the SOS response is shown in (Figure 1-2).

Three genes regulated by the SOS response have significance for SIM due to their ability to replicate damaged DNA by bypassing various DNA lesions (Foster, 2007). These genes encode DNA polymerases, Pol II (*polB*), Pol IV (*dinB*) and Pol V (*umuDC*). The DNA polymerases catalyse error-prone and error-free reactions, known as translesion DNA synthesis (TLS). TLS bypasses DNA lesions by incorporating incorrect or correct nucleotides in opposite lesions (Friedberg et al., 2002; Matic, 2013; Nohmi, 2006). These reactions contribute to mutagenesis. During times of stress, the customarily used high-fidelity DNA Pol III is temporally ineffective in replicating damaged regions of DNA. Instead, Pol IV and Pol V, both from the Y-family of DNA polymerases, can perform TLS. The Y-family polymerases lack 3’ → 5’ exonuclease activity, meaning they have no proofreading ability to

check for errors incorporated during DNA replication (Friedberg et al., 2002; Maslowska et al., 2019; Matic, 2013; Nohmi, 2006). Therefore, Pol IV and Pol V have low accuracy in incorporating the correct bases, known as low fidelity, resulting in error-prone DNA repair. These polymerases compromise their accuracy of DNA replication to enable the bypass of DNA lesions (Matic, 2013). Therefore, mutations appear to be the price to pay for survival. Whereas, DNA polymerase II, belonging to the B-family of DNA polymerases, has 3' → 5' exonuclease proofreading ability but is still involved in error-prone TLS on template DNA (Corzett et al., 2013; Napolitano et al., 2000; Nohmi, 2006).

The SOS polymerases, Pol II, Pol IV, and Pol V, maintain fitness and generate genetic diversity. The three polymerases, Pol II, Pol IV, and Pol V, perform distinct functions (Table 1-1). Pol II is responsible for error-free replication-fork restart. Pol IV is believed to perform error-prone replication-fork rescue, while Pol V is primarily involved in error-prone translesion synthesis (Yeiser et al., 2002). Depending on the lesion encountered, Pol II, Pol IV and Pol V also contribute to error-prone and error-free translesion synthesis (Goodman, 2002; Yeiser et al., 2002).

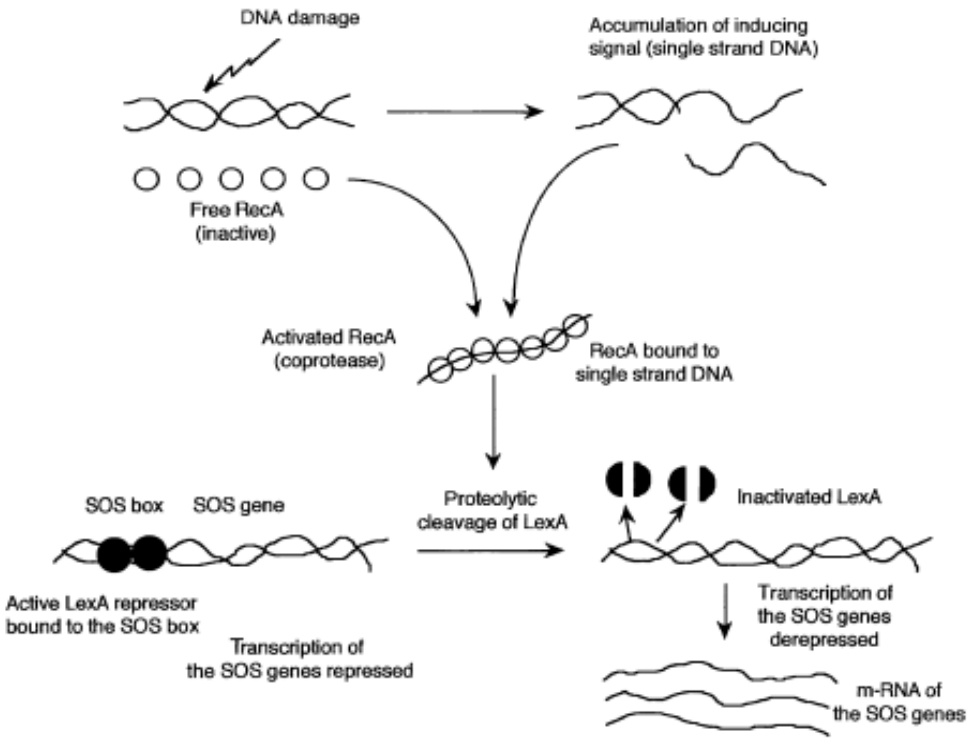

Figure 1-2: The SOS system in response to DNA damage in *Escherichia coli*.
DNA damage results in an accumulation of single stranded DNA (ssDNA), the SOS inducing signal. Inactive RecA proteins bind to the ssDNA to form a RecA-nucleofilament that has co-protease activity. Cleavage of LexA, the SOS repressor, needs to occur for the SOS response to be induced. Self-cleavage of LexA occurs via the co-protease activity of the activated RecA, resulting in activation of the SOS genes. Reproduced from Shinagawa (1996) with permission from Copyright 1996 by Birkhäuser Verlag Basel/Switzerland.

Table 1-1: Key characteristics of *Escherichia coli* DNA polymerases II, III, IV and V

	Pol II	**Pol III**	**Pol IV**	**Pol V**
Structural Gene	*polB*	*polC*	*dinB*	*umuDC*
Family	B	C	Y	Y
Function	Replication restart; TLS; intrastrand cross-link repair	Chromosome replication (elongates DNA)	Replication-fork rescue; TLS; lesion bypass	TLS; lesion bypass
5' → 3' Polymerase Activity	+	+	+	+
3' → 5' Exonuclease Activity	+	+	–	–
SOS inducibility	+	–	+	+
– SOS (molecules/cell)	30–50 [a]	10–20 [b]	250 [c]	15 *umuC* [c] & 200 *umuD* [c]
+ SOS (molecules/cell)	210–350 [a]		2500 [c]	200 *umuC* [c] & 2400 *umuD* [c]
Fidelity on undamaged DNA (error rate per base)	10^{-5}–10^{-6} [d]	10^{-5}–10^{-6} [d]	10^{-3}–10^{-4} [d]	10^{-3}–10^{-4} [d,e]

[a] Bonner et al. (1988); Qiu and Goodman (1997)

[b] Kornberg and Gefter (1972); McHenry (1985); McHenry and Kornberg (1977)

[c] Kuban et al. (2006)

[d] Rattray and Strathern (2003)

[e] Tang et al. (2000)

1.3.1 Pol IV (*dinB*)

The gene *dinB* encodes polymerase IV (Pol IV), a specialized DNA polymerase that performs translesion repair and is involved in DSB repair (Shee, Gibson, et al., 2011; Tang et al., 2000). Despite primarily being upregulated by the SOS induction, the activity of Pol IV is also controlled by the RpoS (σ^S) sigma subunit of the RpoS general stress response (He et al., 2006; Layton & Foster, 2003; Nohmi, 2006; Shee, Gibson, et al., 2011). Its translesion bypass and lack of 3' → 5' exonuclease (proofreading) activity make Pol IV highly error-

prone, leading to a low fidelity and an increase in −1 frameshift mutations (Fuchs & Fujii, 2013; Kim et al., 2001; Nohmi, 2006; Tashjian et al., 2019; Wagner & Nohmi, 2000).

Pol IV plays a crucial role during stationary-phase, and in facilitating adaptive mutations (Foster et al., 2015). Several key findings demonstrate the significance of Pol IV in cell survival and fitness. McKenzie et al. (2001) showed that around 85% of stress-induced point mutations require Pol IV, and the rest (15%) depend on Pol II (Frisch et al. (2010). Secondly, Kim et al. (2001) discovered that the expression levels of *dinB* increase approximately 10-fold, from 250 to 2500 molecules/cell during SOS induction (Foster et al., 2015; Fuchs & Fujii, 2013; Kobayashi et al., 2002; Kuban et al., 2006). Thirdly, Yeiser et al. (2002) observed that Pol IV and Pol V confer a selective advantage during competition in the stationary phase.

1.3.2 Pol V (*umuDC*)

Pol V, like Pol IV, belongs to the Y-family of DNA polymerases and has low processivity and accuracy (Williams & Foster, 2012). Pol V is induced in response to DNA damage (Nohmi, 2006). Pol V's lack of proofreading ability results in high error rates of around 10^{-3} to 10^{-4} when measuring the fidelity of nucleotide incorporation of undamaged DNA. At the same time, Pol IV's error rates are five to tenfold more accurate (Tang et al., 2000).

As explained in section 1.3, RecA forms the active RecA* nucleoprotein filament when bound to single-stranded DNA with ATP present. Not only is RecA* involved in regulating and implementing the SOS response, but RecA* co-protease activity is also necessary for creating Pol V, a mutagenic TLS polymerase. Pol V is created by cutting the *UmuD* protein into a shorter and more mutagenic form, *UmuD',* which dimerises and binds to *UmuC* to form a heterotrimeric complex, $umuD'_2C$ (Foster, 2007; Goodman et al., 2016; Jaszczur et al., 2016; Kuban et al., 2006; Matic, 2013). However, $umuD'_2C$ needs to be activated, which is achieved through transferring a RecA* subunit to $UmuD'_2C$ to form the Pol V Mut complex with ATP ($UmuD'_2C$-RecA-ATP) (Goodman et al., 2016; Jaszczur et al., 2016; Jaszczur et al., 2019; Revitt-Mills & Robinson, 2020).

Pol V is responsible for base substitutions, such as UV radiation, during the SOS response after DNA damage (Kato & Nakano, 1981). Pol V is also found to play an essential role in

frameshift mutations. According to research findings by Kokubo et al. (2005), the deletion of Pol V significantly reduces −2 frameshift mutations caused by four class III chemicals in *Salmonella typhimurium* (i.e., 1-Nitropyrene and 1,8-Dinitropyrene). In addition, the absence of Pol II leads to a 30% to 60% decrease in the mutagenicity of all four class III chemicals. Therefore, TLS resulting in −2 frameshift mutations involves the collaboration of Pol II and Pol V.

Despite *umuC* having low levels in normal cells (~15 molecules per cell), full induction of the *umuDC* operon results in the production of approximately 200 molecules per cell of *umuC,* while *umuD* is present at ~200 molecules per uninduced cell, increasing to ~2400 molecules per induced cell (Kuban et al., 2006; Livneh, 2004; Opperman et al., 1999; Woodgate & Ennis, 1991). Pol V can bypass UV-induced pyrimidine dimers, [6-4] photoproducts and abasic sites, making it a critical factor in damage-induced mutagenesis (Friedberg et al., 2002; Kuban et al., 2006; Smith & Walker, 1998; Sutton et al., 2000). The *umuDC* operon's promoter strongly resembles the consensus LexA repressor binding site, leading to its delayed induction in the SOS response (Jaszczur et al., 2016). Full de-repression of the operon occurs around 15 minutes after DNA damage, with peak levels of $UmuD'_2C$ proteins taking place around 45 minutes after damage (Goodman et al., 2016; Jaszczur et al., 2016).

1.3.3 Pol II (*polB*)

DNA polymerase II, encoded by the *polB* (*dinA*) gene, belongs to the B-family of DNA polymerases (Fijalkowska et al., 2012). Pol II plays a crucial role in evolutionary fitness and has greater fidelity than Pol IV and Pol V due to its 3′→5′ exonuclease activity. Pol II is involved in various DNA repair processes, including TLS, intrastrand cross-link repair and bypassing abasic sites (Berardini et al., 1999; Nohmi, 2006). It is also involved in spontaneous mutagenesis in nutritionally stressed cells containing F′ plasmids and is essential for restarting replication after UV irradiation due to it being the first alternative polymerase to access blocked DNA replication forks (Dapa et al., 2017; Foster, 2007; Nohmi, 2006; Tang et al., 2000). Pol II generates -2 frameshift mutations from the chemical carcinogen *N*-2-acetylaminofluorene (Friedberg et al., 2002; Fuchs & Fujii, 2013; Napolitano et al., 2000). The expression levels of *polB* increase approximately from 30-50 molecules/cell when

uninduced to increase 7-fold (210-350 molecules/cell) during SOS induction (Bonner et al., 1988; Fijalkowska et al., 2012; Kobayashi et al., 2002; Qiu & Goodman, 1997). Corzett et al. (2013) asserted that Pol II confers a fitness advantage during rapid growth without SOS induction by facilitating efficient replication and creating genetic diversity.

The study by Dapa et al. (2017) investigated the role of the RpoS-regulated Pol II in repairing DNA damage caused by the genotoxic agent mitomycin C (MMC) in *E. coli*. MMC strongly induces the SOS response in *E. coli* and causes DNA damage through DNA cross-links and alkylation, as well as the generation of reactive oxygen species (Dapa et al., 2017). This study showed that Pol II is the most critical contributor to the repair of MMC-induced DNA lesions in growing cells due to Pol II being involved in processing intrastrand cross-links (Berardini et al., 1999; Nohmi, 2006). The sensitivity of the Δ*polB* mutant to oxidative stress suggests that Pol II may also play a role in processing MMC-induced oxidative DNA damage (Escarceller et al., 1994). The survival rates of mutant and wild-type cells exposed to hydrogen peroxide provide evidence as the Δ*polB* mutant was more sensitive to oxidative stress than the wild-type (Escarceller et al., 1994). The *polB* gene's expression was also coregulated by RpoS (Dapa et al., 2017). MMC is important as I used it as the SOS inducer in the experiments presented in this thesis.

1.4 The RpoS general stress response

For *E. coli* and its relatives, a physiological state that is highly resistant to stress is achieved by inducing the RpoS general stress response (Battesti et al., 2011). The RpoS general stress response is under the control of one of seven *E. coli* RNA polymerase sigma factors, σ^S (also called σ^{38} or RpoS), which is a transcriptional activator (Layton & Foster, 2003; Matic, 2013; Nohmi, 2006; Rosenberg et al., 2012; Shee et al., 2013; Weber et al., 2005). The RpoS general stress response is induced when *E. coli* cells experience starvation, oxidative stress, pH and temperature changes, or in response to cells entering the stationary phase (Battesti et al., 2011; Foster, 2007; Galhardo et al., 2007; Gottesman, 2019; Hengge-Aronis, 2002; Lombardo et al., 2004; Nohmi, 2006; Poole, 2012; Rosenberg et al., 2012). During exponential growth, genes are transcribed mainly by RpoD, the vegetative sigma factor, also called σ^{70} (Foster, 2007; Matic, 2013). Whereas σ^S is nearly absent in exponentially growing

cells, when *E. coli* cells undergo stress, they strongly induce σ^S, activating the RpoS general stress response (Battesti et al., 2011; Foster, 2007; Hengge-Aronis, 2002).

Weber et al. (2005) state that the activation of a transcriptional activator is necessary to express multiple stress resistances, which enables cells to survive various stressors through cross-protection, as reported by Battesti et al. (2011); Hengge-Aronis (2002). Cross-protection is the ability of cells to become resistant to not only the direct stress facing them but also to other stressful environments they may encounter (Battesti et al., 2011). For example, when cells enter the stationary phase due to exposure to high temperatures, they become resistant to low pH, oxidative stress and carbon starvation (Battesti et al., 2011; Lombardo et al., 2004). RpoS indirectly or directly regulates ~500 genes in *E. coli*, which equates to about 10% of the *E. coli* genome, and many play a role in stress resistance (Battesti et al., 2011; Foster, 2007; Galhardo et al., 2007; Matic, 2013; Weber et al., 2005).

There are currently two mechanisms that have been described by which the RpoS general stress response can increase the mutagenesis of stressed cells (stationary phase mutagenesis), as specified by Foster (2007); Matic (2013). The first mechanism is the induction of the error-prone polymerase *dinB* gene (Pol IV). When *E. coli* cells enter the stationary phase, there is a ~3-fold increase in Pol IV expression levels (Foster, 2007). According to research, the expression of *E. coli* Pol IV is believed to be controlled by σ^S, and this increase in expression is associated with RpoS (Layton & Foster, 2003). It was observed that if the gene encoding σ^S in RpoS is defective, the expression level of Pol IV decreases significantly during the stationary phase (Foster, 2007; Nohmi, 2006). More findings by Layton and Foster (2003, 2005) showed that the RpoS general stress response upregulates Pol IV, causing a 2-fold increase in its level (Pomerantz et al., 2013; Ponder et al., 2005). During the stationary phase, Pol IV levels can reach up to 5,000 molecules/cell, making it the most abundant DNA polymerase in growth-limited cells (Pomerantz et al., 2013). As Pol IV is an error-prone DNA polymerase, it promotes most adaptive mutations under growth-limiting conditions (Pomerantz et al., 2013). Hence, the expression of Pol IV, which is dependent on RpoS, may significantly impact cell mutations while in the stationary phase (Nohmi, 2006).

The second mechanism by which RpoS has been found to enhance spontaneous mutation rates during stress is by downregulation of the mismatch repair (MMR) system (Foster, 2007; Matic, 2013). The MMR complex in *E. coli* and other bacteria is a DNA repair pathway that recognizes mispaired bases in DNA and excises the newly synthesized strand, utilizing the

original strand as a guide for new synthesis (Foster, 2007; Galhardo et al., 2007). *E. coli* can distinguish between the possibly flawed newly synthesized strand and the accurate template strand through their methylation status. The newly synthesized DNA remains unmethylated shortly following replication (Foster, 2007). Though the MMR system remains active in stationary phase cells, levels of two MMR proteins, MutS and MutH, decrease in a manner dependent on RpoS (Feng et al., 1996; Foster, 2007; Harris et al., 1997; Matic, 2013; Tsui et al., 1997). This reduction in MMR proteins has been linked to increased mutation rates, as seen in cases when MMR proteins are overproduced and when MMR is genetically removed (Bjedov et al., 2003; Foster, 2007; Matic, 2013).

1.5 Potential to create anti-evolution drugs

Bacteria have been evolving the ability to combat antibiotics by gaining resistance to them via spontaneous mutations or horizontal gene transfer (Baym et al., 2016; Fitzgerald, 2019; MacLean & San Millan, 2019). These drug-resistant bacteria pose a significant threat to the health of humans. Therefore, finding a way to design drugs that can limit this resistance is highly beneficial. The mechanism of SIM has provided possible insight into creating such drugs. Drugs can be designed to target and inhibit the function of specific proteins to prevent the increase in mutation rate generated by SIM and, ultimately, the evolution of resistance. These proteins, namely Pol IV, Pol V, and Pol II are involved in the induction of the SOS response through the cleavage of LexA and the expression of error-prone DNA polymerases (Cirz & Romesberg, 2006, 2007; Culyba et al., 2015).

Cirz and Romesberg (2006) performed research showing the evolution of resistance to ciprofloxacin. The data suggest that inhibitors of either LexA or SOS polymerases may significantly affect treating strains of bacteria with an abnormally high mutation rate (hypermutable). The results also showed that it might help combat bacteria that evolve resistance to a single antibiotic and bacteria that can evolve multidrug resistance (Cirz & Romesberg, 2006). Work has already been completed on finding potential molecules that inhibit essential proteins in the SOS response. For example, Lee et al. (2005) found a molecule, N^6-(1-Naphthyl)-ADP, that inhibits RecA filamentation required for LexA cleavage and SOS induction in *E. coli*. Pribis et al. (2019) conducted recent research that tested edaravone, an FDA-approved drug, as a potential anti-evolution drug. The study

demonstrated that treatment with edaravone can inhibit the stress response by removing toxic molecules called reactive oxygen species (ROS) induced by antibiotics like ciprofloxacin. Additionally, edaravone reduced ciprofloxacin-induced mutations without interfering with the antibiotic's activity (Pribis et al., 2019). The types of potential drugs that can be produced would be combined with current antibiotics to slow down bacteria's evolution of resistance, as shown in Figure 1-3.

Furthermore, understanding the mechanism of SIM and how to select it can contribute to designing drugs that combat the evolution of antibiotic-resistant pathogens, which is of great clinical value (Shee et al., 2013). However, finding molecular drug targets or potential drugs is costly and time-consuming. Nevertheless, the benefits of creating drugs that treat humans infected with pathogenic bacteria far outweigh the costs. Moreover, potential drugs may not be limited to antibiotic resistance, as targeting hypoxia stress-induced mutagenesis could also slow the evolution of malignancy and chemotherapy resistance in cancer therapy (Fitzgerald et al., 2017).

1.6 Evolvability

Evolvability is the intrinsic capacity of biological populations to adapt and evolve to changing environments (Galhardo et al., 2007). The ability for organisms to display evolvability to new environments can have consequences. Evolvability is prevalent in bacteria who evolve the ability to combat antibiotics – an environmental stressor – by gaining resistance to them. This resistance poses a significant threat to the health of humans (Aljeldah, 2022). Therefore, finding a way to combat the evolvability of bacteria to antibiotics is of great importance. Studying the important aspects of stress-induced mutagenesis allows for understanding how SIM can contribute to evolvability. Conducting a long-term evolution experiment under controlled conditions, subjecting *E. coli* populations to a specific stressor is one way evolvability can be measured, and is shown in this thesis.

1.7 Objectives

I conducted this study to determine if stress-induced mutagenesis contributes to evolvability. To accomplish this, I deleted key error-prone polymerases and examined SIM^- strains' mutation, growth, and evolvability compared to their otherwise isogenic SIM^+ ancestors.

The specific objectives of this study were to:

1. Identify the impact of removing error-prone polymerase genes on evolvability.
2. Using experimental evolution, investigate how the SOS response pathway affects the relationship between stress-induced mutagenesis and evolvability.

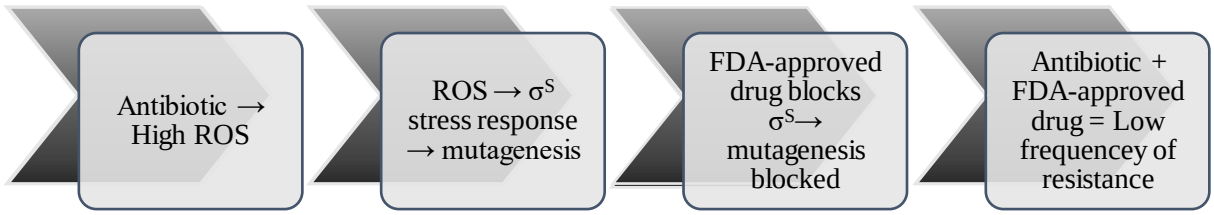

Figure 1-3: Basic schematic of how anti-evolution drugs can be used to lower the evolution of resistance.
Antibiotics induce a high volume of ROS. ROS induce the σ^S stress response which results in mutagenesis. Anti-evolution drugs could work by inhibiting this stress response, consequently blocking mutagenesis. Therefore, antibiotics can be used in combination with anti-evolution drugs to reduce the frequency of antibiotic resistant mutants.

2. MATERIALS AND METHODS

2.1 Bacterial strains, plasmids, and growth conditions

All bacterial strains are laboratory *E. coli K-12* and *E. coli B* (Table 2-1). The plasmids used in this work are listed in Table 2-2, while the primers are shown in Table 2-3. Davis Mingioli medium (DM; potassium phosphate (dibasic trihydrate) 5.34 g/L, potassium phosphate (monobasic anhydrous) 2 g/L, ammonium sulphate 1 g/L, sodium citrate (trisodium, dihydrate) 0.5 g/L with 1 mL 10% $MgSO_4^{2-}$ and 1 mL 0.2% thiamine added after autoclaving) supplemented with glucose at 250 μg/ml (DM250) was used as growth media for cultures in reporter assays, fluctuation tests, and evolution and competition assays. DM250 glucose supports a stationary phase cell density of ~5 x 10^8 cells/ml (Lampe et al., 2019). Lysogeny broth (LB; 10 g/L NaCl, 10 g/L tryptone, 5 g/L yeast extract; LB Agar being LB + 15 g/L agar) was used for reviving strains and routine molecular work involved in removing genes. Overnight cultures were made by adding a frozen aliquot of bacteria to 3 mL of LB or DM250 media or using an inoculation loop to select an isolated colony from a media plate and shaking the loop into plastic test tubes of LB or DM250. Cultures were grown at 30°C (when the functionality of temperature-sensitive plasmids was required) or 37°C with constant shaking at 250 rpm for liquid cultures in test tubes or 1000 rpm for 96-well microtiter and 96-well deep well plates. When needed, the following concentrations of antibiotics were used: ampicillin – 100 μg/mL, chloramphenicol – 65 μg/mL, rifampicin – 100 μg/mL and kanamycin – 50 μg/mL.

All plasmids used were transformed into REL606 and MG1655. The red helper plasmid used in transformations to disrupt genes was pORTMAGE-2 (AmpR), which has temperature-sensitive replication (30°C). pORTMAGE-2 expresses the λ red recombinase proteins (*exo*, *bet* and *gam*) from the *p*L operon under the control of cI857, the temperature-sensitive (ts) repressor (Datta et al., 2006; Nyerges et al., 2016). The template plasmid used was pKD3, which has a chloramphenicol resistance cassette flanked by FRT sites. These FRT sites allow removing the resistance cassette once inserted into the bacterial chromosome by inducing the FLP expressing the temperature-sensitive plasmid, pCP20 (Amp^R) (Datsenko & Wanner, 2000).

Table 2-1: List of bacterial strains

Strain	**Parent**	**Genotype**	**Reference**
TC1276		pKD3 in BT2514k Cm^R in *Escherichia coli K-12*	Datsenko and Wanner (2000)
TC2835		MG1655 pORTMAGE-2 temperature-sensitive (Amp^R)	Nyerges et al. (2016)
TC2837		REL606 pORTMAGE-2 temperature-sensitive (Amp^R)	Nyerges et al. (2016)
CA698		REL606 (*Escherichia coli B)*	Lab stock
CA639		BT340 =DH5alpha (pCP20)	Cherepanov and Wackernagel (1995)
TC1972		MG1655 (*Escherichia coli K-12)*	Lab stock
CA637		P*sulA*-GFP (pUA66)	Zaslaver et al. (2006)
CA638		P*yiaG*-GFP (pUA66)	Zaslaver et al. (2006)
CA640	CA637	REL606 (pUA66 Ω P*sulA*-GFP)	This study
CA641	CA637	MG1655 (pUA66 Ω P*sulA*-GFP)	This study
CA642		REL606 (pUA66 Ω P*bolA*-GFP)	Lab stock
CA643		MG1655 (pUA66 Ω P*bolA*-GFP)	This study
CA644	CA638	REL606 (pUA66 Ω P*yiaG*-GFP)	This study
CA645	CA638	MG1655 (pUA66 Ω P*yiaG*-GFP)	This study
TC1126		REL606 rhaA::P(AI)*cfp*	Lab stock
TC1127		REL606 rhaA::P(AI)*yfp*	Lab stock
CA617	TC2835	MG1655 Δ*polB*, Cm^R from pKD3	This study
CA623	TC2837	REL606 Δ*polB*, Cm^R from pKD3	This study
CA628	TC2835	MG1655 Δ*dinB*, Cm^R from pKD3	This study

Table 2-1: List of bacterial strains (Continued)

Strain	Parent	Genotype	Reference
CA646	CA623	REL606 Δ*polB*	This study
CA649	CA617	MG1655 Δ*polB*	This study
CA652	CA628	MG1655 Δ*dinB*	This study
CA655	CA646	REL606 Δ*polB* + pORTMAGE-2 Amp^R	This study
CA661	CA652	MG1655 Δ*dinB* + pORTMAGE-2 Amp^R	This study
CA664	CA655	REL606 Δ*polB* + Δ*dinB*, Cm^R from pKD3	This study
CA667	CA661	MG1655 Δ*dinB* + Δ*polB*, Cm^R from pKD3	This study
CA674	CA664	REL606 Δ*dinB* Δ*polB*	This study
CA680	CA667	MG1655 Δ*dinB* Δ*polB*	This study
CA692	CA674	REL606 Δ*dinB* Δ*polB* + pORTMAGE-2 Amp^R (replicate 1)	This study
CA693	CA674	REL606 Δ*dinB* Δ*polB* + pORTMAGE-2 Amp^R (replicate 2)	This study
CA696	CA680	MG1655 Δ*dinB* Δ*polB* + pORTMAGE-2 Amp^R (replicate 1)	This study
CA697	CA680	MG1655 Δ*dinB* Δ*polB* + pORTMAGE-2 Amp^R (replicate 2)	This study

2.1.1 Glycerol stocks

All strains for making glycerol stocks were grown overnight, and a sample of 660 µL of each culture was mixed with 330 µL of 60% glycerol and kept at −80° for storage in a cryovial tube (Gallet et al., 2012).

2.1.2 Gel electrophoresis

Before conducting electrophoresis on all gels, 0.5 μg/ml of ethidium bromide (EtBr) was added. Electrophoresis was then performed at 100 V for 1 hour. Afterwards, the gel was subjected to UV light, and a picture of it was captured using a gel documentation system.

2.1.3 Plasmid isolation and purification

For each plasmid used (Table 2-2), isolation occurred from 3 mL of liquid overnight culture using the QIAprep Spin Miniprep Kit (Qiagen), according to the manufacturer's instructions. Plasmid DNA was eluted in 30 μL nuclease-free water and stored at -20ºC. According to the manufacturer's instructions, plasmid DNA was quantified using the NanoDrop spectrophotometer (ACT Gene Asp-3700).

Table 2-2: List of plasmids

Plasmid name	**Relevant characteristics**	**Reference**
pKD3	Cm^R; template plasmid used to help in the removal of genes of interest	Datsenko and Wanner (2000)
pCP20	Amp^R; plasmid used to remove chloramphenicol resistance cassette, which is flanked by FRT sites	Datsenko and Wanner (2000) and Cherepanov and Wackernagel (1995)
pORTMAGE-2	Amp^R; temperature-sensitive plasmid expressing the heat shock-induced λ red recombinase	Nyerges et al. (2016)

Table 2-3: List of primers

Primer	Sequence (5'→3')	Details	Reference
pKD3_*dinB*_F [a]	CTGAAATCACTGTATACTTTACCAGTGTTGAGAGGTGAGCgtgtaggctggagctgcttc	Forward primer for removal of *dinB* gene	This study
pKD3_*dinB*_R [a]	CCTCATAATAATGCACACCAGAATAGACATAATAGTATACcatatgaatatcctccttag	Reverse primer for removal of *dinB* gene	This study
pKD3_*polB*_F [a]	GTCACGCATCAAAATGGTATCTGGCGAACTCTTTTTTTTGgtgtaggctggagctgcttc	Forward primer for removal of *polB* gene	This study
pKD3_*polB*_R [a]	CAGGCTATAATCAAGCCTGGTTTTTTGATGGAATTACAGCcatatgaatatcctccttag	Reverse primer for removal of *polB* gene	This study
pKD3_umuDC_F [a]	GAACAGACTACTGTATATAAAAACAGTATAACTTCAGGCAGgtgtaggctggagctgcttc	Forward primer for removal of *umuDC* gene	This study
pKD3_umuDC_R [a]	CCATTCGGCGCTCCTGCGGGAGCGCTTTTTTCCTGCCGCcatatgaatatcctccttag	Reverse primer for removal of *umuDC* gene	This study

[a]The lower-case letters are complementary to pKD3, and the upper-case letters are homologous to sequences in the gene of interest (GOI).

Table 2-3: List of primers (Continued)

Primer	Sequence (5'→3')	Details	Reference
*dinB*_200bp-away_F	CAAAAATCCGCAAAGCGCGG	Detection of *dinB* gene replaced with Cm^R gene. Locus-specific primer	This study
*dinB*_200bp-away_R	CCTCTTGTTCAGCAAGCATG	Detection of *dinB* gene replaced with Cm^R gene. Locus-specific primer	This study
*polB*_200bp-away_F	CCAAGTCCCAATTCGCTTTC	Detection of *polB* gene replaced with Cm^R gene. Locus-specific primer	This study
*polB*_200bp-away_R	CGGTGCATAACGCCATCGTG	Detection of *polB* gene replaced with Cm^R gene. Locus-specific primer	This study
umuDC_200bp-away_F	GTCATTATGGCGAATGCTTC	Detection of *umuDC* gene replaced with Cm^R gene. Locus-specific primer	This study
umuDC_200bp-away_R	GGGTGCCGCAAGTGTTTGTC	Detection of *umuDC* gene replaced with Cm^R gene. Locus-specific primer	This study
CmR_F	AGCATTCTGCCGACATGGAA	Detection of *dinB*, *polB* and *umuDC* gene replaced with Cm^R gene. Insertion-specific primer	This study
CmR_*dinB*_R	TGCGCTGGCACTTAAGAGAT	Detection of *dinB* gene replaced with Cm^R gene. Insertion-specific primer	This study
CmR_*polB*_R	GCGAAGGCATATTACGGGCA	Detection of *polB* gene replaced with Cm^R gene. Insertion-specific primer	This study
CmR_umuDC_R	CGTGATCTGTTCGGTCGCTA	Detection of *umuDC* gene replaced with Cm^R gene. Insertion-specific primer	This study
p_RhaA_F	GACCACTCAACTGGAACAGGCC	To amplify CFP/YFP gene insert from TC1126 and TC1127 to generate PCR products with a fluorescent marker	This study
p_RhaA_R	CTCTTCCAGCAGTGCCAGAC	To amplify CFP/YFP gene insert from TC1126 and TC1127 to generate PCR products with a fluorescent marker	This study
pUA66_F	AATAGGCGTATCACGAGG	To sequence reporter-fusion strains in REL606 and MG1655 to check if GFP has been incorporated	Lab stock; Huei-Yi Lai

2.2 Process of strain construction (Recombineering)

Recombineering is a method of genetic engineering in bacteria that involves the incorporation of DNA into the genome through homologous recombination (Diner et al., 2011; Marinelli et al., 2012; Sharan et al., 2009; Wannier et al., 2021). Bacteriophage-encoded homologous recombination functions, such as the λ red system, are involved in the process. The λ red system uses three phage-encoded proteins, *exo*, *beta* and *gam*, to degrade one strand of DNA, bind the single-stranded DNA (ssDNA) and prevent degradation of the double-stranded DNA (dsDNA) substrate, respectively (Marinelli et al., 2012; Sharan et al., 2009; Wannier et al., 2021). Recombineering allows for precise genetic modifications, including deletions, insertions, gene knockouts, point mutations, and in vivo cloning (Marinelli et al., 2012).

The goal of using recombineering is to construct strains that lack genes involved in stress-induced mutagenesis (SIM), specifically *dinB*, *polB*, and *umuDC*. Constructing strains that lack SIM associated genes allows for further experiments to be conducted that display the impact of these three genes on evolvability.

Table 2-4: Process of strain construction by recombineering

Steps	Experiment	Description	Achievement
1	PCR	pKD3 was used as a template plasmid to attach primers with ~39-41bp homology arms from each gene (*dinB, polB* and *umuDC)* at their 5' ends.	PCR products called *dinB*-Cm, *polB*-Cm and *umuDC*-Cm
2	Transformation of the red helper plasmid	The red helper plasmid pORTMAGE-2 Amp^R was electroporated into MG1655 and REL606 cells.	REL606 and MG1655 carrying pORTMAGE-2
3	Transformation with PCR products	PCR products *dinB*-Cm^R, *polB*-Cm^R and *umuDC*-Cm^R were electroporated into MG1655 and REL606 carrying pORTMAGE-2.	REL606 Δ*dinB*-Cm^R, REL606 Δ*polB*-Cm^R, MG1655 Δ*dinB*-Cm^R and MG1655 Δ*polB*-Cm^R. Was unsuccessful in transforming cells with *umuDC*-Cm^R
4	Transformation with pCP20	The plasmid pCP20 (Amp^R) was electroporated into REL606 Δ*dinB*-Cm^R, REL606 Δ*polB*-Cm^R, MG1655 Δ*dinB*-Cm^R and MG1655 Δ*polB*-Cm^R.	REL606 Δ*dinB*-Cm^R pCP20, REL606 Δ*polB*-Cm^R pCP20, MG1655 Δ*dinB*-Cm^R pCP20 and MG1655 Δ*polB*-Cm^R pCP20
5	Loss of antibiotic resistance	Strains were grown at 43ºC as heat shock for simultaneously losing CmR and pCP20 (AmpR) plasmid.	REL606 Δ*dinB*, REL606 Δ*polB*, MG1655 Δ*dinB* and MG1655 Δ*polB*

Table 2-4: Process of strain construction by recombineering (Continued)

Steps	Experiment	Description	Achievement
6	Transformation of the red helper plasmid	The red helper plasmid pORTMAGE-2 Amp^R was electroporated into REL606 Δ*dinB*, REL606 Δ*polB*, MG1655 Δ*dinB* and MG1655 Δ*polB* cells.	REL606 Δ*dinB*, REL606 Δ*polB*, MG1655 Δ*dinB* and MG1655 Δ*polB* carrying pORTMAGE-2
7	Transformation of PCR products	PCR products *dinB*-Cm^R, *polB*-Cm^R and *umuDC*-Cm^R were electroporated into REL606 Δ*dinB*, REL606 Δ*polB*, MG1655 Δ*dinB* and MG1655 Δ*polB* carrying pORTMAGE-2.	REL606 Δ*dinB* Δ*polB*-Cm^R and MG1655 Δ*dinB* Δ*polB*-Cm^R. Was unsuccessful in transforming cells with *umuDC*-Cm^R
8	Transformation with pCP20	The plasmid pCP20 (Amp^R) was electroporated into REL606 Δ*dinB* Δ*polB*-Cm^R and MG1655 Δ*dinB* Δ*polB*-Cm^R.	REL606 Δ*dinB* Δ*polB*-Cm^R pCP20 and MG1655 Δ*dinB* Δ*polB*-Cm^R pCP20
9	Removal of antibiotic resistance	Strains were grown at 43ºC as heat shock for simultaneously losing CmR and pCP20 (AmpR) plasmid.	REL606 Δ*dinB* Δ*polB* and MG1655 Δ*dinB* Δ*polB*

2.3 Preparation of PCR products for recombineering

To construct strains lacking SIM, I used recombineering to delete the genes *dinB*, *polB*, and *umuD*C (Table 2-4). PCR products were generated using several pairs of 59- to 61-nt long primers containing a 20-nt priming sequence of template plasmid, pKD3, and 39- to 41-nt long homology arms for each error-prone polymerase gene shown in Table 2-3. The pKD3 strain (TC1276) was used as template DNA (Tables 2-1 and 2-2). PCR was performed following the recipe and protocol outlined in Tables 2-5 and 2-6. The PCR products had regions of the target gene (*dinB*, *polB* and *umuDC*) be disrupted, flanking a region of the

pKD3 plasmid encoding FRT sites and the *cat* gene conferring resistance to chloramphenicol (1016 bp). *dinB*, *polB,* and *umuDC* gene sizes are 1056 bp, 2352 bp and 1689 bp, respectively. Gel electrophoresis was run using the 1 kb Plus DNA ladder (100 bp – 10 kb) from New England Biolabs. PCR products were purified using the Wizard SV Gel and PCR Clean-Up System.

Table 2-5: Creating linear fragments for homologous recombination

Reagents	**Volume**
DreamTaq Green PCR Master Mix 2X	12.5 µL
Isolated plasmid pKD3 as template DNA	1 µL
Primer pKD3_*dinB*_F, or pKD3_*polB*_F, or pKD3_*umuDC*_F	1 µL
Primer pKD3_*dinB*_R, or pKD3_*polB*_R, or pKD3_*umuDC*_R	1 µL
Water	9.5 µL
Total	**25 µL**

Table 2-6: Steps involved in PCR thermal cycling

Steps	**Temperature (°C)**	**Time**	**Number of Cycles**
Initial denaturation	95	2 min	1
Denaturation	95	30 s	30
Annealing	58	30 s	
Extension	72	1 min	
Final Extension	72	5 min	1

2.4 Preparation of electrocompetent cells

To generate electrocompetent cells needed for recombineering, I followed a protocol as described by Datsenko and Wanner (2000), with modification. Overnight cultures of LB + Amp were made of MG1655 or REL606 strains carrying pORTMAGE-2, incubating at 30ºC. 100 µL of each overnight culture was used to inoculate 10 mL of fresh LB media with ampicillin and grew until they reached OD_{600} = ~0.5. Cultures were transferred to a water bath at 42ºC for 15 minutes to induce the red recombination genes. After induction, cultures were immediately placed on ice. Cultures were transferred to chilled 15 mL centrifuge tubes, and cells were collected by centrifugation at 4,000 rpm for 8 minutes at 4ºC. Supernatants were decanted, and cell pellets were carefully resuspended in 10 mL of chilled 10% glycerol before centrifugation at 4,000 rpm for 5 minutes, repeated for two wash cycles. The cell pellets of the second wash cycle were resuspended in 1 mL of 10% glycerol in a chilled sterile Eppendorf tube before centrifugation at 14,000 × *g* for 1 minute at 4ºC for the third and final wash cycle. The cell pellets were resuspended in 100 µL of 10% glycerol and divided into two chilled sterile Eppendorf tubes in 50 µL aliquots that were stored on ice for electroporation.

2.5 Transformation by electroporation

To transform the electrocompetent cells with the PCR product, two different procedures were performed. Firstly, red-induced cells were mixed with the PCR product, while secondly, red-induced cells were used without the PCR product as a negative control. The electrocompetent cells and PCR products were kept on ice. A total of 5 µL of PCR product was aliquoted into 50 µL of electrocompetent cells immediately before electroporation, and H_2O was used for the negative control. The cells were gently mixed and transferred into a pre-chilled 0.1 cm electroporation cuvette. The cuvette was pulsed at 1.80 kV in an electroporator, and then immediately, 1 mL of SOC was added to the cuvette. The shocked cells were then transferred to a sterile Eppendorf tube and incubated at 37ºC for 1 hour while constantly shaking at 250 rpm to facilitate cell recovery before antibiotic selection. After incubation, 100 µL of cells were spread onto LB agar plates containing chloramphenicol to select for Cm^R transformants. The plates were then incubated at 37ºC for 24 h. If no mutants grew within 24 h, the remaining transformed cells were left standing overnight at room temperature before

spreading. Chloramphenicol-resistant colonies were then streaked onto LB agar plates and incubated for 24 h. The resulting colonies were tooth-picked with a plastic tip onto LB-only agar and LB agar containing ampicillin to test for antibiotic sensitivity. The selected mutants were expected to have lost the red protein expression plasmid at 37ºC and should be sensitive to ampicillin. Mutants that grew on LB agar only and not on LB agar with ampicillin indicated the loss of the red helper plasmid and were selected for PCR verification.

2.6 PCR Verification

To verify that the transformants had successfully integrated the PCR product and created a target gene deletion, PCR was carried out using the method described by Datsenko and Wanner (2000). Freshly isolated mutants were suspended in 20 µL of water, and 5 µL aliquots were used in separate 25 µL PCR reactions (Table 2-7). Locus-specific primers were used to test if mutants had the correct structure, located about 200 bp upstream and downstream from the specific gene of interest (GOI) to confirm the loss of the target error-prone polymerase gene and the gain of the antibiotic cassette (Tables 2-3 and 2-7). To determine the expected band size, I added the size of the *cat* gene (1016 bp) or the gene of interest (*dinB*, *polB*, and *umuDC* gene sizes are 1056 bp, 2352 bp, and 1689 bp, respectively) to the size of the homology arms, ~40 bp). I then added the distance between the locus-specific primers and the gene of interest, ~200 bp. This calculation gave the expected product size (Figure 2-1).

For *polB*, there was a noticeable difference of ~1250 bp between the control (2698 bp) and the expected band size for mutants (1442 bp). While for *dinB*, there was little difference between the expected band size for mutants (1435 bp) and the WT (1395 bp), making it hard to distinguish if the *dinB* gene had been replaced with the Cm^R gene. Therefore, insertion-specific primers were designed to facilitate screening for the intended genetic change. These components included a forward primer sequence (CmR_F) situated within the chloramphenicol resistance cassette (Table 2-3), and a reverse primer sequence located outside *dinB* or *polB* genes. If the chloramphenicol-resistant transformants had the antibiotic resistance cassette but lost the error-prone polymerase gene, a detectable band should be observed in the PCR results when using the designated primers, indicating successful achievement of both single and double mutants. This band would indicate the presence of the

Cm^R gene at the site where the error-prone polymerase gene was targeted. No band should be present for the wild-type or chloramphenicol resistance strains when the cassette has been integrated at an off-target location. Control colonies of the WT strain (MG1655 or REL606) were constantly tested side-by-side. PCRs were run with the same thermal cycling conditions (Table 2-6).

Table 2-7: Checking for the removal of GOI and antibiotic-resistant cassette

Reagents	**Volume**
DreamTaq Green PCR Master Mix 2X	12.5 µL
Colony inoculated in 20 µL water	5 µL
Forward primer (CmR_F or ~200bp away)	1 µL
Reverse primer (CmR_R or ~200bp away)	1 µL
Water	5.5 µL
Total volume	**25 µL**

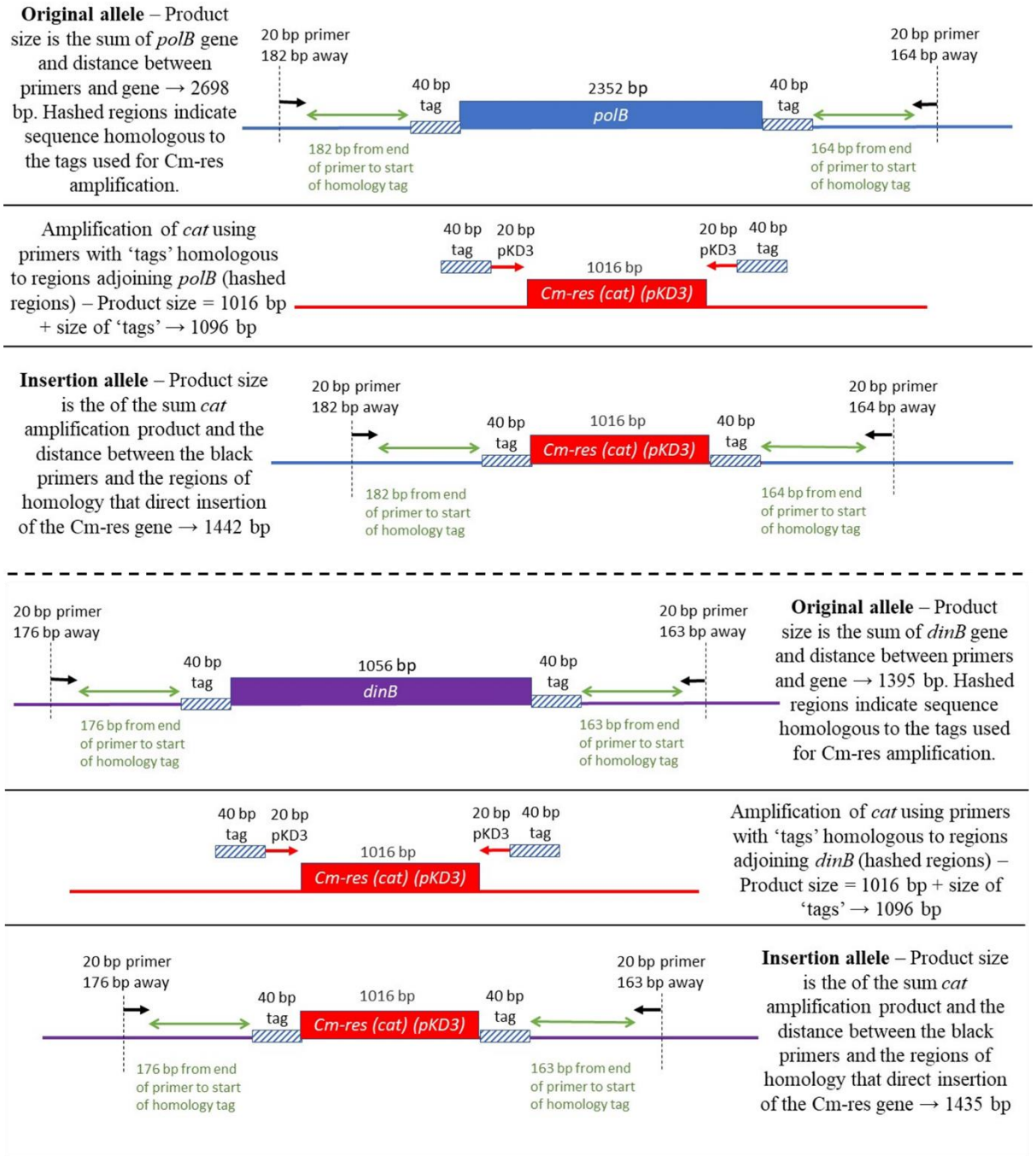

Figure 2-1: Schematic showing how to calculate *cat* gene amplification product size in place of the target gene (*dinB* and *polB*).

2.7 Elimination of antibiotic resistance gene

To remove the *cat* gene flanked by FRT sites, a temperature-sensitive FLP helper plasmid, pCP20, that confers chloramphenicol and ampicillin resistance was utilized following the protocol by Datsenko and Wanner (2000) and Barrick et al. (2023), with modifications. The excision of the *cat* gene leaves behind an 82- to 85-nt scar (Datsenko & Wanner, 2000). First, Cm^R transformants were transformed with pCP20, and Amp^R transformants were selected overnight at 30°C. Resistant colonies were streaked onto LB-only plates and incubated at 42°C overnight for colony purification. The loss of antibiotic resistance was confirmed by tooth-picking six individual colonies from streaked plates onto LB + Amp, LB + Cm, and LB-only plates, in that order, to ensure the absence of growth on the antibiotic-containing plates was not due to insufficient cells. Plates were incubated overnight at 37°C for LB + Cm and LB-only plates and 30°C for LB + Amp plates. The successful mutants were expected to be chloramphenicol and ampicillin-sensitive, indicating that the FRT-flanked chloramphenicol resistance gene and the FLP helper plasmid (pCP20) were simultaneously lost. PCR verification followed the same protocol as in Table 2-7, using locus-specific primers. The expected band size for successful mutants was approximate ~500 bp. Controls for wild-types and single mutants with the cat gene without pCP20 transformation were used to compare band sizes.

2.8 Preparing single mutant strains for the subsequent gene deletion

To enable a second deletion of SIM genes, the single mutant strains required the reintroduction of the red helper plasmid, pORTMAGE-2. Therefore, the REL606 and MG1655 strains carrying pORTMAGE-2 were grown overnight with ampicillin (100 µg/mL) at 30°C and then their plasmids were purified using the QIAprep Spin Miniprep Kit for subsequent transformations. The single mutants were made electrocompetent, transformed with pORTMAGE-2 and then grown overnight on LB + Amp at 30ºC. Single colonies were streaked onto LB + Amp plates for growth overnight, and then colonies were picked to create overnight cultures for freezer stock to be used for transformations of the second gene to be removed. The second removal of the error-prone polymerase gene followed the same strain construction protocol described above.

2.9 Reporter assay for SOS and RpoS response

To measure the extent of SOS induction in various environments, an SOS reporter, which consisted of the *gfp* gene controlled by the *sulA* promoter, was utilized (Bos et al., 2015; Friedberg et al., 2005b; McCool et al., 2004; Pennington & Rosenberg, 2007). The *sulA* gene in *E. coli* is thought to inhibit cell division by binding to FtsZ, which is involved in forming a structural component at the division site of bacterial cell division (Cordell et al., 2003; Friedberg et al., 2005b; McCool et al., 2004; Trusca et al., 1998). The expression of *sulA* is repressed by the SOS repressor, *LexA*, and DNA-damaging agents, such as UV irradiation, can trigger the synthesis of *sulA* protein (Cole, 1983; Cordell et al., 2003; Friedberg et al., 2005b; Huisman & D'Ari, 1981; McCool et al., 2004). Therefore, the P*sulA*-GFP reporter can be used alongside flow cytometry to measure the level of SOS induction in various environments that may induce the SOS response.

To evaluate the role of SIM in a long-term evolution experiment, it is essential to identify a robust environmental inducer of the SOS response that can induce stress-induced mutagenesis without affecting the growth rate of *E. coli*. After researching relevant literature, two potential candidates were identified: mitomycin C (MMC) and nalidixic acid (Nal). In previous studies, both are strong inducers of the SOS response (Dapa et al., 2017; Friedberg et al., 2005a, 2005b; Huisman & D'Ari, 1981). MMC, an antitumour antibiotic used in cancer chemotherapy, inhibits DNA synthesis by inducing DNA cross-links and alkylation (Dapa et al., 2017; Keller et al., 2001; Suresh Kumar et al., 1997). Nal belongs to the quinolone class of antibiotics and acts as an enzyme inhibitor of DNA gyrase and topoisomerase IV, which coil and uncoil DNA. Nal creates double-stranded breaks (DSB), resulting in single-stranded DNA that induces the SOS response (Foster, 2007; Huisman & D'Ari, 1981). SOS reporter assays using flow cytometry were combined with growth curves to determine which stressor produces the most substantial inducing effect with minimal changes to the growth rate. Using a stressor that has a limited effect on growth, I can isolate and study the stress response pathways without interfering with the growth-dependent biological processes (Jaramillo-Riveri et al., 2022).

2.9.1 Strain construction of reporter-GFP fusions

The following protocol was implemented to incorporate the plasmid DNA for each reporter-GFP isolate into wild-type strains to assess the efficacy of P*sulA*-GFP, P*yiaG*-GFP, and P*bolA*-GFP reporters in various environments. I already have pUA66 Ω P*bolA*-GFP introduced into REL606 from a previous study. First, a colony from a streaked LB plate containing each reporter was picked and used to create an overnight culture in LB media, which was incubated in a 37ºC shaking incubator. DNA of the reporter plasmids was then obtained from lab stocks using the QIAprep Spin Miniprep Kit and eluted in 30 mL H_2O before being stored in a -20ºC freezer. To incorporate the plasmid DNA for each reporter-GFP isolate into both REL606 and MG1655 wild-type strains, relevant wild-type cells were made electrocompetent and transformed with the plasmid DNA for each reporter-GFP combination, as previously described. The transformed cells were then plated onto LB + kanamycin (Km) plates overnight, and the next day, transformed colonies were viewed under a fluorescent microscope to identify transformed GFP^+ cells. Fluorescent mutant colonies were picked and streaked onto LB + Km plates overnight at 37ºC. For future use, an individual colony was chosen for each reporter-GFP, and a stock of each isolate was created and stored in a cryovial.

2.9.2 SOS reporter assay

To determine the optimal range for inducing SOS stressors, MMC and Nal, an SOS reporter assay was implemented. Overnight cultures of REL606 and MG1665 wild-type strains and REL606 and MG1665 strains with P*sulA*-GFP reporter-gene fusions (listed in Table 2-1) were prepared in plastic test tubes. The wild-type strains were reserved for future growth curves, while the reporter-GFP fusion strains were for flow cytometry. The next day, cultures were diluted 1:1,000 into 3 mL of fresh DM250 medium and incubated overnight. On day three, each culture was diluted 1:100 into fresh DM250 medium (total volume of 200 µL) in a 96-well microtiter plate containing a specific concentration of the desired stressor (MMC or Nal). Growth curves were performed at 0.725 ng/mL and 0.65 ng/mL concentration of inducer, while flow cytometry used the same concentrations plus 0.8 ng/mL. Each combination of strain and inducer concentration had six replicates. The 96-well microtiter

plates were incubated for 24 hours for flow cytometry and growth curve analysis the following day.

Preliminary experiments were conducted using glucose and glycerol-supplemented media (at 250 µg/mL) to narrow the inducer concentration range. This decision was based on research conducted by Jaramillo-Riveri et al. (2022), which found that slow growth conditions (glycerol-supplemented media) resulted in a higher proportion of cells exhibiting high SOS induction compared to fast growth conditions (glucose-supplemented media).

2.9.3 Flow cytometry for SOS reporter assay

To measure GFP expression levels in both reporter and control cultures described in section 2.9.2, a BD FACSCanto II Flow Cytometer was used. Before analysis by flow cytometry, the wells of the incubated plate were first diluted 1:5 into fresh DM0 and subsequently transferred to a new 96-well microtiter plate. During the preliminary experiments, two replicates were conducted for each strain-stressor combination. Six replicates were performed for each strain-stressor combination for the final SOS reporter assay using flow cytometry. GFP plots were manually assessed, and thresholds were applied to define each population's boundaries, separate cells from noise, and identify GFP^+ populations from GFP^- populations.

2.9.4 Growth curves for SOS reporter assay

To determine the impact of stressors on growth rates, cultures from section 2.9.2 were diluted at a 1:50 ratio into fresh DM250 in a new 96-well microtiter plate to a final volume of 200 µL per well. For the SOS reporter assay using growth curves, six replicates were performed for each strain-stressor combination. The plate was then incubated at 37ºC in a Spectramax machine with five seconds of shaking before taking an OD_{450} reading every five minutes over 24 hours. Growth curve data were analysed using Curveball (Ram et al. (2019).

2.9.5 Process of RpoS reporter assay

To identify the most efficient reporter fusion, a reporter assay was conducted using four treatments and four strains, namely REL606 and MG1655, with reporter fusions P*bolA*-GFP and P*yiaG*-GFP. The aim was to determine an environment that induces the RpoS response effectively. Treatments were starvation for 12, 24, 48 and 72 hours. Five replicates were performed for each strain-treatment combination.

Cells from each strain were grown overnight from freezer stocks in a 15 mL glass tube with a plastic lid containing LB media shaken at 250 rpm and incubated at 37ºC. A 10^4-fold dilution was made into 990 µL DM medium supplemented with 25 µL/mL glucose (DM25) and incubated in a 37ºC shaking incubator for 24 hours. DM25 was selected because of its minimal glucose supply, which makes starvation happen more quickly. The next day, cultures underwent a 100-fold dilution into fresh DM25 media and were left shaking for 24 hours at 37ºC. Each treatment was initiated on different days to allow the analysis of results by flow cytometer on the same day for all treatments. To quantify the effect of different starvation periods on reporter expression, cultures of cells were analysed by flow cytometry to determine the distribution of GFP expression in cells sampled from each treatment (Figure 2-3). Thresholds were manually applied on the GFP plots to determine the boundaries of each population.

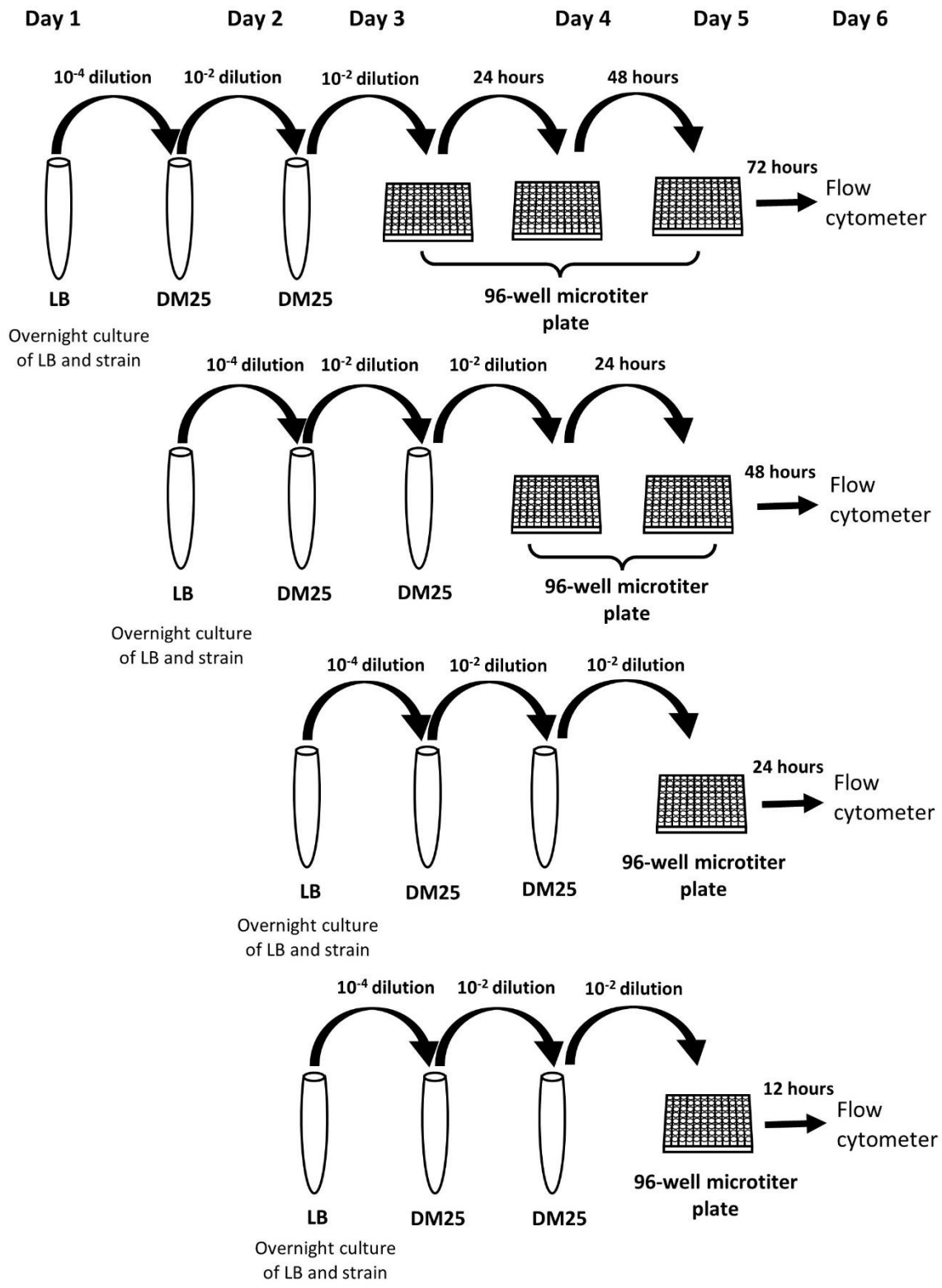

Figure 2-2: Schematic of reporter assay for RpoS response.

2.10 Verification of SIM$^-$ strains and reporter-gene fusions

To confirm the successful removal of each SIM gene and the correct placement of reporter-GFP fusions, sequencing of SIM$^-$ and reporter strains was carried out. The samples were sent to Macrogen for sequencing, and primers that bind ~200bp away from target genes were used for the SIM$^-$ strains. For the reporter strains, the pUA66_F primer (listed in Table 2-3) was used.

2.11 Construction of chromosomal fluorescent markers in SIM$^+$ and SIM$^-$ strains

I attempted to introduce Cyan Fluorescent Protein (CFP) and Yellow Fluorescent Protein (YFP) markers at the *rhaA* locus in both SIM$^+$ and SIM$^-$ ancestral wildtype and mutant strains using the one-step inactivation of chromosomal genes technique developed by Datsenko and Wanner (2000).

Firstly, I performed PCR using p-RhaA primers to amplify a cassette comprising the P_{AI} promoter driving *cfp* and *yfp* genes from lab stocks of REL606 already containing *yfp* and *cfp* genes (Tables 2-1 and 2-3). Since I already had REL606 containing YFP and CFP markers, the focus was on incorporating *yfp* and *cfp* genes into the MG1655 ancestral wildtype and the mutant strains of both MG1655 and REL606. The PCRs followed the protocol in Tables 2-5 & 2-6. I then used the PCR products containing *cfp* and *yfp* genes to transform electrocompetent cells of REL606 and MG1655 SIM$^-$ strains and the SIM$^+$ MG1655 strain that all have pORTMAGE-2 present as a red helper plasmid (Table 2-1). After electroporation, strains were incubated for 1 hour at 37°C in Eppendorf tubes, and then 100 µL plated onto LB only and incubated at 42°C overnight to get rid of the red helper plasmid. The next day, visible colonies on each plate were viewed under a fluorescent microscope to determine if any colonies contained the fluorescent markers. Unfortunately, I did not observe any fluorescent colonies in the three times the experiment was conducted. Hence, I could not proceed with competition experiments on MG1655 evolved and ancestral mutant strains as I did not have the ancestral strain containing a YFP or CFP marker. A MG1655 YFP or CFP strain is essential to compete the evolved and ancestral lines of MG1655 against for competition experiments. Therefore, I could only proceed with competition experiments of the REL606 ancestral and evolved mutant strains against the REL606 YFP or CFP strains.

2.12 Fluctuation test

To test whether SOS induction elevates mutation rates in ancestral SIM^+ (REL606 and MG1655) but not SIM^- (REL606 Δ*dinB* Δ*polB* and MG1655 Δ*dinB* Δ*polB*) strains, the following steps were taken. First, the strains were grown overnight in LB shaking at 250rpm in a 37ºC incubator. The next day, a 1:100 dilution of overnight culture was transferred into fresh DM250 and incubated under identical conditions. Each of the four test strains had fifteen replicate plastic test tubes. Three were used as controls on non-selective plates, and the remaining 12 were for selective plates. On day two, another 100-fold dilution was performed for each of the 15 replicates of each isolate into fresh DM250. On day three, a 1,000,000-fold dilution was made, resulting in inoculations of ~500 cells into 3 mL cultures that were incubated for 48 hours at 37ºC. Dilutions were carried out in both DM250 alone, and DM250 supplemented with 0.65 ng/mL of MMC, which served as an inducer for the SOS response. These two conditions were used to observe any effect on the mutation rate when adding a specific stressor to induce the SOS response. After incubation, the cultures to be plated on selective media were spun down by centrifugation at 4,000 rpm for eight minutes to pellet cells. The supernatants were removed, leaving 200 µL of concentrated cells plated on LB supplemented with rifampicin selective plates and incubated for 48 hours at 37ºC. The cultures to be plated on non-selective LB-only plates had appropriate dilutions before being spread on LB-only plates and incubated at 37ºC for 24 hours. On the following day, non-selective plates were counted and recorded. The next day, selective plates were counted and recorded.

2.13 Long-term evolution experiment

To determine whether strains that lack SIM show reduced evolvability, an evolution experiment was conducted using SIM^+ (REL606 and MG1655) and SIM^- (REL606 Δ*dinB* Δ*polB* and MG1655 Δ*dinB* Δ*polB*) strains. An evolution experiment allows the impact of stress-induced mutagenesis on evolvability to be addressed by subjecting SIM^+ and SIM^- strains of *E. coli* to a specific stressor (mitomycin C) and then observing how each strain's ability to generate adaptive genetic changes is affected comparatively over successive generations through conducting a competition experiment.

Initially, overnight cultures of each strain were grown in LB at 37°C with shaking at 250 rpm. The next day, a 1:100 dilution of each culture was transferred into 3mL fresh DM250 and incubated under identical conditions. On day four, 10,000-fold dilutions of each strain were inoculated into a 96-well deep well plate containing DM250 with 0.65 ng/mL MMC or with no inducer (NI) in a checkerboard pattern with negative control (DM250 only) (Appendix 1). Twenty-four replicates of each strain in each environment were split over two plates to minimize temperature variation in the incubator. The plates were incubated at 37°C with shaking, and every 48 hours, cells were transferred 1:10,000 into fresh medium to promote starvation of cells and RpoS induction. Cryovials with 30% glycerol were used to store cells every 100 generations (Figure 2-4). The number of generations per transfer cycle (n) was calculated using Equation (1), where DF represents the dilution factor (10,000-fold):

$$n = log2(DF) \quad (1)$$

As a result, 13.29 generations occurred during each transfer, equivalent to 7.52 transfers every 100 generations. The experiment was halted temporarily after 300 generations, and the cells were stored at -80ºC. A 100-fold dilution was made into fresh DM250 in a 96-well deep well plate to revive the cells, and they were incubated with shaking at 37ºC. The next day, the transfers were restarted using the overnight cultures. The experiment ran for 400 generations, comprising 30 transfers (60 days), and the evolved lines were stored at -80ºC for future use in competition experiments (Figure 2-5).

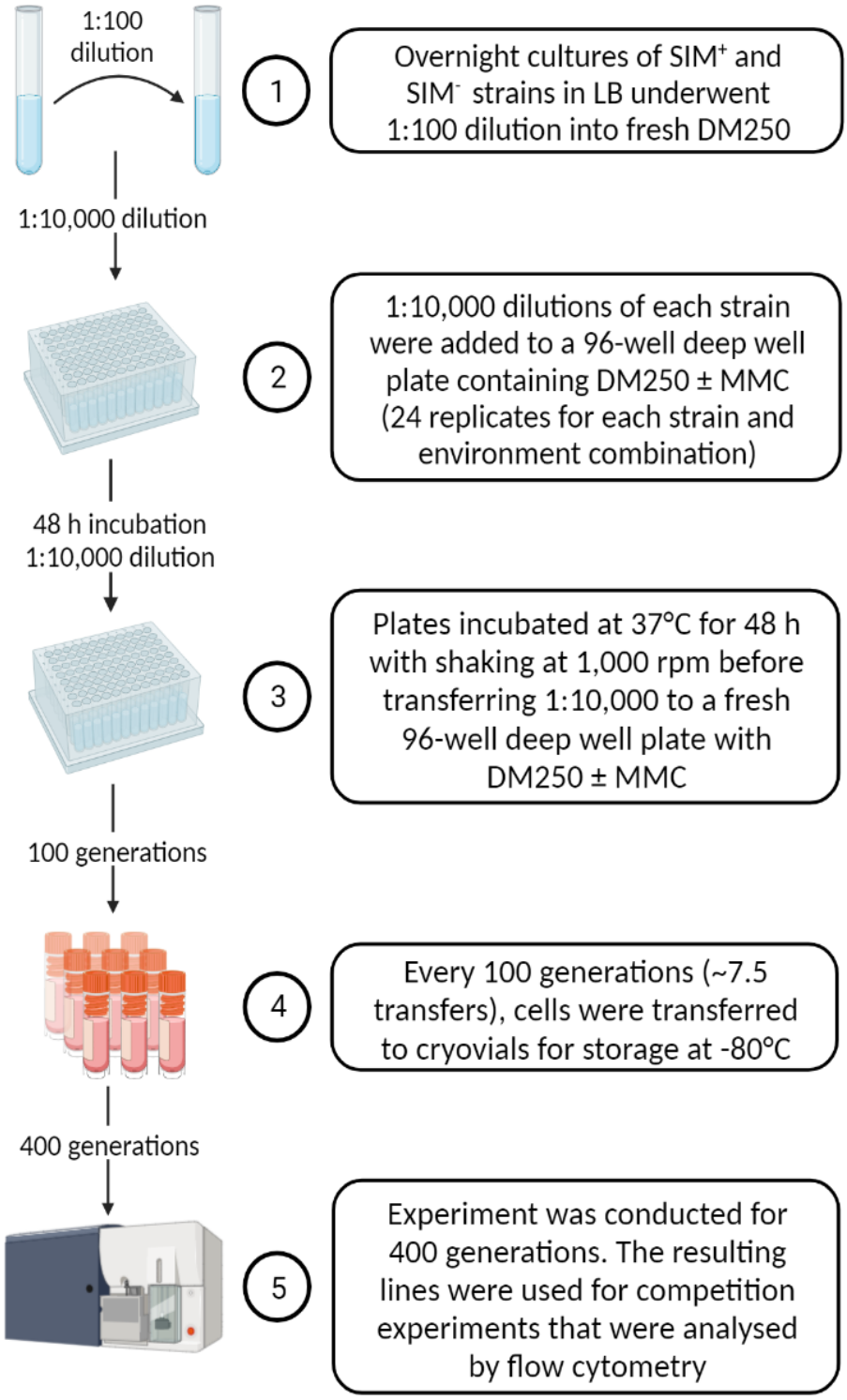

Figure 2-3: Schematic of evolution experiment.
Created with Biorender.com.

2.14 Competition experiment

To evaluate the ability of SIM^+ and constructed SIM^- strains from evolved and ancestral lines to adapt to selection environments, competition experiments were conducted against a reference strain with a YFP marker. The change in the relative frequency of each strain was measured to estimate their relative fitness using the method described by Gallet et al. (2012). Relative fitness in this case refers to how well each strain (SIM^+, constructed SIM^-, and reference strains) are adapted to their selection environments. It is a quantitative assessment of the reproductive success and competitive advantage of each strain compared to the reference strain with a YFP marker. Four competition types were conducted to measure the fitness effect of deleting error-prone polymerases in evolved and ancestral REL606 lines while controlling for potential fluorescent marker effects. These types included (a) REL606 *yfp* vs. REL606 Δ*dinB* Δ*polB* (ancestor), (b) REL606 *yfp* vs. REL606 Δ*dinB* Δ*polB* (evolved), (c) REL606 *yfp* vs. REL606 (ancestor), (d) REL606 *yfp* vs. REL606 (evolved). Two environments, MMC and Nal, were used for the competitions, while MG1655 evolved strains were excluded due to unsuccessful YFP and CFP gene insertion.

The following protocol was adapted from Gallet et al. (2012) and consisted of five days. On the first day, strains were cultivated separately from glycerol stock in 200 µL/well of DM250 in a 96-well deep well plate at 37ºC overnight while shaking at 1,000 rpm. On the second day, a 1:100 dilution of each culture was transferred to a fresh 96-well deep well plate and incubated for 24 hours. On the third day, competitors were diluted 100-fold before mixing in a 1:1 ratio in DM250 with and without MMC into a new 96-well deep-well plate. 200 µL was removed and stored at 4ºC before completing flow cytometry one hour later (0 hours). The remaining culture was kept for further incubation overnight. On the fourth day, a 100-fold dilution was performed into fresh DM250 with and without MMC, and 200 µL was removed and stored at 4ºC before completing flow cytometry one hour later (24 hours). On the final day, a 100-fold dilution was performed into 200 µL of fresh DM0 in a 96-well microtiter plate, and flow cytometry was completed one hour later after storage at 4ºC (Figure 2-5). Using DM250 as the growth medium allowed for visible growth and the assessment of hundreds of thousands of cells using small sample volumes (Gallet et al., 2012). Evolved competitions had three experimental blocks with 24 evolved lines for each competitor combination per plate. Ancestral competitions had 12 replicates of each competitor

combination per plate and were conducted over three experimental blocks, excluding the last block from analysis due to machine failure.

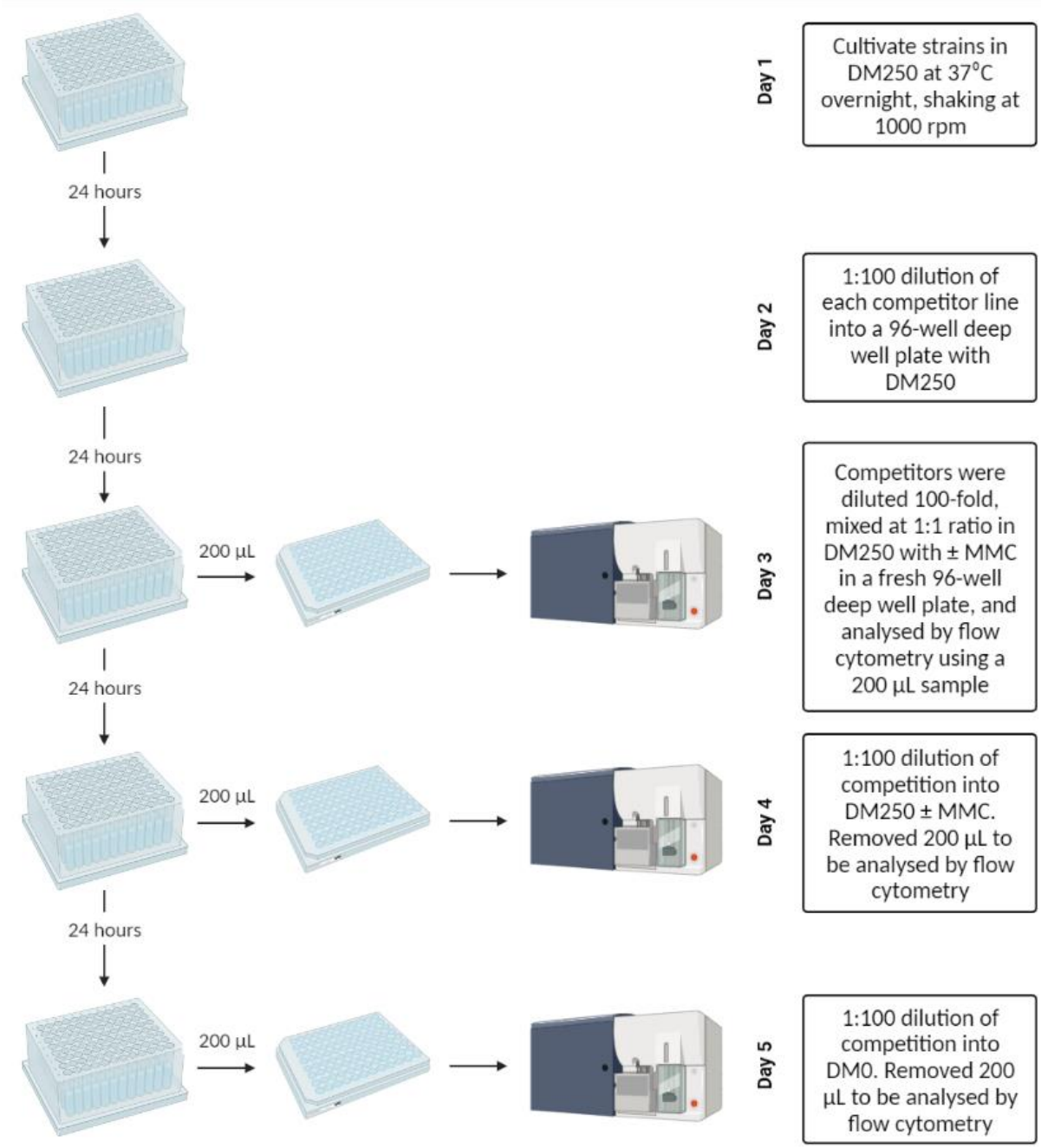

Figure 2-4: Schematic of competition experiment.
Competitors are evolved or ancestral lines competed against a reference strain (REL606 with YFP marker). Created by Biorender.com.

2.14.1 Flow cytometry for competition experiment

The BD FACSCanto II flow cytometer was used to measure the frequency of YFP-marked competitors at 0-, 24-, and 48- hours following the mixing of competing genotypes (Gallet et al., 2012). Gating was performed on a bivariate normal distribution to focus on the central cluster of events in an FSC-SSC plot, capturing approximately 68% of cells in each competition experiment. Manual thresholds were subsequently applied to YFP histogram plots to determine the boundaries of each YFP^+ (reference) and YFP^- population. The count data were filtered to ensure consistency and accuracy in analysing evolved competition data. This filtering included only YFP^+ and YFP^- values within 20% of an equal proportion of count values (50:50) at time zero of the competition. This range was chosen because the count data at time zero was not evenly distributed, with most competitor counts deviating by 10-20% from equivalence (50-50). Excluding competitions from analysis that deviated by more than a 20% range from equivalence obtained the most minor 95% confidence intervals while including sufficient counts. For ancestral competitions, a 10% range from equivalence was used for filtering the count data, which provided a sufficient sample size while preserving the proportion of the count data.

The overall fitness for each strain-environment combination was calculated using fitness values from 0 and 48 hours from the filtered count data. For evolved competitions, the fitness for each of the three replicates was averaged by line (24 lines for each strain-environment combination). Some replicates and lines were lost due to the filtering of count data prior. The resultant lines were then averaged to find the overall fitness for each strain-environment combination. The same was done for ancestral populations, except with the two replicate blocks for the 12 lines of each strain-environment combination. Statistical analyses and plots were generated from the fitness values. From the ancestral competitions of REL606 vs REL606 YFP, a marker cost of 26.70% and 27.50% was calculated in the MMC environment and in its absence, respectively. This marker cost was then subtracted from the reference strain, ancestral SIM^+, to eliminate its effects. Marker cost was calculated by removing 1 from the fitness score.

2.15 Statistical analysis

The software bz-rates developed by Gillet-Markowska et al. (2015) was utilized to determine the mutation rate of SIM^+ and SIM^- strains with and without MMC induction of the SOS response. There were 12 replicate populations of each strain-environment combination. The software generated summary mutation rates and corresponding confidence intervals for each combination of strain and environment. The Curveball software created by Ram et al. (2019) was used to visualize growth curve data. It fits growth models to growth curve data using a command line interface (CLI) and a programmatic interface (API) that works directly with growth curve measurements from 96-well microtiter plates.

Statistical analysis was performed using R Statistical Software (v4.2.2; R Core Team 2022). FlowCore (v2.10.0; Ellis et al. 2022), flowStats (v4.10.0; Hahne et al. 2022), flowWorkspace (v4.10.1; Finak & Jiang 2022), rmarkdown (v2.19; Allaire et al. 2022 and Xie et al. 2018 and Xie et al. 2020), dplyr (v1.0.10; Wickham et al. 2022), ggcyto (v1.26.4; Van et al. 2018), fda (v6.0.5; Ramsay et al. 2022), rstudioapi (v0.14; Ushey et al. 2022), and lattice (v0.20.45; Sarkar 2008) packages were used to process and analyse flow cytometry and growth curve data.

Two-way ANOVA tests were used for competition experiment data, followed by Tukey HSD post hoc comparisons and calculation of effect sizes using pooled standard deviations. I used ANOVA to test for significant effects of environment and genotype. ANOVAs were performed on the summary data of 24 evolved and 12 ancestral population lines in the four strain-environment combinations. The data from each line in evolved competitions was filtered and averaged, using up to three replicates from three experimental blocks. For ancestral competitions, up to two replicates from two experimental blocks were used for each line summary data. Six replicates of each strain and inducer combination were used for growth curve data analysis. As only summary results containing confidence intervals were obtained, growth curve and fluctuation test data were subjected to two-sample t-tests.

3. RESULTS

3.1 Construction of SIM$^-$ strain

The bacterial genome underwent recombineering to construct a SIM$^-$ strain by removing specific error-prone polymerase genes associated with stress-induced mutagenesis (SIM). This genetic manipulation is expected to prevent the increase in mutation rates generated by SIM, facilitating adaptation to stressful environments.

3.1.1 Insertion of *cat* gene in place of *dinB*, *polB* or *umuDC* genes

The process of recombineering was used to replace a gene of interest (*dinB*, *polB*, or *umuDC*) with an FRT-flanked chloramphenicol resistance cassette from the *cat* gene in the template plasmid, pKD3. These FRT sites allow the removal of the resistance cassette once inserted into the bacterial chromosome with a temperature-sensitive FLP helper plasmid, pCP20 (Amp^R) (Datsenko & Wanner, 2000). PCR verifications of transformants were conducted to determine if candidate gene-replacement strains lost the target error-prone polymerase gene and gained the antibiotic cassette. PCR verifications involved the use of two different primer pairs. One primer pair had locus-specific primers located ~200 bp upstream and downstream from the specific gene of interest (GOI) to show if all the mutants had a loss of the error-prone polymerase gene and gain of the antibiotic cassette. The second primer pair had insertion-specific primers, with one primer inside the resistance gene and the other outside the region, flanking the insertion site. This primer pair will only produce a product if the expected construct has been created, where the *cat* gene has been successfully inserted into the target gene. Full details on the conditions of the PCR reactions can be found in section 2.6 (Tables 2-3 and 2-7).

Section 2.6 and Figure 2-1 present the band sizes calculations for gene size replacement experiments. The expected band sizes for replacing the *polB* gene with the *cat* gene using locus-specific primers in REL606 and MG1655 were 1442 bp, while the control band size for wild-type only was 2698 bp, showing a difference of approximately 1250 bp. For *dinB* gene replacement with the *cat* gene in MG1655, the expected band size was 1435 bp, and the

control band size for wild-type only was 1395 bp, showing a difference of approximately 40 bp. My results in Figure 3-1 confirm that the mutants have the expected structures. However, for MG1655 Δ*dinB*, the experiment's results show that the band sizes are similar to the original and insertion allele, making it difficult to determine if the *dinB* gene has been replaced with the *cat* gene using these specific primers. No gel images show *umuDC* deletion due to being unable to grow transformed mutant colonies after electroporation. Thus, no successful Δ*umuDC* mutants were obtained.

The primers used in this experiment are not specific enough to detect if the replacement occurred correctly. To further investigate the presence of the *cat* gene, it was necessary to use insertion-specific primers and DNA sequencing to confirm the presence of the replacement construct with accurate results. The presence of a band in the mutants and the absence of a band in the control wild-type strains confirmed the successful replacement of the *dinB* and *polB* genes with the *cat* gene, as determined by the insertion-specific primers (Figure 3-2). Therefore, the correct structures are present in all mutants. Figures 3-1 and 3-2 show band sizes of strains CA623 (REL606 Δ*polB*, Cm^R from pKD3), CA617 (MG1655 Δ*polB*, Cm^R from pKD3) and CA628 (MG1655 Δ*dinB*, Cm^R from pKD3) that were kept stored as glycerol stocks and used for further experiments.

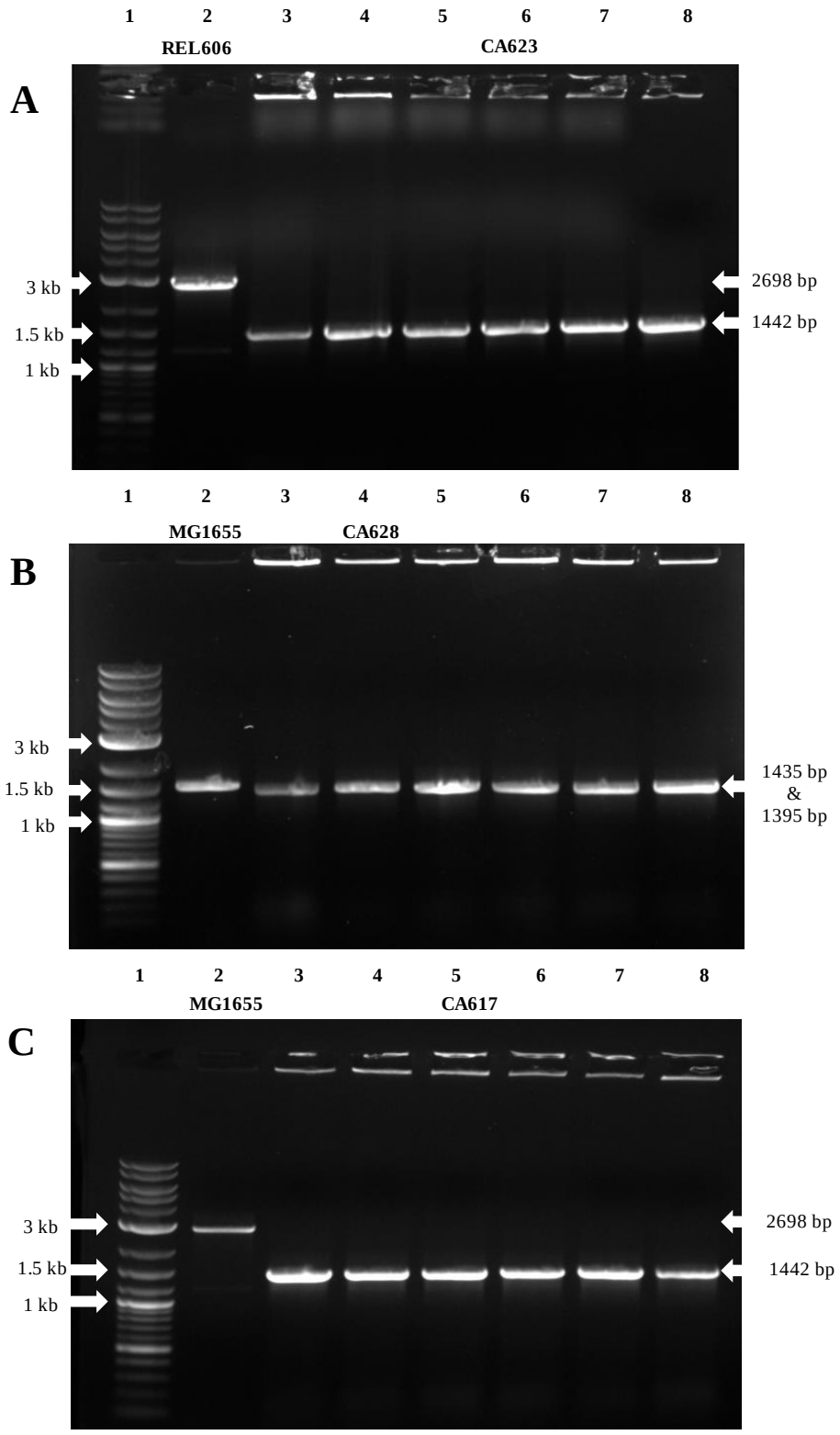

Figure 3-1: Gel image of REL606 Δ*polB* (A), MG1655 Δ*dinB* (B), and MG1655 Δ*polB* (C) with *cat* gene from pKD3 mutants using locus-specific primers.
Lane 1 is a 1 kb Plus DNA ladder. Lane 2 is a control of REL606 WT (2698 bp) or MG1655 (2698 bp or 1395 bp for *polB* and *dinB*, respectively). Lanes 3-8 represent mutants in which a SIM gene within each strain has been substituted with the *cat* gene from pKD3 (1442 bp or 1435 bp for *polB* and *dinB*, respectively).

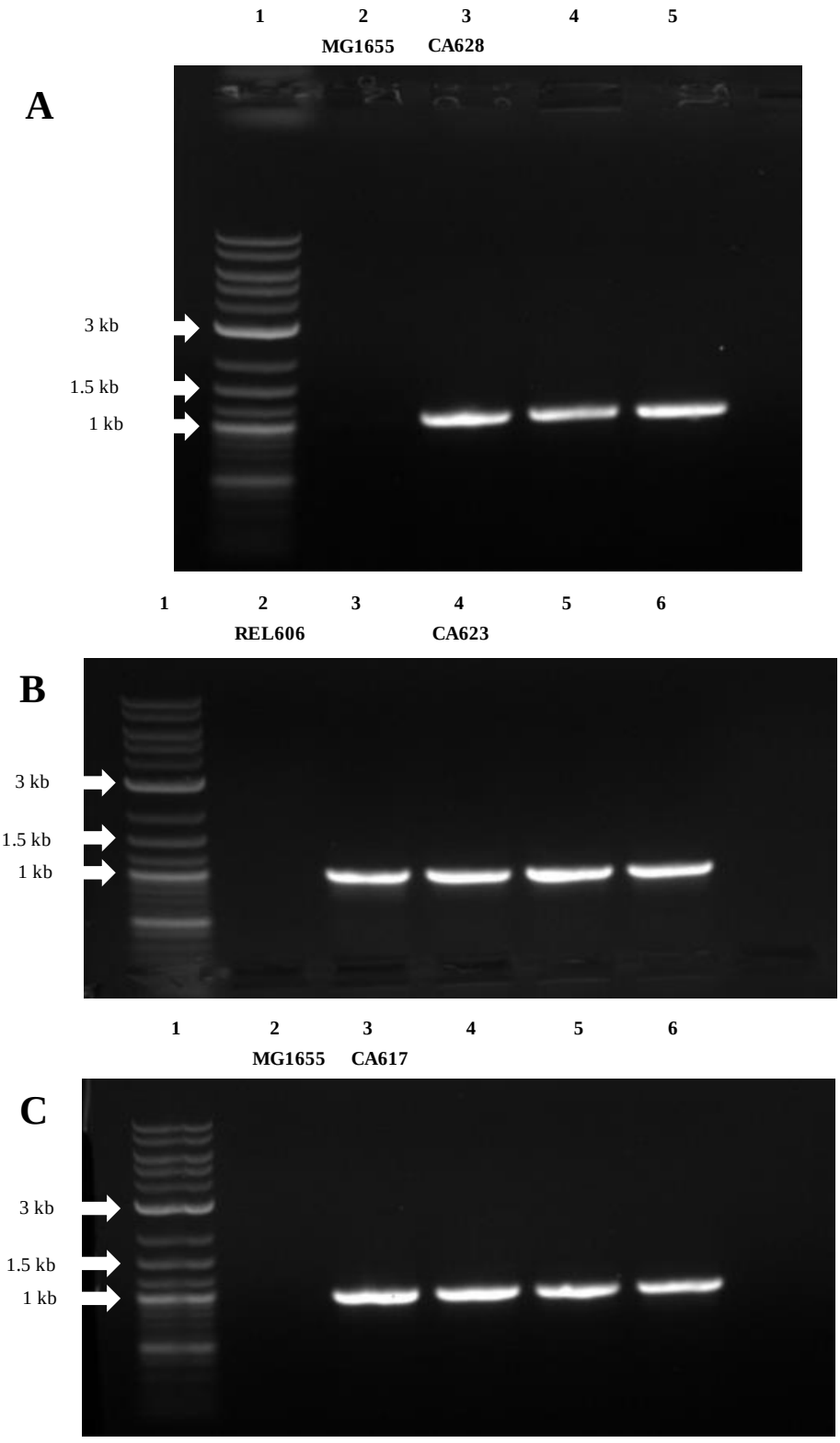

Figure 3-2: Gel image of MG1655 Δ*dinB* (A), REL606 Δ*polB* (B) and MG1655 Δ*polB* (C) with *cat* gene from pKD3 mutants using insertion-specific primers.
No band will be visible if *cat* gene has not replaced *dinB* or *polB* gene. Lane 1 is a 1 kb Plus DNA ladder. Lane 2 is a control of MG1655 WT or REL606 WT. Lanes 3-6 (or lanes 3-5 for (A)) represent mutants in which a SIM gene within each strain has been substituted with the *cat* gene from pKD3.

3.1.2 Removal of *cat* gene in single mutants

After confirming the insertion of the FRT-flanked chloramphenicol resistance gene (*cat* gene) in place of the *dinB* and *polB* genes, my next goal was to remove the *cat* gene. With temperature-sensitive replication, an ampicillin-resistant FLP plasmid, pCP20, was used to remove the *cat* gene (Datsenko & Wanner, 2000). Removing the *cat* gene leaves behind an 82- to 85-nt scar in its place (Datsenko & Wanner, 2000). Mutants were selected based on their simultaneous loss of resistance to chloramphenicol and ampicillin, as described in section 2.7. PCR verifications of selected mutants involved the use of locus-specific primers. The expected band size for mutants that have successfully removed the *cat* gene is approximately ~500 bp. Controls for wild-types and single mutants with the *cat* gene without pCP20 transformation were used to compare band sizes. Results show that all mutants transformed with pCP20 have the expected band size (Figure 3-3). Thus, these mutants have the correct structures with no resistance genes representing MG1655 Δ*dinB*, MG1655 Δ*polB*, and REL606 Δ*polB* single mutants. Band sizes of strains CA646 (REL606 Δ*polB*) and CA652 (MG1655 Δ*dinB*) were stored as glycerol stocks and used for further experiments (Figure 3-3).

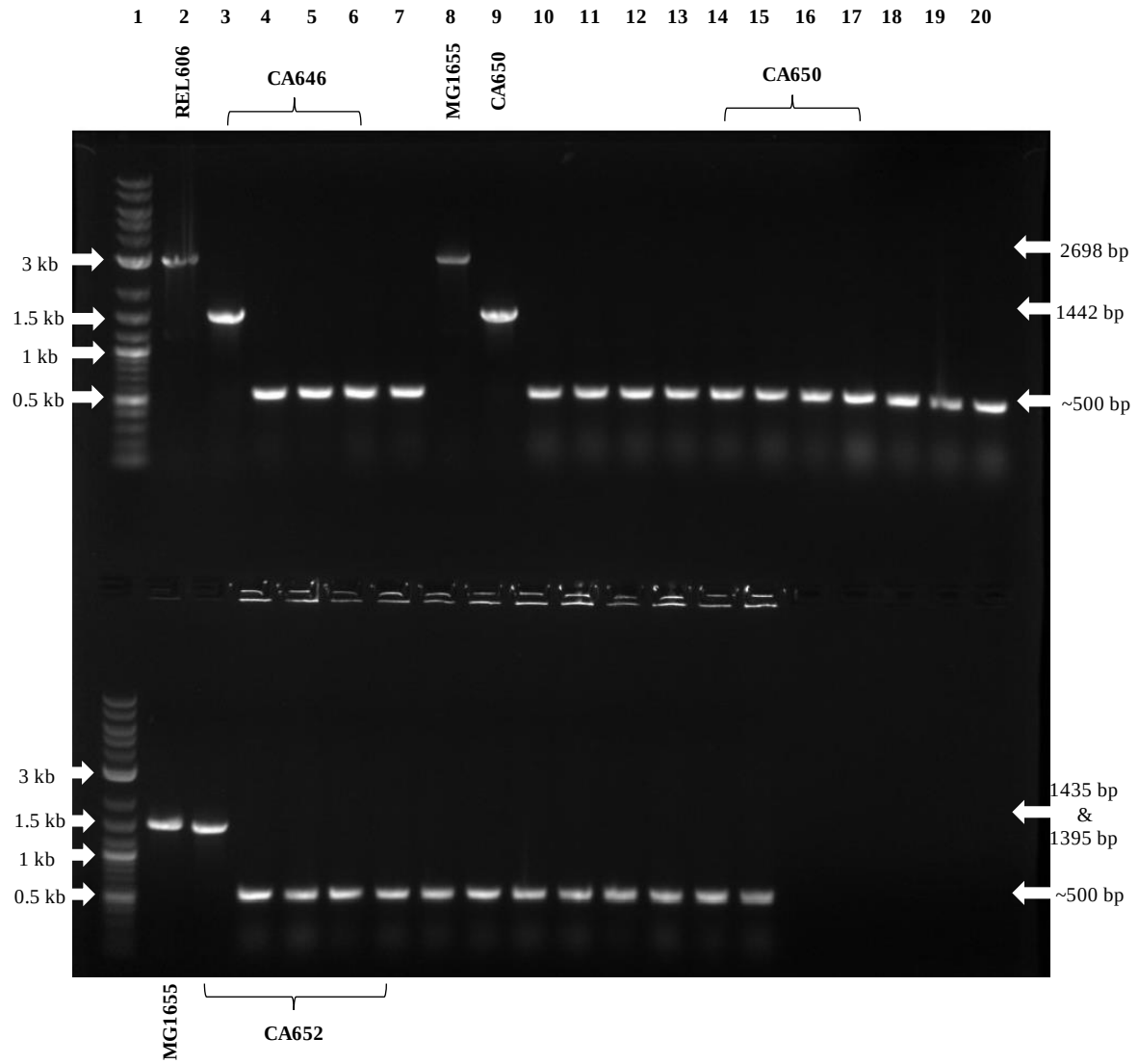

Figure 3-3: Gel image of single mutants with pCP20 to remove *cat* gene. Locus-specific primers were used. Band sizes are expected to be ~500 bp if the removal of *cat* gene (1016 bp) is achieved. **Top:** Lane 1 is a 1 kb Plus DNA ladder. Lane 2 is REL606 WT, lane 3 is a single mutant without pCP20, lanes 4-7 are REL606 Δ*polB* mutants with pCP20. Lane 8 is MG1655 WT, lane 9 is a MG1655 Δ*polB* mutant without pCP20, lanes 10-20 are MG1655 Δ*polB* mutants with pCP20. **Bottom:** Lane 1 is a 1 kb Plus DNA ladder. Lane 2 is MG1655 WT, lane 3 is a MG1655 Δ*dinB* mutant without pCP20, lanes 4-15 are MG1655 Δ*dinB* mutants with pCP20.

3.1.3 Insertion and removal of *cat* gene in place of *dinB* or *polB* genes

Now that single mutants with no resistance have been achieved for *polB* and *dinB*, my next goal was to produce mutants that have lost two error-prone polymerase genes. Double mutants were achieved by reintroducing the pORTMAGE-2 red helper plasmid into the single mutants and replacing a second gene of interest with the FRT-flanked *cat* gene inserted in its place. PCR verification of transformants was conducted to determine if all the mutants had replaced a second error-prone polymerase with the chloramphenicol resistance cassette. PCR verification again involved the use of two different primer pairs: 1) locus-specific primers and 2) insertion-specific primers. Full details on the conditions of the PCR reactions can be found in Tables 2-3 and 2-7.

The expected band sizes are the same as in section 3.1.1. The calculations of band sizes can be found in section 2.3 and Figure 2-1. My results indicate that the band sizes for the original allele and gene replacements of *dinB* and *polB* with the *cat* gene are approximately as expected (Figure 3-4). Therefore, it can be concluded that these mutants possess the appropriate structures, indicating that the *cat* gene from pKD3 has replaced the gene of interest. However, the results from the experiment show no bands present for MG1655 Δ*polB* and a few lanes of MG1655 Δ*dinB*. This lack of bands indicates that mutants do not have the correct structure and have not replaced the gene of interest with the *cat* gene. When undergoing replacement of Δ*dinB* by the *cat* gene in REL606 Δ*polB* and MG1655 Δ*polB* single mutants, only insertion-specific primers were used due to locus-specific primers not being specific enough to detect if the replacement had taken place correctly. Band sizes of strains CA664 (REL606 Δ*polB* + Δ*dinB*, Cm^R from pKD3) and CA667 (MG1655 Δ*dinB* + Δ*polB*, Cm^R from pKD3) that were kept stored as glycerol stocks and used for further experiments (Figure 3-4).

I removed the *cat* gene from double mutant strains using the approach described in section 3.1.2 (Figure 3-5). Notably, the mutants transformed with pCP20 showed an anticipated band size of approximately ~500 bp, indicating they had the correct structures with no resistance genes. Thus, the resulting double mutants were REL606 Δ*dinB* Δ*polB* (CA674) and MG1655 Δ*dinB* Δ*polB* (CA680), which were kept stored as glycerol stocks and used for further experiments.

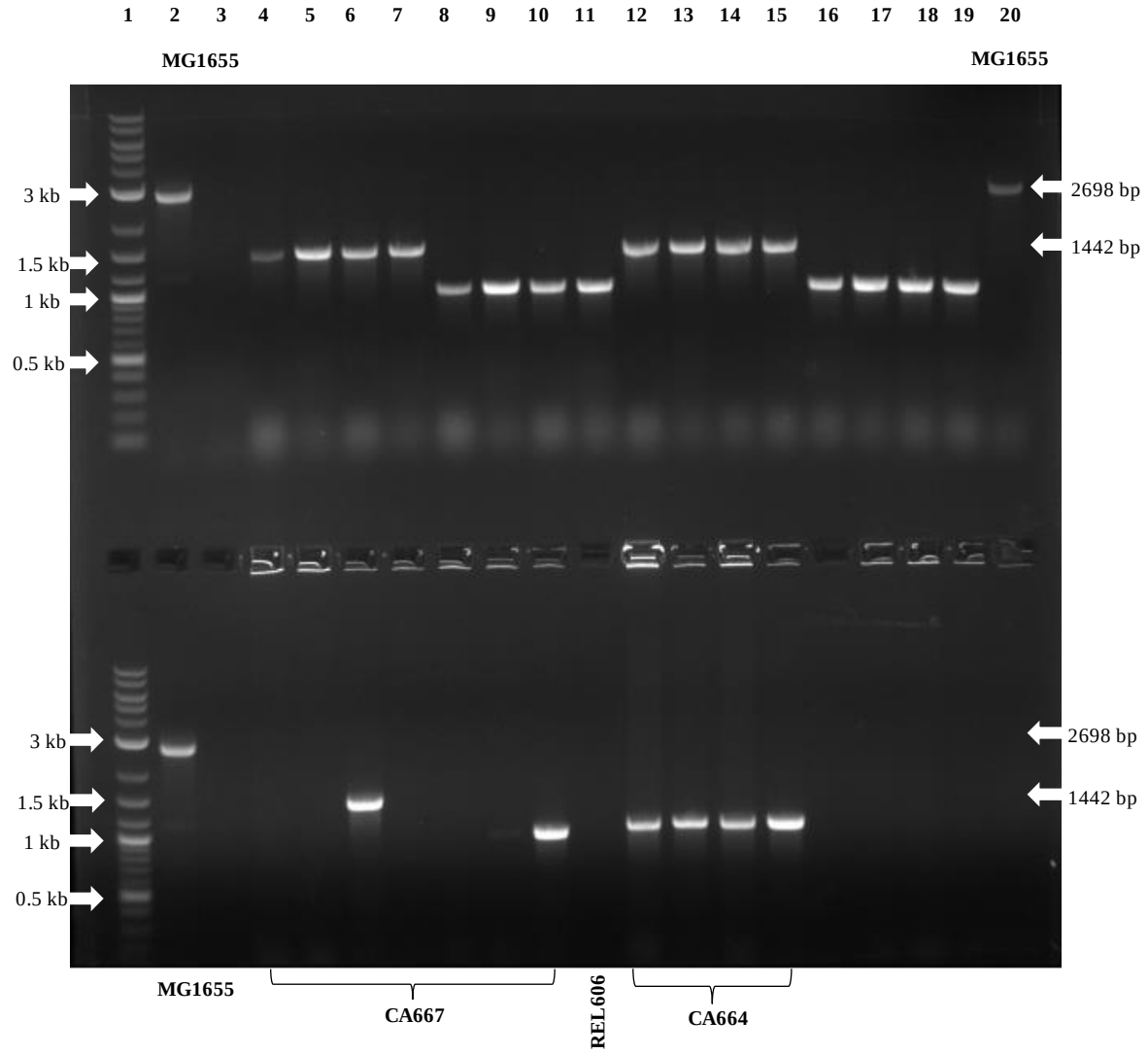

Figure 3-4: Gel image of double mutants with the *cat* gene from pKD3. Locus-specific primers (primer 1) and insertion-specific primers (primer 2) were used to test for the replacement of the *dinB* and *polB* genes by the *cat* gene. If the replacement occurred, primer 1 would show a band size difference from 2698 bp (original allele) to 1442 bp (insertion allele) for *polB*, and primer 2 would have no visible band if the *cat* gene did not replace the *dinB* or *polB* genes. Lane 1 in both panels is a 1 kb Plus DNA ladder, while lanes 2 and 3 show MG1655 WT with primer 1 and primer 2, respectively. **Top:** Lanes 4-20 test for mutants with a second deletion (Δ*polB*) replaced with the *cat* gene. **Bottom:** Only lanes 6 and 10 have the expected band sizes for a double mutant with a second deletion (Δ*polB*) replaced by the *cat* gene. Lanes 11 and 16 are REL606 WT and MG1655 WT, respectively, while lanes 12-15 and 17-20 test for mutants with a second deletion (Δ*dinB*) with the replaced by the *cat* gene.

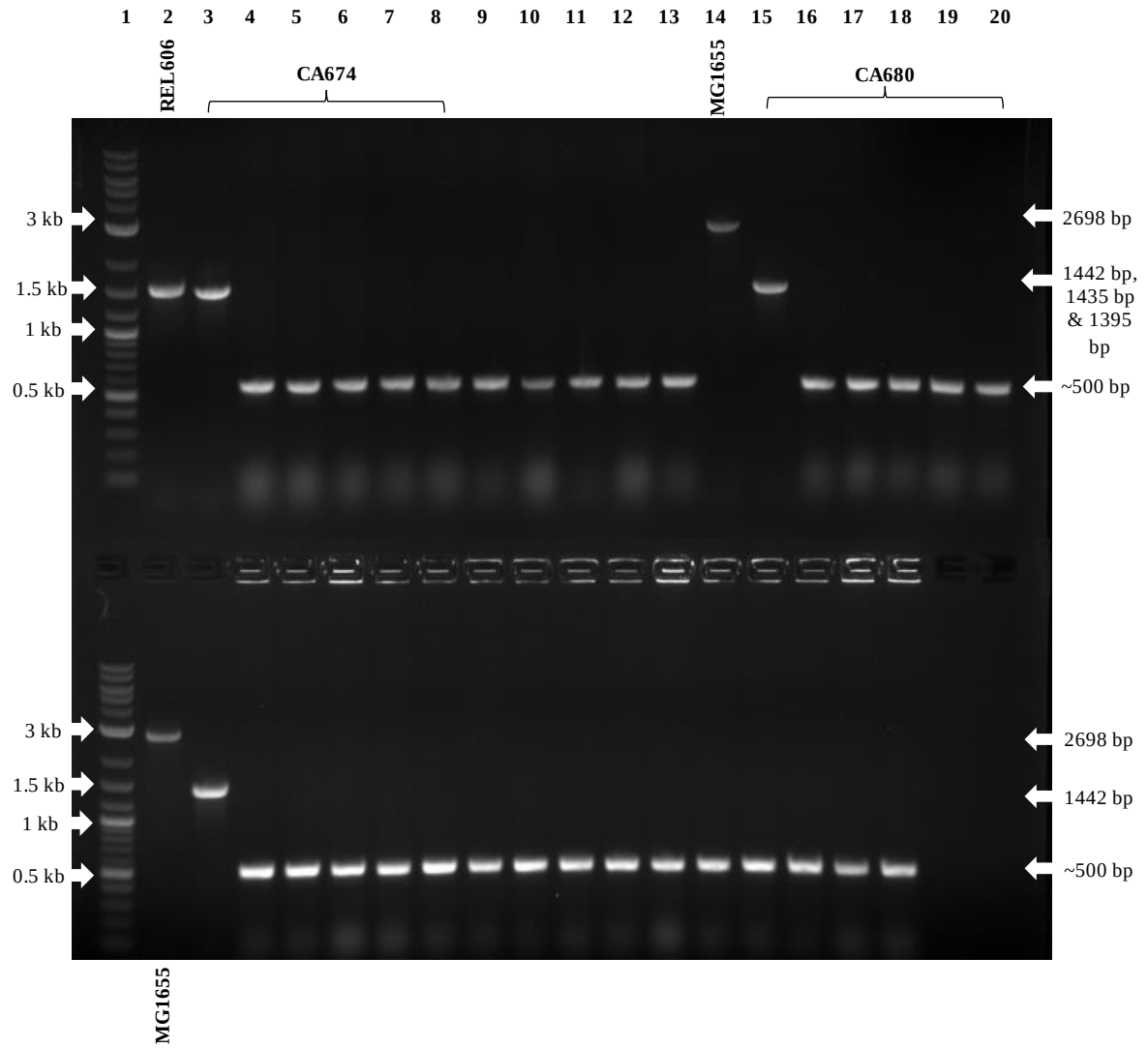

Figure 3-5: Gel image of double mutants with pCP20 to remove *cat* gene.
Band sizes are expected to be ~500 bp if the removal of *cat* gene (1016 bp) is achieved. Locus-specific primers were used. **Top:** Lane 1 is a 1 kb Plus DNA ladder. Lane 2 is REL606 WT, lane 3 is a REL606 double mutant without pCP20. Lanes 4-13 are REL606 double mutants with pCP20. Lane 14 is MG1655 WT, lane 15 is a MG1655 double mutant without pCP20. Lanes 16-20 MG1655 double mutants with pCP20. **Bottom:** Lane 1 is a 1 kb Plus DNA ladder. Lane 2 is MG1655 WT, lane 3 is a MG1655 double mutant without pCP20, lanes 4-18 are MG1655 double mutants with pCP20.

3.2 DNA sequencing

Genome sequencing was conducted to verify the successful removal of target genes from the SIM$^-$ strains, the accurate placement of reporter-GFP fusions in the reporter strains, and as a precaution against potential off-target effects or unintended mutations acquired during the transformation procedures. Macrogen conducted the sequencing of samples using primers binding ~200bp away from target genes for the SIM$^-$ strains, as detailed in section 2.9 (Table 2-3). The sequencing results of single and double mutant strains confirmed the findings from gel images (Figures 3-3 and 3-5). CA646 (REL606 Δ*polB*), CA652 (MG1655 Δ*dinB*), CA674 (REL606 Δ*dinB* Δ*polB*), and CA680 (MG1655 Δ*dinB* Δ*polB*), showed clean deletions of target genes (Appendix 2).

To check that the correct reporter-GFP fusions were being used, plasmid preps of transformed cells were sent to Macrogen for sequencing with the primer pUA66_F (Table 2-3). pUAGG_F was used to check if the region of the pUA66 reporter plasmid corresponding to the inserted promoter maps to the correct promoter in the *E. coli* genome (e.g., P*sulA,* P*yiaG* and P*bolA*). BLAST was run on sequences for the reporter-GFP fusions to check the region of the pUA66 reporter plasmid corresponding to the inserted promoter maps to the promoter it should in the REL606 and MG1655 genomes (P*sulA*, P*bolA*, P*yiaG*) as well as mapping to *gfp* gene sequences (Zhang et al., 2000). Two matches returned for each top alignment when running BLAST, specifically in *E. coli* genomes. These matches equated to *sulA* gene sequences, *bolA* gene sequences, *yiaG* gene sequences and *gfp* gene sequences for strains CA640, CA641, CA643 and CA645. In comparison, CA644 has only *yiaG* gene sequences that have aligned. CA642 did not align with any gene of interest.

3.3 SOS reporter assay

Two tests were done to determine the environmental challenge most suitable for inducing the SOS response. The goal was to identify a concentration of inducer that induces the SOS response but has little effect on the population growth rate, which might select mutants that are resistant to the inducer and, therefore, have a reduced SOS response. The study involved growing cell populations in environments with varying concentrations of mitomycin C (MMC) or nalidixic acid (Nal) to determine their effects on SOS expression and growth rate.

3.3.1 Flow cytometry

Preliminary results from a comprehensive series of experiments conducted to establish the optimal concentration range for SOS-inducing stressors MMC and Nal are presented in Appendix 3. An extensive range of concentrations (µg/mL) was initially selected for SOS reporter flow cytometry that was subsequently reduced (Appendix 3; Figure 8-1). However, the fluorescence intensity for the relative cell numbers of each combination was too high to distinguish small subpopulations of cells exhibiting SOS induction. The impact of slow-growth conditions on the proportion of cells exhibiting high SOS induction was investigated in an SOS reporter assay with lower concentrations of inducers (ng/ml). Still, little difference was observed between glucose and glycerol-supplemented media (Appendix 3; Figure 8-2). However, from these lower concentrations of inducer being used, subpopulations exhibiting SOS induction were displayed. The highest proportion of subpopulations is shown by the small group of cell populations that have a higher fluorescence intensity relative to the main peak of cell populations. Fluorescence intensity of GFP increases along the x-axis from left to right. Therefore, cell populations to the left show lower fluorescence intensities than populations on the right. Fluorescence intensity is indicative of the number of cells expressing GFP. As specifically shown in the REL606-MMC-glucose combination, concentrations of 0.5, 0.65 and 0.8 ng/mL had the highest proportion of subpopulations exhibiting SOS induction, shown by the high fluorescence intensity (GFP-H) signal to the right of the main peak.

The final SOS reporter assay, which aimed to optimize the inducer concentration that balances SOS induction with minimal impact on the population growth rate, was analysed

through parallel flow cytometry and growth curve assays (Figures 3-6 and 3-7). These assays were conducted to compare the efficacy of the SOS response induction and its impact on the growth rate. Flow cytometry analysis was performed using histograms to assess the effect of MMC and Nal inducer concentrations (0.65 ng/mL, 0.725 ng/mL, and 0.8 ng/mL) on SOS induction. In flow cytometry, an increase in induction levels of the SOS response is reflected by an increase in GFP expression since the *gfp* gene is fused to the SOS-inducible *sulA* promoter. The results from the density plot did not show any significant difference in estimated SOS induction among the different concentrations of inducers (Figure 3-6). However, a second peak towards higher GFP expression in the MMC stressor environment indicates a strong induction of the SOS response. In contrast, the Nal environment showed no sign of SOS induction relative to the control treatment.

The mean GFP expression levels were analysed using a mixed distribution model to identify the SOS-on subpopulations based on the highest mean GFP expression level within an overall population. When analysing flow cytometry data, mixed distribution models are a tool for distinguishing various cell types within a larger cell population (Chan et al., 2008). The MMC-induced strains had significantly higher mean GFP expression levels than the Nal-induced strains (Figure 3-7), indicating a more potent induction of the SOS response in the MMC-induced strains. The concentrations 0.65 ng/mL, 0.725 ng/mL, and 0.8 ng/mL of MMC were found to be equally effective in inducing the SOS response in the studied strains, with only a slight difference in mean GFP expression level for the 0.725 ng/mL concentration. These results suggest that combining the density and mean GFP plots can help determine the inducer concentration that best balances SOS-induction and population growth rate. They were compared to the growth curve assay to confirm the significance of the flow cytometer results.

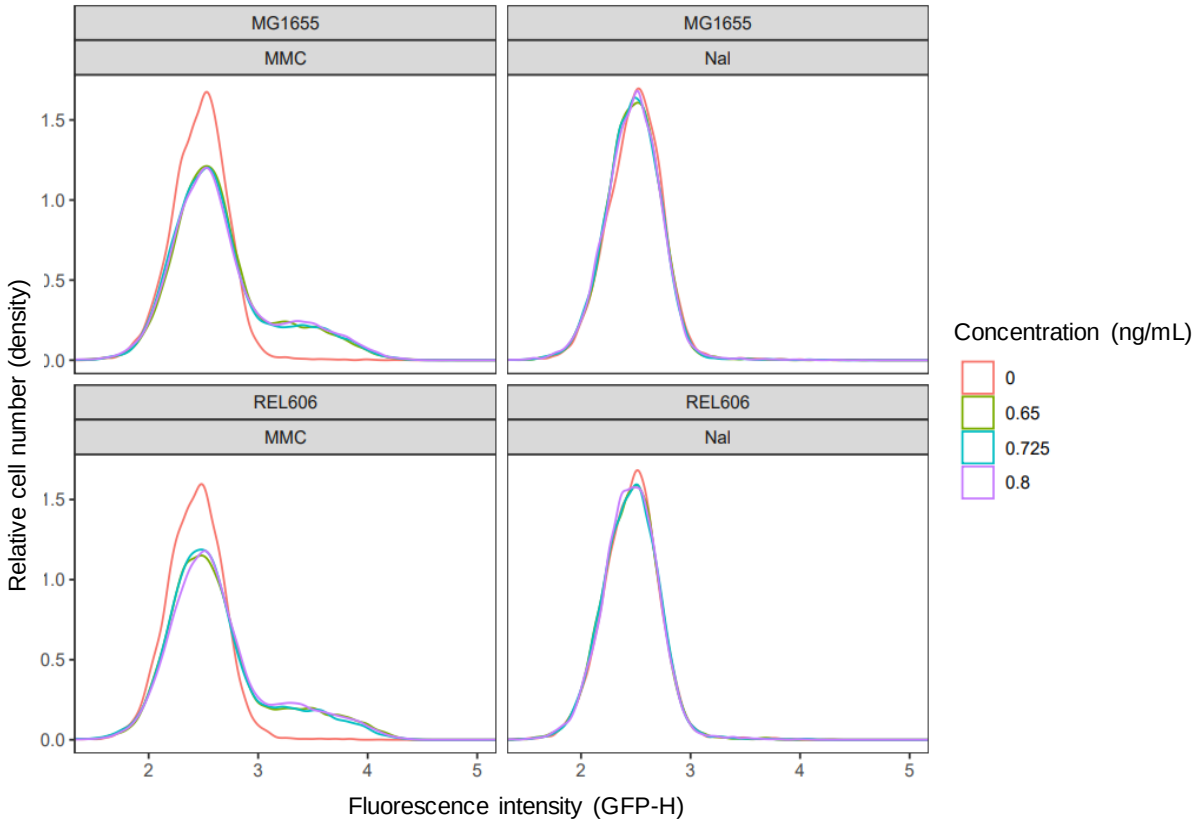

Figure 3-6: Density plots summarizing the effect of mitomycin C (MMC) and nalidixic acid (Nal) inducer concentrations on SOS induction.
Each histogram represents six replicates for each combination of strain and stressor concentration. Concentrations of 0.65, 0.725 and 0.8 ng/mL MMC all showed SOS induction.

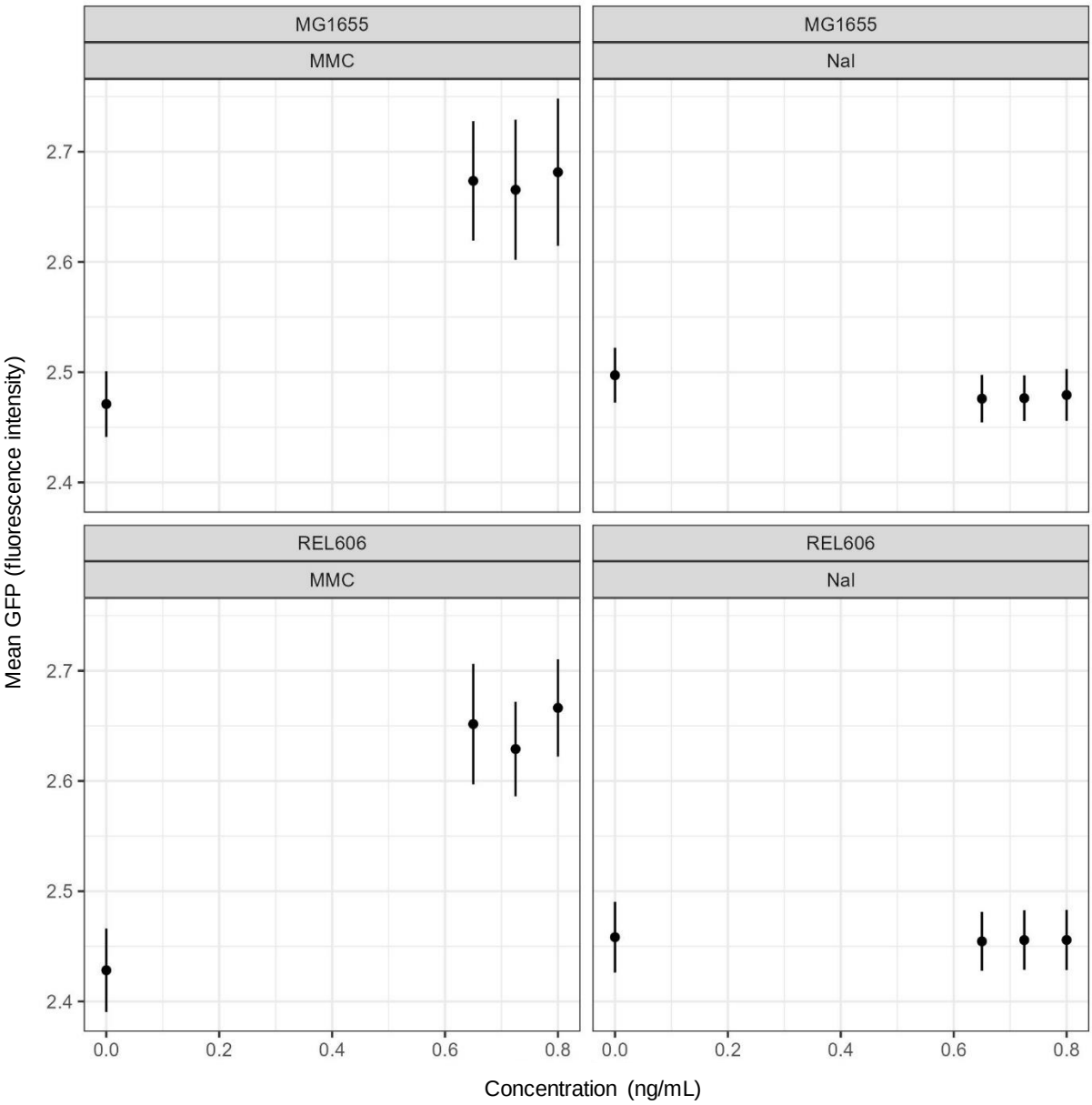

Figure 3-7: Mean GFP plot of the final range of mitomycin C (MMC) and nalidixic acid (Nal) concentrations.
Each symbol indicates six replicates for each combination of strain and stressor concentration. Error bars represent 95% confidence intervals for each mean GFP data point.

3.3.2 Growth curves

To identify a stressor that can induce the SOS response without affecting the growth rate of the wild-type strains (REL606 and MG1655), a growth curve assay was conducted using concentrations of 0.65 ng/mL and 0.725 ng/mL MMC and Nal. The results were analysed using Curveball (Ram et al., 2019) (Figures 3-8 and 3-9). Using solely the information derived from a growth curve experiment, Curveball provides the capability to predict microbial growth (Ram et al., 2019). Models are fitted by comparing Bayesian information criteria (BIC) scores and selecting the one with the smallest BIC value. BIC balances model fit and complexity, making it a common method to assess model fit quality (Ram et al., 2019). Based on the growth curve, no strain-inducer combination significantly affected the growth rate compared to the control group with no inducer (Figures 3-8, 3-9).

Two-sample *t*-tests were performed for each strain-inducer combination to test if a given SOS inducer significantly affects growth rate. Growth of REL606 in environments supplemented with Nal at 0.65 or 0.725 ng/mL did not affect the growth rate. Likewise, growth in the same concentrations of MMC did not affect growth rates (control vs. 0.65 ng/mL, $t_{10} = 0.145$, $P > 0.05$; control vs. 0.725 ng/mL, $t_{10} = 0.260$, $P > 0.05$). Growth of MG1655 in environments supplemented with Nal at 0.65 or 0.725 ng/mL did not affect the growth rate (control vs. 0.65 ng/mL, $t_{10} = 0.437$, $P > 0.05$; control vs. 0.725 ng/mL, $t_{10} = -0.672$, $P > 0.05$). Likewise, growth in the same concentrations of MMC did not affect growth rates (control vs. 0.65 ng/mL, $t_{10} = 1.272$, $P > 0.05$; control vs. 0.725 ng/mL, $t_{10} = -1.306$, $P > 0.05$). A significant difference in growth rate between the two strains in the MMC treatment was displayed, with REL606 exhibiting a substantially higher growth rate in all MMC inducer concentrations than MG1655, as evidenced by the non-overlapping confidence intervals (Figure 3-9).

By integrating flow cytometry and growth curve assays, I determined the optimal concentration for inducing the SOS response to be 0.65 ng/mL. This concentration provided a robust response while allowing average cell growth. Moreover, I identified MMC as the most suitable option for long-term evolution experiments since it could induce the SOS response at all tested concentrations without compromising the growth rate. Narrowing down the concentration range and conducting parallel assays was crucial for me to identify the optimal concentration for subsequent experiments.

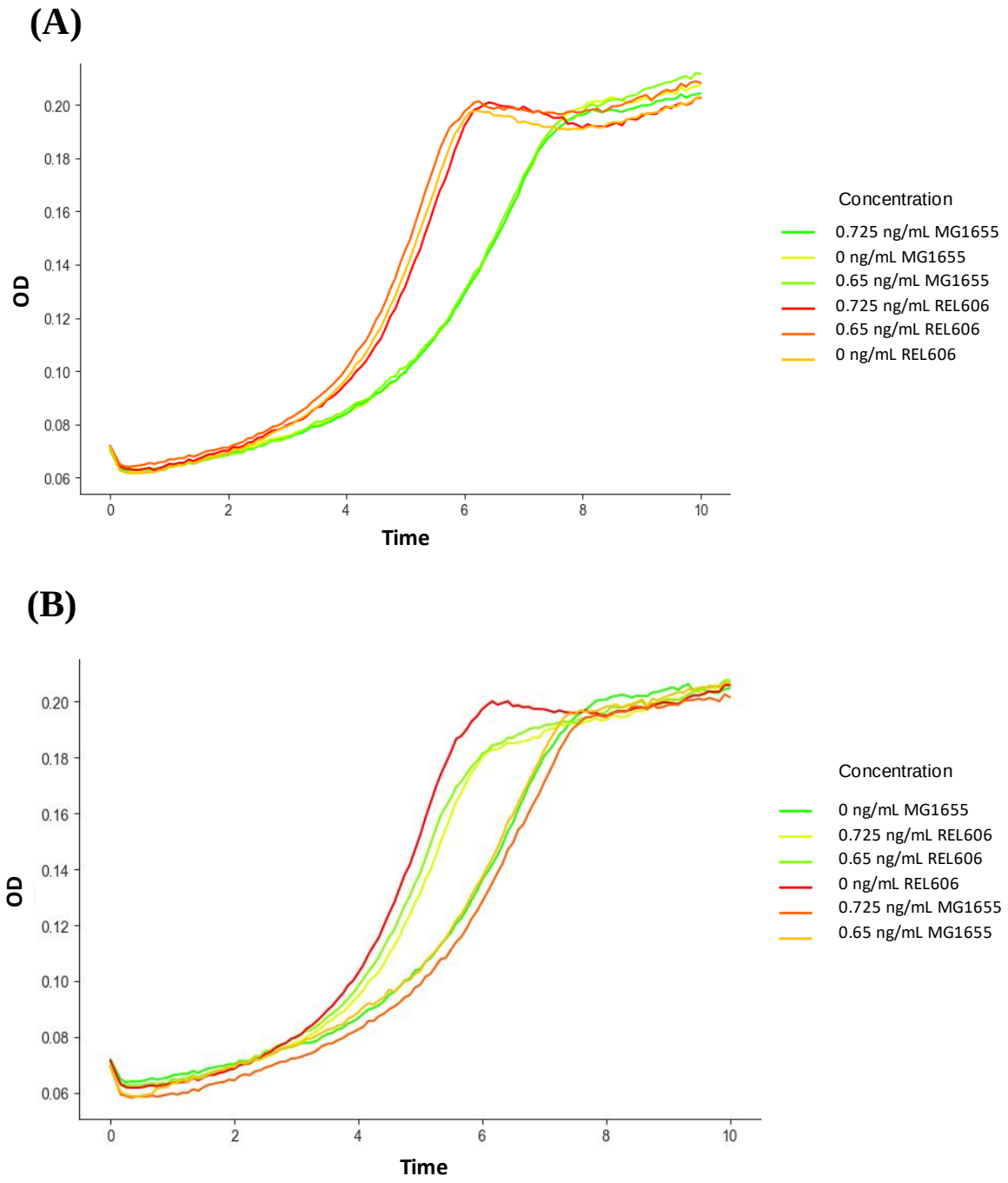

Figure 3-8: Growth curve of SOS reporter assay.
(A) is growth curve of SOS reporter assay with mitomycin C; (B) is growth curve of SOS reporter assay with nalidixic acid. Each growth curve represents six replicates for each combination of strain and stressor concentration.

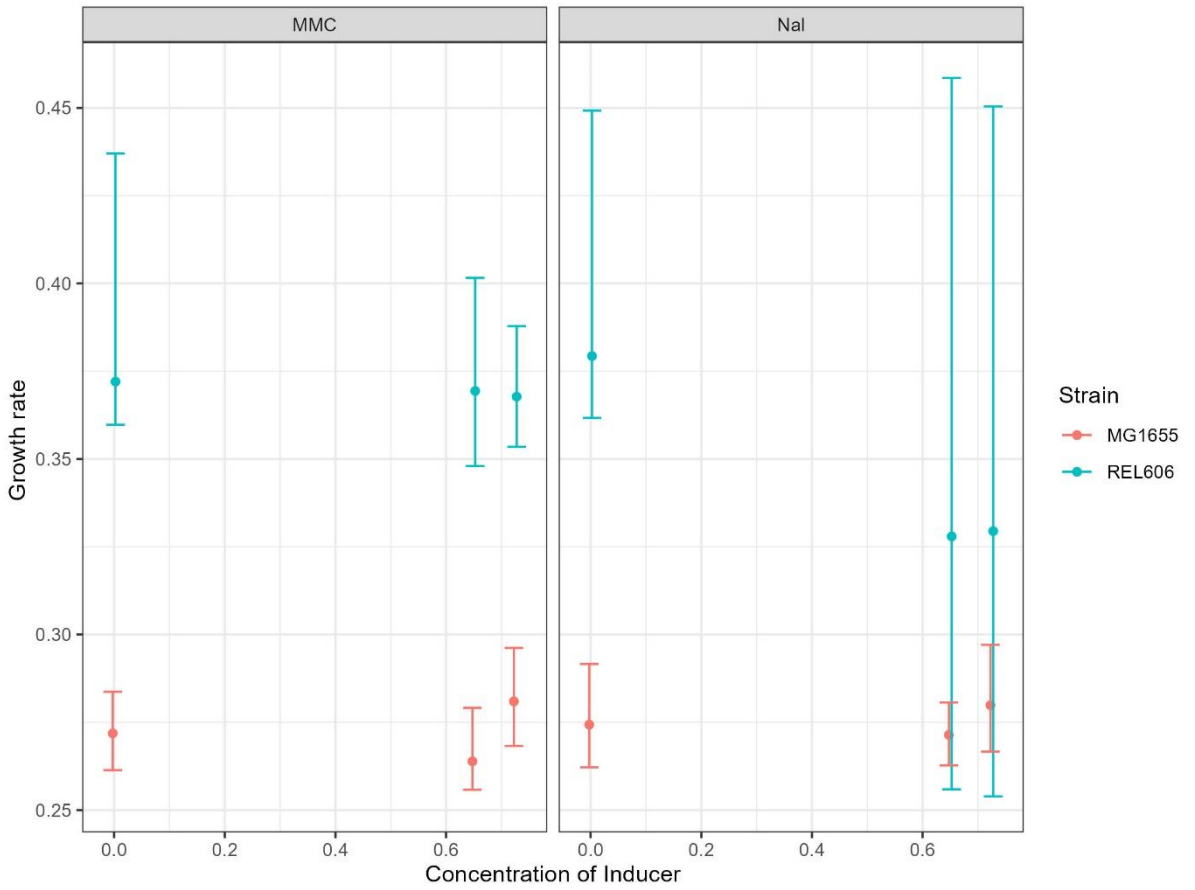

Figure 3-9: Estimated growth rate of mitomycin C (MMC) and nalidixic acid (Nal) induced reporter strains.
Each symbol indicates six replicates for each combination of strain and stressor concentration (ng/mL). Error bars represent 95% confidence intervals. Units for concentrations are ng/mL.

3.4 RpoS reporter assay

In this study, a RpoS reporter assay was utilized to investigate the inducibility of the RpoS response under starvation conditions and whether the timing of the induction would affect the expression of the RpoS response. Two distinct RpoS reporters, *bolA*-GFP and *yiaG*-GFP, were first validated by sequencing to ensure their integrity before being used, section 3.2. The fluorescence intensity of the samples, categorized based on strain-reporter combinations and time intervals, was quantified using histogram plots from flow cytometry analysis. Based on previous experiments and expert advice from the laboratory (pers. comm. T. Cooper), it was hypothesized that a two-day transfer cycle would be optimal to induce the RpoS response. The results demonstrated negligible differences in GFP expression levels across various time intervals for each strain-reporter combination (12, 24, 48, and 72 hours) (Figure 3-10). Nonetheless, noticeable differences in GFP expression were observed between the distinct strain-reporter combinations, further emphasizing the importance of accurately controlling for environmental factors when analysing experimental results. Since the results did not reveal a discernible difference in optimal transfer cycles, with all cycles proving equally effective across three separate instances the experiment was conducted, a consistent two-day transfer cycle was chosen for implementation in both long-term evolution experiments and fluctuation tests.

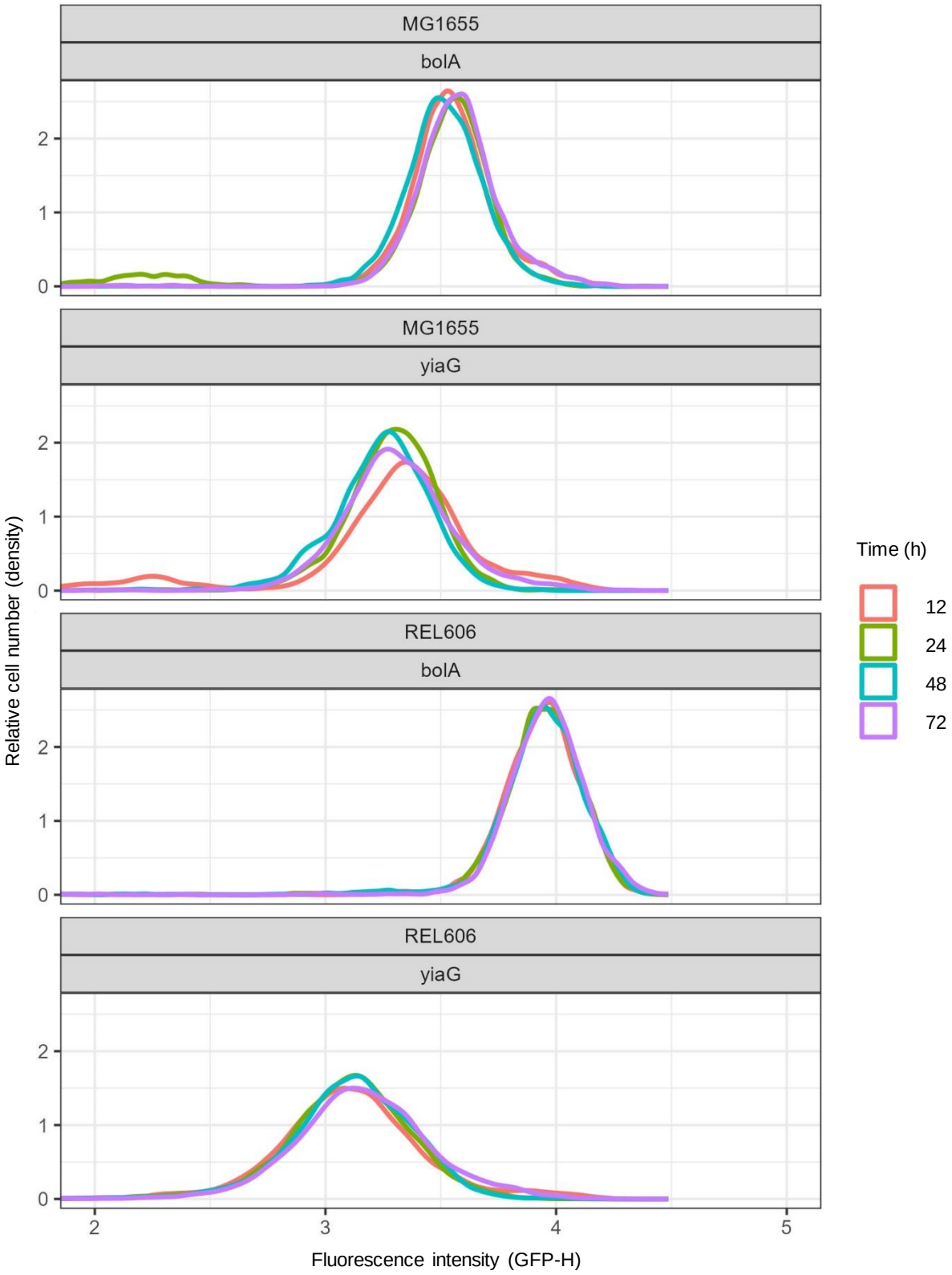

Figure 3-10: Density plots summarizing the effect of time on RpoS induction. Goal was to find optimal environment to induce RpoS response. Each histogram represents five replicates for each treatment and strain combination.

3.5 Effect of SIM and SOS on mutation rate

I performed fluctuation tests to determine the combined effect of deletion of error-prone polymerase and the presence of SOS inducers on mutation rate. In particular, my investigation aimed to validate the hypothesis that the presence of SIM genes in strains undergoing SOS induction would result in a higher mutation rate compared to strains lacking *dinB* and *polB* genes or strains that were not induced to express the SOS response. To evaluate this hypothesis, I estimated mutation rates in replicate populations comprising four experimental treatments: the presence and absence of MMC, a specific SOS inducer, and the presence and absence of SIM. I used 12 replicate populations to estimate the mutation rate to rifampicin resistance per cell per generation in each strain and environment combination. From here on, I use SIM^- to refer to double mutant (Δ*dinB* and Δ*polB*) strains and SIM^+ to refer to wild-type strains. I will use MMC to refer to the induction of the SOS response by MMC and no-inducer (NI) to refer to the absence of MMC and SOS induction.

I found that both MMC and SIM are mutagenic. In REL606 and MG1655, the presence of both SIM and MMC increased mutation rates 4.4- and 4-fold relative to the absence of both (Figure 3-11 and Appendix 4; REL606 SIM^+MMC^+ vs SIM^-MMC^-, $t_{22} = 4.51$, $P < 0.001$; MG1655 SIM^+MMC^+ vs SIM^-MMC^-, $t_{22} = 4.57$, $P < 0.001$, respectively).

I expected MMC induction of the SOS response and the SIM system to interact to cause higher mutation rates than expected by either individual factor. I discovered that the presence of MMC increased mutation rates 2.3- and 2.2-fold relative to the absence of MMC in SIM^+ strains, while SIM^- strains increased mutation rates 3.3- and 2.4-fold relative to the absence of MMC (Figure 3-11 and Appendix 4; REL606 SIM^+MMC^+ vs SIM^+MMC^-, $t_{22} = 3.13$, $P < 0.005$; MG1655 SIM^+MMC^+ vs SIM^+MMC^-, $t_{22} = 3.11$, $P < 0.01$; REL606 SIM^-MMC^+ vs SIM^-MMC^-, $t_{22} = 3.52$, $P < 0.002$; MG1655 SIM^-MMC^+ vs SIM^-MMC^-, $t_{22} = 2.74$, $P < 0.02$, respectively). While the presence of SIM increased mutation rates by 1.3- and 1.7-fold relative to the absence of SIM in stressed environments, while unstressed environments increased mutation rates by 1.89- and 1.82-fold relative to the absence of SIM (Figure 3-11 and Appendix 4; REL606 SIM^+MMC^+ vs SIM^-MMC^+, $t_{22} = 1.15$, $P > 0.05$; MG1655 SIM^+MMC^+ vs SIM^-MMC^+, $t_{22} = 2.12$, $P < 0.05$; REL606 SIM^+MMC^- vs SIM^-MMC^-, $t_{22} = 2.11$, $P < 0.05$; MG1655 SIM^+MMC^- vs SIM^-MMC^-, $t_{22} = 2.17$, $P < 0.05$, respectively). The estimated interaction effect is relatively small and judged by the overlap of confidence

intervals, not statistically significant relative to the individual mutagenic effects of MMC and SIM (Figure 3-11).

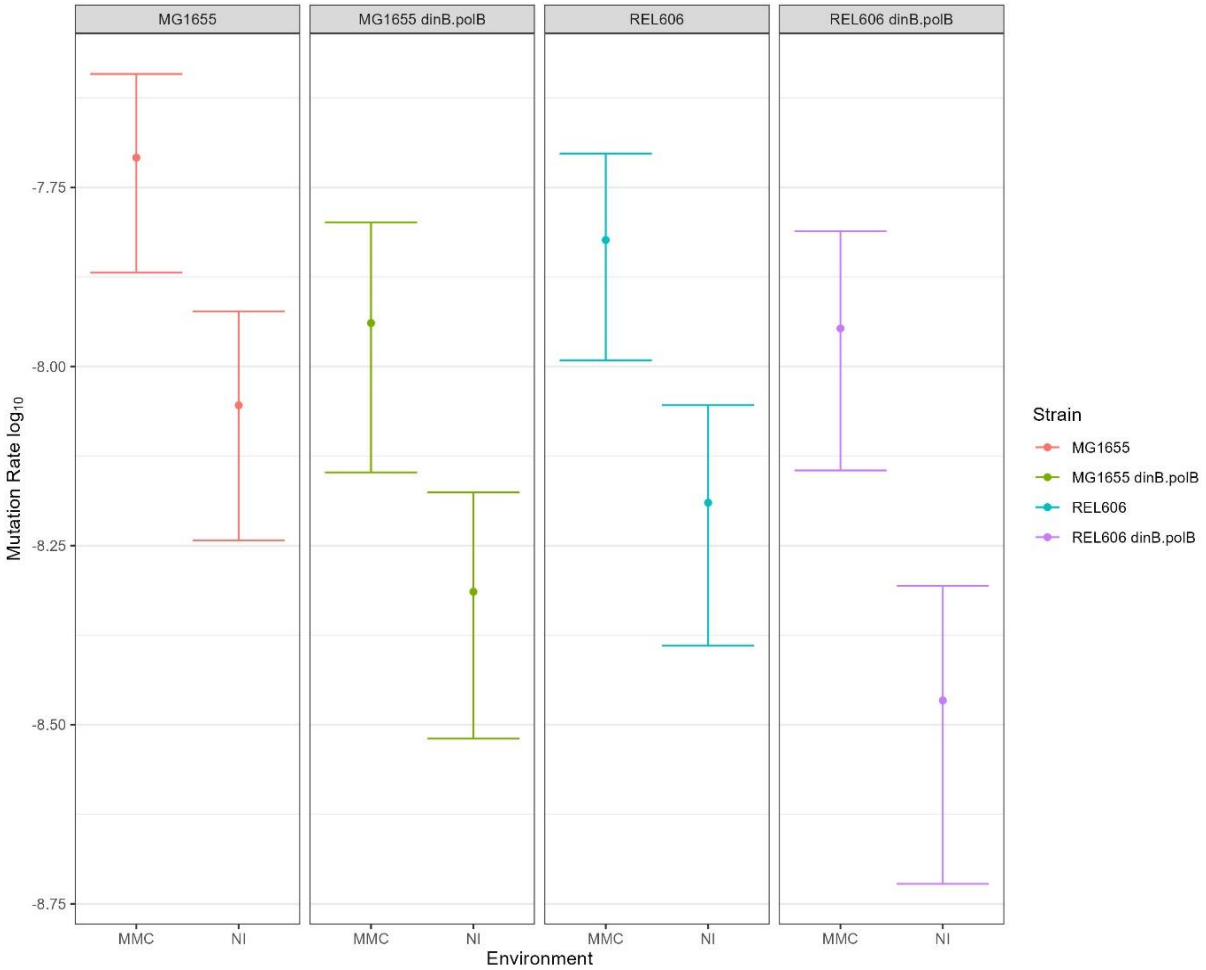

Figure 3-11: Log_{10} transformed mutation rate of SIM^- and SIM^+ strains with and without mitomycin C (MMC).
Symbols indicate mean mutation rates calculated using fluctuation tests comprising 12 replicate populations for each strain-environment combination. REL606 dinB.polB indicates the SIM^- strains, while REL606 is indicative of SIM^+ strains. Error bars represent 95% confidence intervals.

3.6 Effect of SIM on SOS evolvability

To test if SIM and SOS combine to increase evolvability, I evolved 24 independent replicate populations for each of the REL606 and MG1655 background strains in each of the following conditions: SIM^+SOS^+, SIM^+SOS^-, SIM^-SOS^+, and SIM^-SOS^-. Together this represents a total of 192 populations. After 400 generations of selection, I carried out competition assays to estimate the fitness changes of evolved populations (Table 2-1; Figure 3-12). Unfortunately, a suitable reference strain was not identified for evolved populations started with MG1655, so these evolved populations were not considered further.

I found that populations selected in the MMC environment had higher fitness than those selected in the no-inducer (NI) environment, with the MMC-selected SIM^+ populations having the highest overall fitness (Figure 3-13). Fitness change depended on both MMC and the presence of SIM ($P = 0.043$; Appendix 4). The presence of both SIM and MMC increased fitness by 4.3% relative to the absence of SIM and MMC in evolved populations (SIM^+MMC^+ vs SIM^-MMC^-). Having both SIM and MMC present resulted in a 1.7% increase in fitness compared to having SIM present but MMC absent (SIM^+MMC^+ vs SIM^+MMC^-), and also resulted in a 1.7% increase in fitness compared to having MMC present but SIM absent (SIM^+MMC^+ vs SIM^-MMC^+) (Appendix 4; SIM^+MMC^+ vs SIM^+MMC^-, $P = 0.714$; SIM^+MMC^+ vs SIM^-MMC^+, $P = 0.727$).

I also tested the individual effects of SIM and MMC on evolvability. Environment and strain had marginally non-significant effects on fitness change (Appendix 4; MMC status: $F_{1,74} = 3.481$, $P = 0.066$; SIM status: $F_{1,74} = 3.932$, $P = 0.051$), respectively. The presence of MMC individually increased fitness by 1.7% in SIM^+ populations and 2.6% in SIM^- populations relative to environments without MMC (Figure 3-13). While SIM genes increased fitness by 1.7% in the presence of MMC and 2.6% in the absence of MMC, compared to populations with SIM genes. My results show that the combination of stress and error-prone polymerase has a significantly higher fitness change relative to their individual effect on fitness in evolved populations, highlighting the significance of their presence together in an evolutionary context.

Determining SIM and MMC's combined effects on evolved populations' fitness improvements could be challenging because the SIM^+ and SIM^- strains have different initial fitness levels. These varying fitness levels may independently impact subsequent changes in

fitness, regardless of any direct effect of SIM, which could confound the interpretation of results. In other words, any observed differences between the SIM^+ and SIM^- strains may be due in part to their differing initial fitness levels rather than solely due to the presence or absence of the SIM variable. The immediate relative fitness of SIM^+ and SIM^- in the ancestral strains used to start the evolution experiment was assessed by carrying out additional competitions. I found a significant immediate fitness effect of SIM and SIM^- populations in the ancestral competitions; $F_{1,38} = 85.640$, $P < 0.001$ (Appendix 4). The SIM^- strain, which lacks error-prone DNA polymerases, unexpectedly showed an increase in fitness of 13.3% and 15% relative to SIM^+ strains in ancestral populations measured in MMC and NI environments, respectively (Figure 3-14; Appendix 4).

It is important to note that while the overall fitness of the ancestral SIM^- populations is higher than that of the SIM^+ populations, the fitness of both evolved populations is lower than that of their respective ancestors (Figures 3-13 and 3-14). The evolved strains are estimated to be less fit than their ancestor, with a 13.7% and 16.3% decrease in fitness for SIM^- in MMC and NI environments, respectively, and a 12% and 13.7% decrease in fitness for SIM^+ in MMC and NI environments, respectively (Figure 3-13).

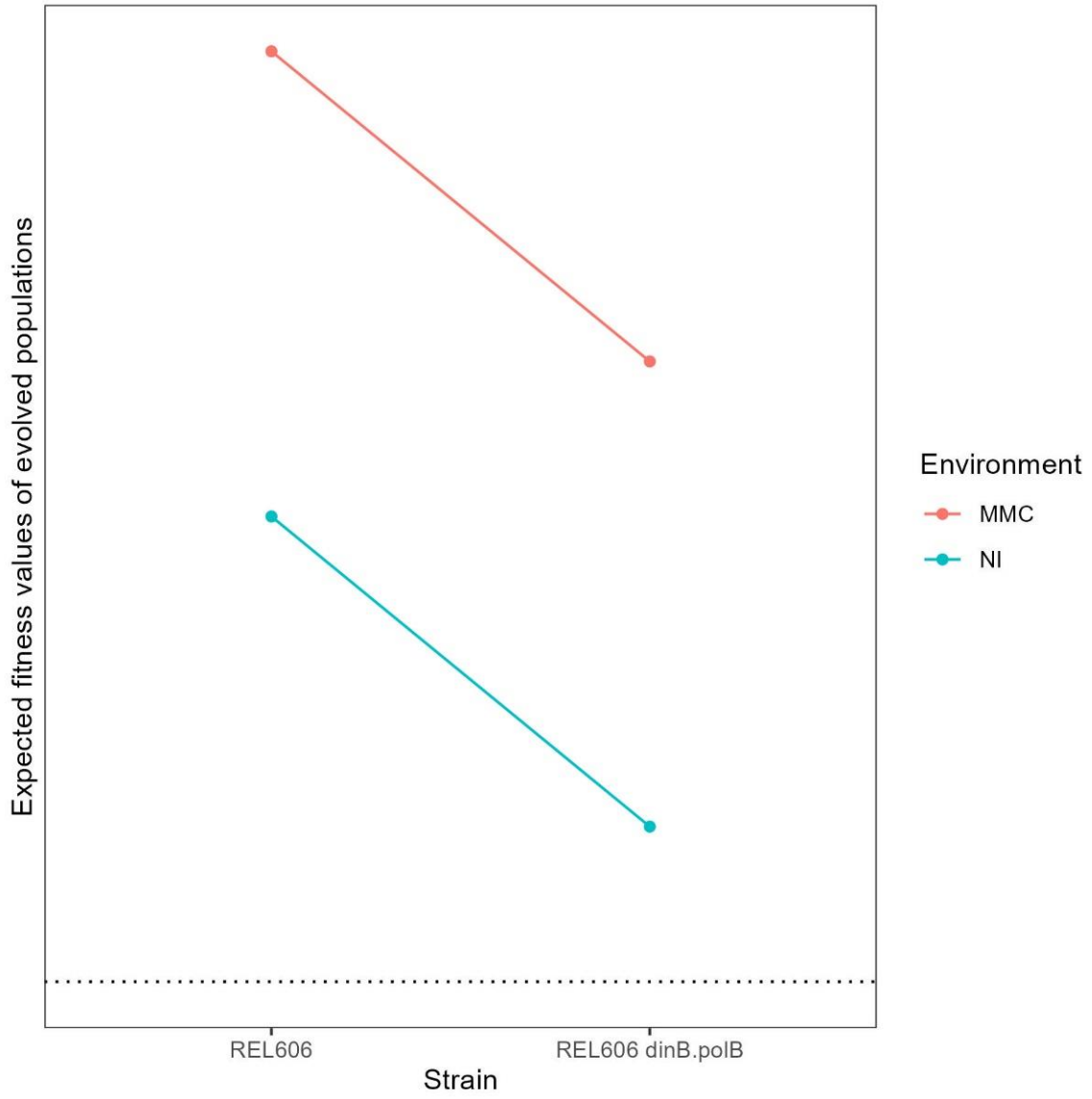

Figure 3-12: Schematic showing an expected fitness model of evolved and ancestral populations. Units are arbitrary.
Expect evolved populations to have higher fitness values than reference strain. Expect SIM^+ (REL606) strains to have higher fitness values than SIM^- (REL606 dinB.polB) for evolved and ancestral populations. Expect MMC selected evolved populations to have higher fitness than NI selected evolved populations. Dashed line represents reference strain.

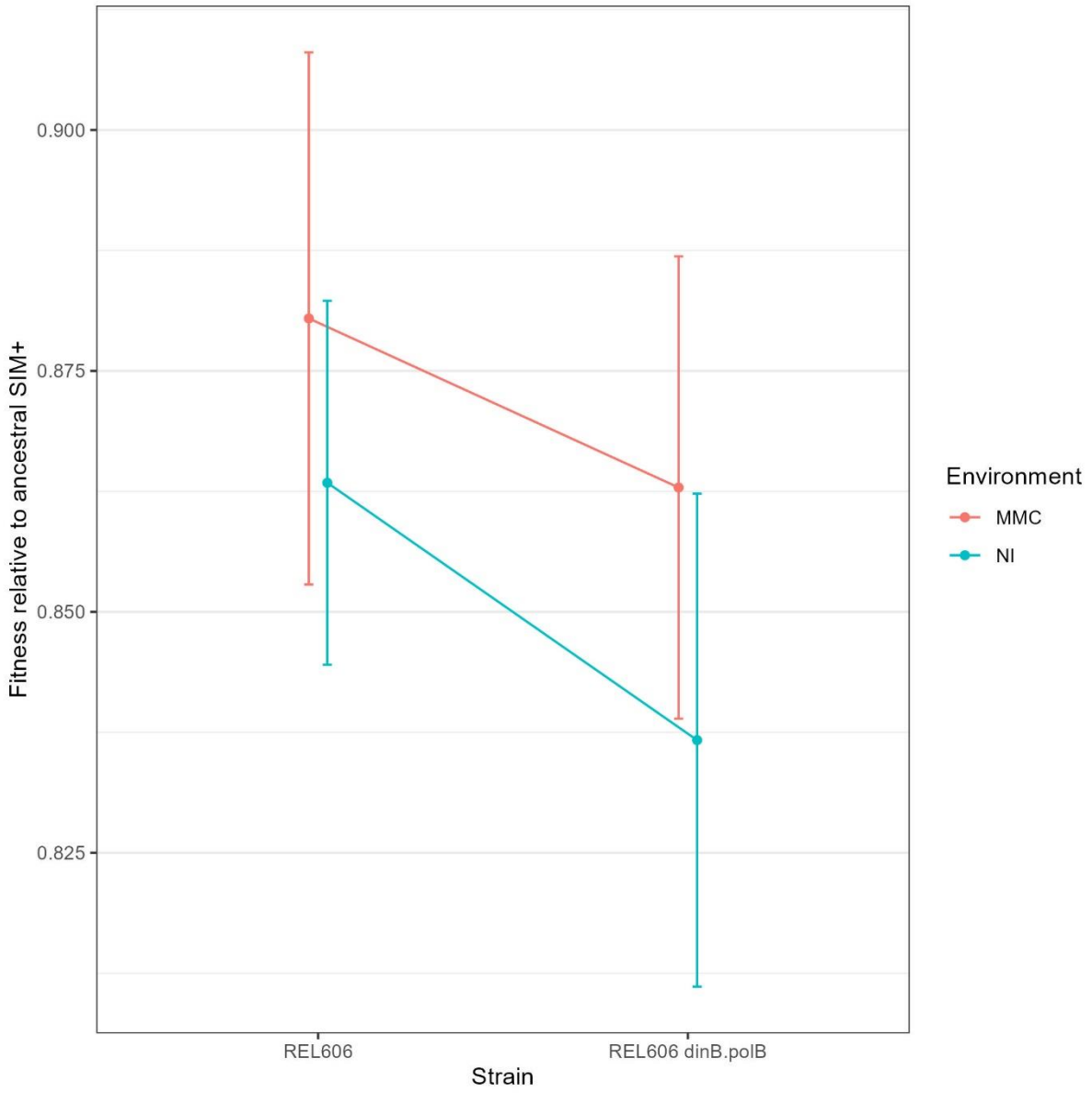

Figure 3-13: The fitness of evolved populations competition assays relative to the reference strain (ancestral REL606).
Values below one indicates strains are less fit than reference strain after accounting for YFP marker effect. REL606 dinB.polB indicates the SIM^- strains, while REL606 is indicative of SIM^+ strains. Symbols indicates the mean of up to 24 evolved population replicates, each measured on three different occasions. Error bars represent 95% confidence intervals.

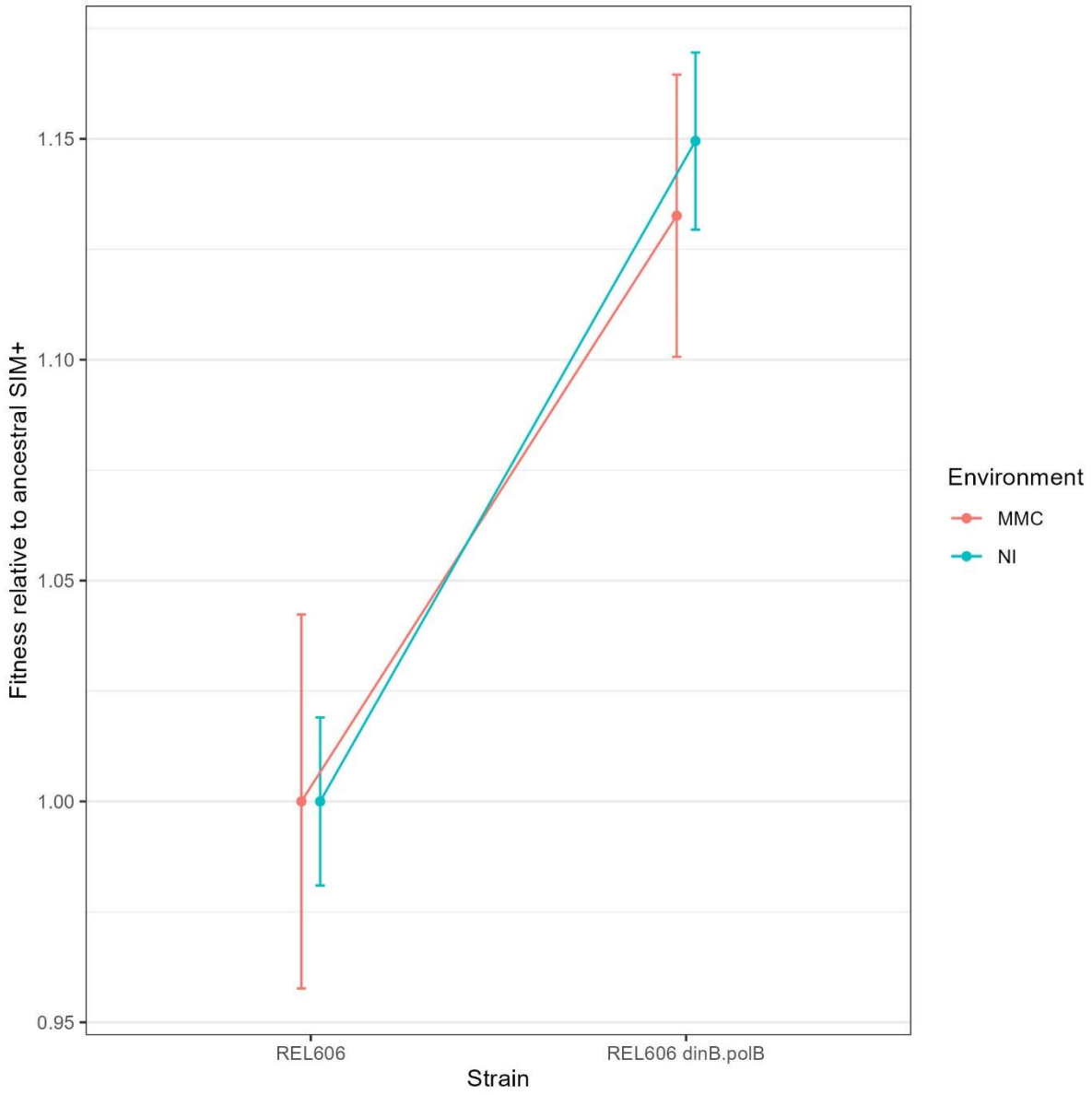

Figure 3-14: Fitness of ancestral populations competition assays relative to the reference strain (ancestral REL606).
Values above one indicates strains are more fit than reference strain after accounting for YFP marker effect. REL606 dinB.polB indicates the SIM^- strains, while REL606 is indicative of SIM^+ strains. Symbols indicates the mean of up to 12 ancestral strain replicates, each measured on two different occasions. Error bars represent 95% confidence intervals.

4. DISCUSSION AND CONCLUSIONS

4.1 Discussion

To investigate whether stress-induced mutagenesis (SIM) contributes to evolvability, I created SIM^- strains by deleting two error-prone polymerases. Then, I compared the mutation rate, growth rate, and evolvability of the SIM^- strains to their otherwise isogenic SIM^+ ancestors. Overall, my findings demonstrate the critical importance of error-prone polymerases in the stress-induced mutagenesis pathways of *E. coli* and suggest that targeting these polymerases may be a viable strategy to combat antibiotic resistance.

I used fluctuation tests to evaluate the hypothesis that error-prone polymerases are induced by the SOS response to confer the SIM phenotype. I found that environmental stress, such as the mutagen, mitomycin C (MMC), and SIM increased mutation rates in bacterial populations. Notably, the combination of SIM and MMC significantly increased mutation rates in both REL606 and MG1655 strains (Figure 3-11 & Appendix 4; $P < 0.001$). MMC also increased mutation rates in both SIM^+ and SIM^- populations, consistent with prior research demonstrating that sub-inhibitory MMC concentrations can result in a 2- to 3-fold increase mutation rates in parent and MG1655 strains containing error-prone polymerases (Csörgő et al., 2012). This effect is comparable to my 2.3- and 2.2-fold increase in mutation rates in REL606 and MG1655 SIM^+ strains when exposed to MMC, respectively (Figure 3-11 & Appendix 4; $P < 0.005$ and $P < 0.01$, respectively). However, I found an unexpected 3.3- and 2.4-fold increase in mutation rates in REL606 and MG1655 SIM^- strains when exposed to MMC, respectively, which contradicts previous results Csörgő et al. (2012) (Figure 3-11 & Appendix 4; $P < 0.002$ and $P < 0.02$, respectively).

One potential explanation for the effect of MMC in increasing mutation rates in my SIM^- populations could be that the SIM^- strain is more sensitive to the specific stressors used in the study. SIM^- strains may be more sensitive to genotoxic stress due to their lack of error-prone polymerases and translesion DNA synthesis (TLS) that help with DNA repair past lesions caused by stress (Friedberg et al., 2002). Sensitivity affects mutation rates as strains more vulnerable to stress may have a less effective DNA repair system, making them more likely to accumulate mutations over time (Vincent & Uphoff, 2020). This explanation is consistent with previous findings by Dapa et al. (2017), who found that inactivation of the *polB* gene

can increase sensitivity to MMC-induced genotoxic stress compared to the reference strain. This finding from my research and Dapa et al. (2017) implies that the *polB* gene plays a crucial role in the adaptive response to MMC-induced genotoxic stress. The absence of *polB* and *dinB* genes in the double mutant may have resulted in an even greater vulnerability to MMC-induced damage, leading to a higher mutation rate than the SIM^+ strain (Dapa et al., 2017). The discrepancy between my findings and Csörgő et al. (2012) concerning the effect of MMC on mutation rates in SIM^- strains highlights the complexity of bacterial adaptive responses to environmental stressors and emphasises the importance of further research to comprehend the underlying mechanisms.

Another key finding from my research is that the absence of *dinB* and *polB* genes reduces mutation rates in MMC and NI environments, as expected. This result is consistent with earlier research by Csörgő et al. (2012) which saw a 50% decrease in the mutation rate of a Δ*dinB* and Δ*polB* SIM^- *E. coli* strain in an unstressed environment. My SIM^+ strains had higher mutation rates than SIM^- strains, with 1.89- and 1.82-fold increases in mutation rates in the absence of MMC in the REL606 and MG1655 strain backgrounds, respectively. When MMC was present, the SIM^+ strains had 1.3- and 1.7-fold increases in mutation rates compared to SIM^- strains in the REL606 and MG1655 backgrounds, respectively. My results align with previous studies that found that removing all three inducible polymerases can significantly decrease post-exposure mutation rates in the presence of ciprofloxacin (Cirz et al., 2005). Furthermore, my findings support an earlier report that deleting *dinB* significantly reduces base substitution and frameshift mutations in a Lac^+ reversion system and a rifampicin resistance assay (Strauss et al., 2000). My findings demonstrate the importance of *dinB* and *polB* genes in promoting genetic variability and the potential evolution of antibiotic resistance in bacterial populations under stressed and unstressed environments.

My fluctuation test findings and previous studies here shed light on the critical role of stress-induced mutagenesis in bacterial evolution and adaptation. Overall, the increase in mutation rates during the SOS response is proposed to be an adaptive mechanism that allows bacteria to generate genetic diversity in response to DNA damage or other stresses, which can aid in their survival and adaptation (Podlesek & Žgur Bertok, 2020). My results offer valuable information regarding how the induction of SOS response and the presence of error-prone polymerases affect mutation rates. These findings can help towards developing strategies to

manage bacterial infections and prevent the evolution of antibiotic resistance (Cirz et al., 2005; Torres-Barceló et al., 2015).

Consistent with my evolvability hypothesis, I found that induction of the SOS response by MMC and the presence of error-prone polymerases interacted to affect the fitness of evolved populations (Appendix 4; MMC-SIM interaction term, $P = 0.043$). The combination of SIM and MMC increased fitness by 4.3% relative to the absence of both in evolved populations, indicating that stress and error-prone polymerases interact positively to increase evolvability (Figure 3-13).

Complicating the interpretation of the combined dependence on SIM and MMC on increased fitness improvements of evolved populations is my finding that deleting error-prone polymerases to make the SIM^- strain caused an immediate increase in fitness relative to a SIM^+ reference strain. This benefit occurred in environments with and without MMC. There are reasons to be cautious in interpreting this result, as results represent a considerable difference from expectations and previous findings. A decrease in the fitness of SIM^- strains relative to SIM^+ was seen by Yeiser et al. (2002) when competing SIM mutants against wild-type *Escherichia coli*. Another finding by Torres-Barceló et al. (2015) observed a short-term effect of wild-type *Pseudomonas aeruginosa* outcompeting a SIM-deficient mutant lacking an SOS response, adapting faster to the ciprofloxacin antibiotic stress. This finding contradicts the short-term effect on my ancestral populations where the SIM^- strain, in the absence and presence of MMC, shows a significant immediate increase in fitness relative to the reference strain.

Based on previous findings of Yeiser et al. (2002) and Torres-Barceló et al. (2015), my competition assay findings may be influenced by a complication affecting other aspects of the experiment. One possible candidate is the influence of an inadvertent difference between selection and competition environments, which I discuss in detail in section 4.2. In ancestral populations grown in both MMC and NI environments, the SIM^- strain showed an unexpected increase in fitness compared to the SIM^+ strain. This increase may be attributed to other factors, such as epistatic interactions between genes, which could have influenced the initial fitness differences between the two strains (Elena & Lenski, 2003; Orr, 2005).

Unexpectedly, I observed that the evolved strains had lower fitness than their ancestors. It may be attributed to the fact that the SIM-deficient ancestral populations showed a significant

increase in fitness in the presence and absence of MMC relative to the SIM^+ reference strain. This result likely had implications for the fitness of the evolved strains observed. It is essential to understand that the decreased fitness of evolved strains compared to their respective ancestors does not necessarily indicate the absence of adaptive mutations. It is possible that the evolved populations produced new beneficial mutations that have not yet been fixed, leading to a decrease in fitness relative to their ancestors (De Visser & Rozen, 2005; Wilke, 2004). These unexpected findings suggest that the relationship between mutation rates, adaptation, and evolvability is complex and cannot be generalised without considering the specific genetic and environmental contexts.

Overall, my estimates of the fitness of evolved strains indicate that the combination of stress and error-prone polymerases can enhance evolvability. This finding is supported by the higher fitness of populations selected in the MMC environment, and the significant increase in fitness observed in populations with SIM and MMC. However, the unexpected increase in fitness of the SIM^- strain relative to the SIM^+ strain in ancestral populations selected in MMC and NI environments indicates the need for caution when interpreting the result. The observed decreased fitness of the evolved strains compared to their respective ancestors is also unexpected. These results underscore the need for further research to understand the factors that influence the evolution of microbial populations.

4.2 Limitations

My thesis provides evidence that bacterial mutation rates are higher in the presence of error-prone polymerases and in response to SOS induction. While the difference in mutation rates between SIM^+ and SIM^- strains was insignificant, populations selected in a stressful environment with error-prone polymerases exhibited higher overall fitness. However, my results also reflect limitations in my experimental design that may have impacted results, as evidenced by unexpected outcomes such as the decreased fitness of evolved populations and the increase in SIM^- ancestral populations relative to ancestral populations.

Maintaining experimental consistency is crucial for obtaining reliable and reproducible results. Inconsistent experimental conditions can introduce variability, leading to inaccurate conclusions and potentially false discoveries. Differences between competition and evolution

experimental conditions are a potential explanation for the apparent lack of adaptation (Lenski, 2023). Using a different 1-day transfer cycle for competition experiments compared to the 2-day cycle used in a long-term evolution experiment and fluctuation test may have led to misleading fitness estimates if fitness changes across the two growth treatments were not correlated. Altering the transfer cycle can affect the experimental organisms' growth rate, population size, and evolutionary trajectory, resulting in differences in adaptation and genetic changes over time. Inconsistent experimental conditions can also hinder comparing and integrating results from different experiments, which is vital for understanding the underlying mechanisms and principles governing the system under study. However, it is important to note that other factors may have also affected these unexpected results. Further investigation is needed to fully understand the underlying causes and ensure consistency in experimental conditions to obtain reliable and reproducible results.

Another limitation of this study is that only *dinB* and *polB* were deleted, while the third error-prone polymerase, coded by *umuDC,* could not be removed. As the SIM mechanism involves multiple genes and responses, including those controlled by *umuDC,* my results may not fully represent the overall impact of SIM on mutation rates and fitness. My study's findings may not be generalisable to other genes involved in the SIM pathway, as the role and function of these genes may differ from those of *dinB* and *polB.* This limitation has several implications. First, the presence of the *umuDC* genes may confound the interpretation of the results as they are responsible for error-prone DNA repair, leading to increased mutagenesis. Second, it suggests that the impact of the SIM mechanism on mutation rates may be more significant than reported in this study. Third, it highlights the need for further research to understand the contribution of each gene and response to the overall mutagenic response. Therefore, this limitation emphasises the complexity of the SIM mechanism and the challenges associated with studying it. Further studies are necessary to remove all components of the SIM mechanism to understand its impact on mutation rates.

The inability to introduce the YFP and CFP markers into the ancestral strains presents a significant challenge for testing the evolved lines. The YFP and CFP markers are helpful for visualising gene expression and monitoring growth and behaviour under various conditions. However, its absence limits important information about evolved lines starting with MG1655 and derivatives, emphasising the need for careful selection of experimental techniques and alternative approaches. Furthermore, the inability to analyse the evolved lines from MG1655

in an evolutionary experiment is a significant scientific limitation. Monitoring the evolution of each strain, including potential adaptations or mutations, is critical, and not studying the evolved lines from MG1655 reduces the scope of the study and available information for analysis. The failure to draw applicable conclusions for both strains could limit the generalizability of the results and opportunities for identifying new mutations or adaptations in this strain, potentially limiting the overall scientific impact of the study.

Testing multiple strains of *E. coli* has several benefits. Firstly, different strains can have unique physiological, metabolic, and genetic characteristics. By testing multiple strains, researchers can obtain a more comprehensive understanding of the biological processes involved and how they vary between strains. Secondly, testing multiple strains can improve the reliability and validity of experimental results by identifying common trends and patterns that are less likely to be due to chance or random variation. Finally, studying multiple strains can provide insights into the evolutionary processes that occur within bacterial populations. By comparing the evolutionary trajectories of different strains, researchers can better understand the factors that contribute to adaptation and evolution.

Research has demonstrated the crucial role of SOS and RpoS responses in bacterial adaptation to DNA damage and nutrient limitation, respectively. However, the specific mechanisms and timing of SOS and RpoS induction may vary depending on the bacterial species and growth conditions being studied. It is important to acknowledge the limitations of current research in this area. For instance, the study only investigated the effects of two inducers for SOS, MMC and Nal, and one inducer for RpoS, nutrient starvation. Other inducers may have different effects on the response. Therefore, exploring the effectiveness of alternative inducers in inducing the SOS response would be beneficial.

Additionally, I only examined the impact of inducer concentrations on the SOS response and population growth rate under laboratory conditions, not reflecting the complexity of the response in natural settings. Therefore, the relevance of my findings to real-world situations may be limited. Moreover, I focused on the SOS and RpoS response to MMC selection and nutrient starvation in *E. coli*. Further research is required to establish whether the findings can be extrapolated to other bacterial species. By acknowledging these limitations, future research can identify new areas of investigation and provide a more comprehensive understanding of bacterial stress response mechanisms.

4.3 Conclusion and next steps

I aimed to test if stress-induced mutagenesis contributes to evolvability and to understand its mechanisms by creating SIM^- strains and examining their growth, mutation, and evolvability compared to SIM^+ strains. I had specific objectives: to determine the effects of removing error-prone polymerase genes and SOS responses on evolvability.

I found that the presence of both an SOS inducer, MMC, and SIM increases mutation rates, a requirement of the model that an active SOS response is necessary for error-prone polymerases to increase the evolvability of bacterial populations. SIM populations that have evolved to cope with stress and adapted to the SOS response have higher fitness in the presence of MMC. These findings support the hypothesis that the combination of stress and error-prone polymerases can enhance evolvability. However, the unexpected increase in fitness of SIM^- strains relative to SIM^+ strains in ancestral populations and the observed decrease in fitness of evolved strains compared to their ancestors limit the scope of the study, and caution should be taken when interpreting its results. Additionally, the study did not remove the *umuDC* gene associated with stress-induced mutagenesis, potentially not fully capturing the effects of the SOS response on mutation rates.

An essential next step to gain a comprehensive understanding of the SOS response pathway's contribution to mutagenesis is to investigate the impact of removing all genes involved in the pathway. Additionally, a thorough examination of the effects of each polymerase on mutagenesis could be achieved by evolving each single, double, and triple mutant. This approach would offer a deeper understanding of SOS polymerases in bacterial survival and adaptation, especially under stressful conditions and competition (Yeiser et al., 2002).

To compare evolved lines against their ancestral counterparts, fluorescent markers or barcodes must be incorporated in a competition assay with a two-day transfer cycle to account for the transfer cycle used in the evolution experiment and eliminate variability. The inducer MMC concentration can also be increased incrementally during long-term evolution to avoid acclimation. Extending the time frame to 1,000 generations can provide a more comprehensive understanding of adaptive mechanisms, but it was not feasible in the present study due to time constraints.

Several critical next steps can be taken to understand the results comprehensively. Firstly, using the growth curve machine can provide valuable information about the growth rates of different strains, including the wild type and double mutants with and without YFP, under varying stress conditions. Growth curves can aid in determining whether the observed fitness effects are due to marker cost or other external factors. Secondly, it is necessary to verify the integrity of the strains by sequencing the double mutant strain to ensure that the unexpected fitness effect of deleting the two error-prone polymerases is present and not caused by any unexpected mutations.

To ensure the accuracy and reliability of my study, it is crucial to recognize that the outcomes are limited to the specific experimental conditions used. Therefore, further research should investigate additional factors, such as different stressors or genetic backgrounds, to understand bacterial mutagenesis comprehensively. This knowledge could have significant implications for antibiotic development, as it may help to identify crucial regulators of mutagenesis and provide novel targets for drug development. These steps can refine the experiment's results, verify the accuracy of the observations, and offer important insights into the underlying mechanisms driving the observed effects.

Overall, my study provides valuable insights into bacterial stress responses, which could have significant implications for antibiotic development, particularly in microbial and evolutionary biology, where mutation rates play a vital role in shaping genetic diversity and adaptation. Understanding the effects of the SOS response pathway and associated SIM genes on mutagenesis may help address the urgent need for new approaches to combat antibiotic resistance and develop more effective strategies for treating infections caused by antibiotic-resistant bacteria.

5. BIBLIOGRAPHY

Agashe, D. (2017). The road not taken: Could stress-specific mutations lead to different evolutionary paths? *PLOS Biology*, *15*(6), e2002862. https://doi.org/10.1371/journal.pbio.2002862

Aljeldah, M. M. (2022). Antimicrobial Resistance and Its Spread Is a Global Threat. *Antibiotics (Basel)*, *11*(8). https://doi.org/10.3390/antibiotics11081082

Allaire, J. J., Xie, Y., McPherson, J., Luraschi, J., Ushey, K., Atkins, A., Wickham, H., Cheng, J., Chang, W., & Iannone, R. (2022). *rmarkdown: Dynamic Documents for R*. In R package version 2.19. https://rmarkdown.rstudio.com

Barrick, J., Deatherage, D., & Sowa, S. (2023). *FLP Recombination in E. coli*. https://barricklab.org/twiki/bin/view/Lab/ProcedureFLPFRTRecombination

Battesti, A., Majdalani, N., & Gottesman, S. (2011). The RpoS-mediated general stress response in *Escherichia coli*. *Annu Rev Microbiol*, *65*, 189-213. https://doi.org/10.1146/annurev-micro-090110-102946

Baym, M., Stone, L. K., & Kishony, R. (2016). Multidrug evolutionary strategies to reverse antibiotic resistance. *Science*, *351*(6268), aad3292. https://doi.org/10.1126/science.aad3292

Berardini, M., Foster, P. L., & Loechler, E. L. (1999). DNA Polymerase II (*polB*) Is Involved in a New DNA Repair Pathway for DNA Interstrand Cross-Links in *Escherichia coli*. *Journal of Bacteriology*, *181*(9), 2878-2882. https://doi.org/10.1128/JB.181.9.2878-2882.1999

Bjedov, I., Tenaillon, O., Gérard, B., Souza, V., Denamur, E., Radman, M., Taddei, F., & Matic, I. (2003). Stress-Induced Mutagenesis in Bacteria. *Science*, *300*(5624), 1404-1409. https://doi.org/10.1126/science.1082240

Bonner, C. A., Randall, S. K., Rayssiguier, C., Radman, M., Eritja, R., Kaplan, B. E., McEntee, K., & Goodman, M. F. (1988). Purification and characterization of an inducible *Escherichia coli* DNA polymerase capable of insertion and bypass at abasic lesions in DNA. *J Biol Chem*, *263*(35), 18946-18952.

Bos, J., Zhang, Q., Vyawahare, S., Rogers, E., Rosenberg, S. M., & Austin, R. H. (2015). Emergence of antibiotic resistance from multinucleated bacterial filaments. *Proceedings of the National Academy of Sciences*, *112*(1), 178-183. https://doi.org/10.1073/pnas.1420702111

Brown, T. (2002). Mutation, Repair and Recombination. In *Genomes* (2nd ed.). Wiley-Liss. https://www.ncbi.nlm.nih.gov/books/NBK21114/

Chan, C., Feng, F., Ottinger, J., Foster, D., West, M., & Kepler, T. B. (2008). Statistical mixture modeling for cell subtype identification in flow cytometry. *Cytometry A*, *73*(8), 693-701. https://doi.org/10.1002/cyto.a.20583

Cherepanov, P. P., & Wackernagel, W. (1995). Gene disruption in *Escherichia coli*: TcR and KmR cassettes with the option of Flp-catalyzed excision of the antibiotic-resistance determinant. *Gene*, *158*(1), 9-14. https://doi.org/10.1016/0378-1119(95)00193-a

Cirz, R. T., Chin, J. K., Andes, D. R., de Crécy-Lagard, V., Craig, W. A., & Romesberg, F. E. (2005). Inhibition of mutation and combating the evolution of antibiotic resistance. *PLoS Biol*, *3*(6), e176. https://doi.org/10.1371/journal.pbio.0030176

Cirz, R. T., & Romesberg, F. E. (2006). Induction and Inhibition of Ciprofloxacin Resistance-Conferring Mutations in Hypermutator Bacteria. *Antimicrobial Agents and Chemotherapy*, *50*(1), 220-225. https://doi.org/10.1128/aac.50.1.220-225.2006

Cirz, R. T., & Romesberg, F. E. (2007). Controlling Mutation: Intervening in Evolution as a Therapeutic Strategy. *Critical Reviews in Biochemistry and Molecular Biology*, *42*(5), 341-354. https://doi.org/10.1080/10409230701597741

Cole, S. T. (1983). Characterisation of the promoter for the LexA regulated *sulA* gene of *Escherichia coli*. *Molecular and General Genetics MGG*, *189*(3), 400-404. https://doi.org/10.1007/bf00325901

Cordell, S. C., Robinson, E. J. H., & Löwe, J. (2003). Crystal structure of the SOS cell division inhibitor SulA and in complex with FtsZ. *Proceedings of the National Academy of Sciences*, *100*(13), 7889-7894. https://doi.org/10.1073/pnas.1330742100

Correa, R., Thornton, P. C., Rosenberg, S. M., & Hastings, P. J. (2018). Oxygen and RNA in stress-induced mutation. *Curr Genet*, *64*(4), 769-776. https://doi.org/10.1007/s00294-017-0801-9

Corzett, C. H., Goodman, M. F., & Finkel, S. E. (2013). Competitive fitness during feast and famine: how SOS DNA polymerases influence physiology and evolution in *Escherichia coli*. *Genetics*, *194*(2), 409-420. https://doi.org/10.1534/genetics.113.151837

Csörgő, B., Fehér, T., Tímár, E., Blattner, F. R., & Pósfai, G. (2012). Low-mutation-rate, reduced-genome *Escherichia coli*: an improved host for faithful maintenance of engineered genetic constructs. *Microbial Cell Factories*, *11*(1), 11. https://doi.org/10.1186/1475-2859-11-11

Culyba, M. J., Mo, C. Y., & Kohli, R. M. (2015). Targets for Combating the Evolution of Acquired Antibiotic Resistance. *Biochemistry*, *54*(23), 3573-3582. https://doi.org/10.1021/acs.biochem.5b00109

Dapa, T., Fleurier, S., Bredeche, M. F., & Matic, I. (2017). The SOS and RpoS Regulons Contribute to Bacterial Cell Robustness to Genotoxic Stress by Synergistically Regulating DNA Polymerase Pol II. *Genetics*, *206*(3), 1349-1360. https://doi.org/10.1534/genetics.116.199471

Datsenko, K. A., & Wanner, B. L. (2000). One-step inactivation of chromosomal genes in *Escherichia coli K-12* using PCR products. *Proceedings of the National Academy of Sciences*, *97*(12), 6640-6645. https://doi.org/10.1073/pnas.120163297

Datta, S., Costantino, N., & Court, D. L. (2006). A set of recombineering plasmids for gram-negative bacteria. *Gene*, *379*, 109-115. https://doi.org/10.1016/j.gene.2006.04.018

De Visser, J. A. G. M., & Rozen, D. E. (2005). Limits to adaptation in asexual populations. *Journal of Evolutionary Biology*, *18*(4), 779-788. https://doi.org/10.1111/j.1420-9101.2005.00879.x

Dellus-Gur, E., Ram, Y., & Hadany, L. (2017). Errors in mutagenesis and the benefit of cell-to-cell signalling in the evolution of stress-induced mutagenesis. *Royal Society Open Science*, *4*(11), 170529. https://doi.org/10.1098/rsos.170529

Denamur, E., & Matic, I. (2006). Evolution of mutation rates in bacteria. *Molecular Microbiology*, *60*(4), 820-827. https://doi.org/10.1111/j.1365-2958.2006.05150.x

Diner, E. J., Garza-Sánchez, F., & Hayes, C. S. (2011). Genome engineering using targeted oligonucleotide libraries and functional selection. *Methods in molecular biology (Clifton, N.J.)*, *765*, 71-82. https://doi.org/10.1007/978-1-61779-197-0_5

Elena, S. F., & Lenski, R. E. (2003). Evolution experiments with microorganisms: the dynamics and genetic bases of adaptation. *Nature Reviews Genetics*, *4*(6), 457-469. https://doi.org/10.1038/nrg1088

Ellis, B., Haaland, P., Hahne, F., Le Meur, N., Gopalakrishnan, N., Spidlen, J., Jiang, M., & Finak, G. (2022). *flowCore: flowCore: Basic structures for flow cytometry data*. In R package version 2.10.0.

Erill, I., Campoy, S., & Barbé, J. (2007). Aeons of distress: an evolutionary perspective on the bacterial SOS response. *FEMS Microbiology Reviews*, *31*(6), 637-656. https://doi.org/10.1111/j.1574-6976.2007.00082.x

Escarceller, M., Hicks, J., Gudmundsson, G., Trump, G., Touati, D., Lovett, S., Foster, P. L., McEntee, K., & Goodman, M. F. (1994). Involvement of *Escherichia coli* DNA Polymerase II in response to oxidative damage and adaptive mutation. *Journal of Bacteriology*, *176*(20), 6221-6228. https://doi.org/10.1128/jb.176.20.6221-6228.1994

Feng, G., Tsui, H. C., & Winkler, M. E. (1996). Depletion of the cellular amounts of the MutS and MutH methyl-directed mismatch repair proteins in stationary-phase *Escherichia coli K-12* cells. *J Bacteriol*, *178*(8), 2388-2396. https://doi.org/10.1128/jb.178.8.2388-2396.1996

Fijalkowska, I. J., Schaaper, R. M., & Jonczyk, P. (2012). DNA replication fidelity in *Escherichia coli*: a multi-DNA polymerase affair. *FEMS Microbiol Rev*, *36*(6), 1105-1121. https://doi.org/10.1111/j.1574-6976.2012.00338.x

Finak, G., & Jiang, M. (2022). *flowWorkspace: Infrastructure for representing and interacting with gated and ungated cytometry data sets*. In R package version 4.10.1.

Fitzgerald, D. M. (2019). The road to resistance. *eLife*, *8*, e52092. https://doi.org/10.7554/eLife.52092

Fitzgerald, D. M., Hastings, P. J., & Rosenberg, S. M. (2017). Stress-Induced Mutagenesis: Implications in Cancer and Drug Resistance. *Annual review of cancer biology*, *1*, 119-140. https://doi.org/10.1146/annurev-cancerbio-050216-121919

Fogle, C. A., Nagle, J. L., & Desai, M. M. (2008). Clonal Interference, Multiple Mutations and Adaptation in Large Asexual Populations. *Genetics*, *180*(4), 2163-2173. https://doi.org/10.1534/genetics.108.090019

Foster, P. L. (2007). Stress-Induced Mutagenesis in Bacteria. *Critical Reviews in Biochemistry and Molecular Biology*, *42*(5), 373-397. https://doi.org/10.1080/10409230701648494

Foster, P. L., Lee, H., Popodi, E., Townes, J. P., & Tang, H. (2015). Determinants of spontaneous mutation in the bacterium *Escherichia coli* as revealed by whole-genome sequencing. *Proceedings of the National Academy of Sciences of the United States of America*, *112*(44), E5990-E5999. https://doi.org/10.1073/pnas.1512136112

Friedberg, E. C., Wagner, R., & Radman, M. (2002). Specialized DNA Polymerases, Cellular Survival, and the Genesis of Mutations. *Science*, *296*(5573), 1627-1630. https://doi.org/10.1126/science.1070236

Friedberg, E. C., Walker, G. C., Siede, W., Wood, R. D., Schultz, R. A., & Ellenberger, T. (2005a). Nucleotide Excision Repair. In *DNA Repair and Mutagenesis* (pp. 227-266). https://doi.org/10.1128/9781555816704.ch7

Friedberg, E. C., Walker, G. C., Siede, W., Wood, R. D., Schultz, R. A., & Ellenberger, T. (2005b). The SOS Responses of Prokaryotes to DNA Damage. In *DNA Repair and Mutagenesis* (pp. 463-508). https://doi.org/10.1128/9781555816704.ch14

Frisch, R. L., Su, Y., Thornton, P. C., Gibson, J. L., Rosenberg, S. M., & Hastings, P. J. (2010). Separate DNA Pol II- and Pol IV-Dependent Pathways of Stress-Induced Mutation during Double-Strand-Break Repair in *Escherichia coli* Are Controlled by RpoS. *Journal of Bacteriology*, *192*(18), 4694-4700. https://doi.org/10.1128/jb.00570-10

Fuchs, R. P., & Fujii, S. (2013). Translesion DNA synthesis and mutagenesis in prokaryotes. *Cold Spring Harbor perspectives in biology*, *5*(12), a012682-a012682. https://doi.org/10.1101/cshperspect.a012682

Galhardo, R. S., Do, R., Yamada, M., Friedberg, E. C., Hastings, P. J., Nohmi, T., & Rosenberg, S. M. (2009). *DinB* upregulation is the sole role of the SOS response in stress-induced mutagenesis in *Escherichia coli*. *Genetics*, *182*(1), 55-68. https://doi.org/10.1534/genetics.109.100735

Galhardo, R. S., Hastings, P. J., & Rosenberg, S. M. (2007). Mutation as a Stress Response and the Regulation of Evolvability. *Critical Reviews in Biochemistry and Molecular Biology*, *42*(5), 399-435. https://doi.org/10.1080/10409230701648502

Gallet, R., Cooper, T. F., Elena, S. F., & Lenormand, T. (2012). Measuring selection coefficients below 10(-3): method, questions, and prospects. *Genetics*, *190*(1), 175-186. https://doi.org/10.1534/genetics.111.133454

Gillet-Markowska, A., Louvel, G., & Fischer, G. (2015). bz-rates: A Web Tool to Estimate Mutation Rates from Fluctuation Analysis. *G3 (Bethesda)*, *5*(11), 2323-2327. https://doi.org/10.1534/g3.115.019836

Goodman, M. F. (2002). Error-Prone Repair DNA Polymerases in Prokaryotes and Eukaryotes. *Annual Review of Biochemistry*, *71*(1), 17-50. https://doi.org/10.1146/annurev.biochem.71.083101.124707

Goodman, M. F., McDonald, J. P., Jaszczur, M. M., & Woodgate, R. (2016). Insights into the complex levels of regulation imposed on *Escherichia coli* DNA polymerase V. *DNA repair*, *44*, 42-50. https://doi.org/10.1016/j.dnarep.2016.05.005

Gottesman, S. (2019). Trouble is coming: Signaling pathways that regulate general stress responses in bacteria. *J Biol Chem*, *294*(31), 11685-11700. https://doi.org/10.1074/jbc.REV119.005593

Hahne, F., Gopalakrishnan, N., Khodabakhshi, A., Wong, C., & Lee, K. (2022). *flowStats: Statistical methods for the analysis of flow cytometry data*. In R package version 4.10.0. http://www.github.com/RGLab/flowStats

Harris, R. S., Feng, G., Ross, K. J., Sidhu, R., Thulin, C., Longerich, S., Szigety, S. K., Winkler, M. E., & Rosenberg, S. M. (1997). Mismatch repair protein *MutL* becomes limiting during stationary-phase mutation. *Genes Dev*, *11*(18), 2426-2437. https://doi.org/10.1101/gad.11.18.2426

He, A. S., Rohatgi, P. R., Hersh, M. N., & Rosenberg, S. M. (2006). Roles of *E. coli* double-strand-break-repair proteins in stress-induced mutation. *DNA repair*, *5*(2), 258-273. https://doi.org/10.1016/j.dnarep.2005.10.006

Hede, K. (2014). Antibiotic resistance: An infectious arms race. *Nature*, *509*(7498), S2-S3. https://doi.org/10.1038/509S2a

Hengge-Aronis, R. (2002). Signal transduction and regulatory mechanisms involved in control of the sigma(S) (RpoS) subunit of RNA polymerase. *Microbiology and molecular biology reviews: MMBR*, *66*(3), 373-395. https://doi.org/10.1128/MMBR.66.3.373-395.2002

Huisman, O., & D'Ari, R. (1981). An inducible DNA replication-cell division coupling mechanism in *E. coli*. *Nature*, *290*(5809), 797-799. https://doi.org/10.1038/290797a0

Jaramillo-Riveri, S., Broughton, J., McVey, A., Pilizota, T., Scott, M., & El Karoui, M. (2022). Growth-dependent heterogeneity in the DNA damage response in Escherichia coli. *Molecular Systems Biology*, *18*(5), e10441. https://doi.org/10.15252/msb.202110441

Jaszczur, M., Bertram, J. G., Robinson, A., van Oijen, A. M., Woodgate, R., Cox, M. M., & Goodman, M. F. (2016). Mutations for Worse or Better: Low-Fidelity DNA Synthesis by SOS DNA Polymerase V Is a Tightly Regulated Double-Edged Sword. *Biochemistry*, *55*(16), 2309-2318. https://doi.org/10.1021/acs.biochem.6b00117

Jaszczur, M. M., Vo, D. D., Stanciauskas, R., Bertram, J. G., Sikand, A., Cox, M. M., Woodgate, R., Mak, C. H., Pinaud, F., & Goodman, M. F. (2019). Conformational

regulation of *Escherichia coli* DNA polymerase V by RecA and ATP. *PLoS genetics*, *15*(2), e1007956. https://doi.org/10.1371/journal.pgen.1007956

Jiang, X., Mu, B., Huang, Z., Zhang, M., Wang, X., & Tao, S. (2010). Impacts of mutation effects and population size on mutation rate in asexual populations: a simulation study. *BMC Evolutionary Biology*, *10*(1), 298. https://doi.org/10.1186/1471-2148-10-298

Kato, T., & Nakano, E. (1981). Effects of the umuC36 mutation on ultraviolet-radiation-induced base-change and frameshift mutations in *Escherichia coli*. *Mutation Research/Fundamental and Molecular Mechanisms of Mutagenesis*, *83*(3), 307-319. https://doi.org/10.1016/0027-5107(81)90014-2

Keller, K. L., Overbeck-Carrick, T. L., & Beck, D. J. (2001). Survival and induction of SOS in *Escherichia coli* treated with cisplatin, UV-irradiation, or mitomycin C are dependent on the function of the RecBC and RecFOR pathways of homologous recombination. *Mutation Research/DNA Repair*, *486*(1), 21-29. https://doi.org/10.1016/S0921-8777(01)00077-5

Kim, S. R., Matsui, K., Yamada, M., Gruz, P., & Nohmi, T. (2001). Roles of chromosomal and episomal *dinB* genes encoding DNA pol IV in targeted and untargeted mutagenesis in *Escherichia coli*. *Molecular Genetics and Genomics*, *266*(2), 207-215. https://doi.org/10.1007/s004380100541

Kishony, R., & Leibler, S. (2003). Environmental stresses can alleviate the average deleterious effect of mutations. *Journal of biology*, *2*(2), 14-14. https://doi.org/10.1186/1475-4924-2-14

Kobayashi, S., Valentine, M. R., Pham, P., O'Donnell, M., & Goodman, M. F. (2002). Fidelity of *Escherichia coli* DNA Polymerase IV. *Journal of Biological Chemistry*, *277*(37), 34198-34207. https://doi.org/10.1074/jbc.m204826200

Kokubo, K., Yamada, M., Kanke, Y., & Nohmi, T. (2005). Roles of replicative and specialized DNA polymerases in frameshift mutagenesis: Mutability of *Salmonella typhimurium* strains lacking one or all of SOS-inducible DNA polymerases to 26 chemicals. *DNA repair*, *4*(10), 1160-1171. https://doi.org/10.1016/j.dnarep.2005.06.016

Kornberg, T., & Gefter, M. L. (1972). Deoxyribonucleic Acid Synthesis in Cell-free Extracts: IV. Purification and catalytic properties of deoxyribonucleic acid Polymerase III. *Journal of Biological Chemistry*, *247*(17), 5369-5375. https://doi.org/10.1016/S0021-9258(20)81114-4

Kuban, W., Banach-Orlowska, M., Schaaper, R. M., Jonczyk, P., & Fijalkowska, I. J. (2006). Role of DNA polymerase IV in *Escherichia coli* SOS mutator activity. *J Bacteriol*, *188*(22), 7977-7980. https://doi.org/10.1128/jb.01088-06

Lampe, N., Marin, P., Coulon, M., Micheau, P., Maigne, L., Sarramia, D., Piquemal, F., Incerti, S., Biron, D. G., Ghio, C., Sime-Ngando, T., Hindre, T., & Breton, V. (2019). Reducing the ionizing radiation background does not significantly affect the evolution

of *Escherichia coli* populations over 500 generations. *Scientific Reports*, *9*(1), 14891. https://doi.org/10.1038/s41598-019-51519-9

Lanfear, R., Kokko, H., & Eyre-Walker, A. (2014). Population size and the rate of evolution. *Trends in Ecology & Evolution*, *29*(1), 33-41. https://doi.org/10.1016/j.tree.2013.09.009

Layton, J. C., & Foster, P. L. (2003). Error-prone DNA polymerase IV is controlled by the stress-response sigma factor, RpoS, in *Escherichia coli*. *Molecular Microbiology*, *50*(2), 549-561. https://doi.org/10.1046/j.1365-2958.2003.03704.x

Layton, J. C., & Foster, P. L. (2005). Error-Prone DNA Polymerase IV Is Regulated by the Heat Shock Chaperone *GroE* in *Escherichia coli*. *Journal of Bacteriology*, *187*(2), 449-457. https://doi.org/10.1128/JB.187.2.449-457.2005

Lee, A. M., Ross, C. T., Zeng, B.-B., & Singleton, S. F. (2005). A Molecular Target for Suppression of the Evolution of Antibiotic Resistance: Inhibition of the *Escherichia coli* RecA Protein by N6-(1-Naphthyl)-ADP. *Journal of Medicinal Chemistry*, *48*(17), 5408-5411. https://doi.org/10.1021/jm050113z

Lenski, R. E. (2023). Revisiting the Design of the Long-Term Evolution Experiment with *Escherichia coli*. *Journal of Molecular Evolution*, *91*(3), 241-253. https://doi.org/10.1007/s00239-023-10095-3

Livneh, Z. (2004). *UmuC, D* Lesion Bypass DNA Polymerase V. In W. J. Lennarz & M. D. Lane (Eds.), *Encyclopedia of Biological Chemistry* (pp. 308-312). Elsevier. https://doi.org/10.1016/B0-12-443710-9/00040-5

Lodish, H., Berk, A., Zipursky, S., Matsudaira, P., Baltimore, D., & Darnell, J. (2000a). DNA Damage and Repair and Their Role in Carcinogenesis. In *Molecular Cell Biology* (4th ed.). W. H. Freeman. https://www.ncbi.nlm.nih.gov/books/NBK21554/

Lodish, H., Berk, A., Zipursky, S., Matsudaira, P., Baltimore, D., & Darnell, J. (2000b). Mutations: Types and Causes. In *Molecular Cell Biology* (4th ed.). W. H. Freeman. https://www.ncbi.nlm.nih.gov/books/NBK21578/

Lombardo, M. J., Aponyi, I., & Rosenberg, S. M. (2004). General stress response regulator RpoS in adaptive mutation and amplification in *Escherichia coli*. *Genetics*, *166*(2), 669-680. https://doi.org/10.1534/genetics.166.2.669

Lukačišinová, M., Novak, S., & Paixão, T. (2017). Stress-induced mutagenesis: Stress diversity facilitates the persistence of mutator genes. *PLOS Computational Biology*, *13*(7), e1005609. https://doi.org/10.1371/journal.pcbi.1005609

MacLean, R. C., & San Millan, A. (2019). The evolution of antibiotic resistance. *Science*, *365*(6458), 1082-1083. https://doi.org/10.1126/science.aax3879

MacLean, R. C., Torres-Barceló, C., & Moxon, R. (2013). Evaluating evolutionary models of stress-induced mutagenesis in bacteria. *Nature Reviews Genetics*, *14*(3), 221-227. https://doi.org/10.1038/nrg3415

Maharjan, R., & Ferenci, T. (2014). Stress-induced mutation rates show a sigmoidal and saturable increase due to the RpoS sigma factor in *Escherichia coli*. *Genetics*, *198*(3), 1231-1235. https://doi.org/10.1534/genetics.114.170258

Marinelli, L. J., Hatfull, G. F., & Piuri, M. (2012). Recombineering: A powerful tool for modification of bacteriophage genomes. *Bacteriophage*, *2*(1), 5-14. https://doi.org/10.4161/bact.18778

Maslowska, K. H., Makiela-Dzbenska, K., & Fijalkowska, I. J. (2019). The SOS system: A complex and tightly regulated response to DNA damage. *Environmental and molecular mutagenesis*, *60*(4), 368-384. https://doi.org/10.1002/em.22267

Matic, I. (2013). Stress-Induced Mutagenesis in Bacteria. In D. Mittelman (Ed.), *Stress-Induced Mutagenesis* (pp. 1-19). Springer New York. https://doi.org/10.1007/978-1-4614-6280-4_1

McCool, J. D., Long, E., Petrosino, J. F., Sandler, H. A., Rosenberg, S. M., & Sandler, S. J. (2004). Measurement of SOS expression in individual *Escherichia coli K-12* cells using fluorescence microscopy. *Molecular Microbiology*, *53*(5), 1343-1357. https://doi.org/10.1111/j.1365-2958.2004.04225.x

McHenry, C. (1985). DNA polymerase III holoenzyme of *Escherichia coli*: Components and function of a true replicative complex. *Molecular and Cellular Biochemistry*, *66*(1). https://doi.org/10.1007/bf00231826

McHenry, C., & Kornberg, A. (1977). DNA polymerase III holoenzyme of *Escherichia coli*. Purification and resolution into subunits. *J Biol Chem*, *252*(18), 6478-6484.

McKenzie, G. J., Harris, R. S., Lee, P. L., & Rosenberg, S. M. (2000). The SOS response regulates adaptive mutation. *Proceedings of the National Academy of Sciences*, *97*(12), 6646-6651. https://doi.org/10.1073/pnas.120161797

McKenzie, G. J., Lee, P. L., Lombardo, M.-J., Hastings, P. J., & Rosenberg, S. M. (2001). SOS Mutator DNA Polymerase IV Functions in Adaptive Mutation and Not Adaptive Amplification. *Molecular Cell*, *7*(3), 571-579. https://doi.org/10.1016/S1097-2765(01)00204-0

Moore, J. M., Correa, R., Rosenberg, S. M., & Hastings, P. J. (2017). Persistent damaged bases in DNA allow mutagenic break repair in *Escherichia coli*. *PLoS genetics*, *13*(7), e1006733-e1006733. https://doi.org/10.1371/journal.pgen.1006733

Mothersill, C., & Seymour, C. (2013). Radiation-Induced Bystander Effects and Stress-Induced Mutagenesis. In D. Mittelman (Ed.), *Stress-Induced Mutagenesis* (pp. 199-222). Springer New York. https://doi.org/10.1007/978-1-4614-6280-4_10

Napolitano, R., Janel-Bintz, R., Wagner, J., & Fuchs, R. P. P. (2000). All three SOS-inducible DNA polymerases (Pol II, Pol IV and Pol V) are involved in induced mutagenesis. *The EMBO Journal*, *19*(22), 6259-6265. https://doi.org/10.1093/emboj/19.22.6259

Nohmi, T. (2006). Environmental Stress and Lesion-Bypass DNA Polymerases. *Annual Review of Microbiology*, *60*(1), 231-253. https://doi.org/10.1146/annurev.micro.60.080805.142238

Nyerges, Á., Csörgő, B., Nagy, I., Bálint, B., Bihari, P., Lázár, V., Apjok, G., Umenhoffer, K., Bogos, B., Pósfai, G., & Pál, C. (2016). A highly precise and portable genome engineering method allows comparison of mutational effects across bacterial species. *Proceedings of the National Academy of Sciences*, *113*(9), 2502-2507. https://doi.org/10.1073/pnas.1520040113

Opperman, T., Murli, S., Smith, B. T., & Walker, G. C. (1999). A model for a *umuDC*-dependent prokaryotic DNA damage checkpoint. *Proceedings of the National Academy of Sciences*, *96*(16), 9218-9223. https://doi.org/10.1073/pnas.96.16.9218

Orr, H. A. (2005). The genetic theory of adaptation: a brief history. *Nature Reviews Genetics*, *6*(2), 119-127. https://doi.org/10.1038/nrg1523

Pennington, J. M., & Rosenberg, S. M. (2007). Spontaneous DNA breakage in single living *Escherichia coli* cells. *Nature Genetics*, *39*(6), 797-802. https://doi.org/10.1038/ng2051

Podlesek, Z., & Žgur Bertok, D. (2020). The DNA Damage Inducible SOS Response Is a Key Player in the Generation of Bacterial Persister Cells and Population Wide Tolerance [Mini Review]. *Frontiers in Microbiology*, *11*. https://doi.org/10.3389/fmicb.2020.01785

Pomerantz, R. T., Goodman, M. F., & O'Donnell, M. E. (2013). DNA polymerases are error-prone at RecA-mediated recombination intermediates. *Cell Cycle*, *12*(16), 2558-2563. https://doi.org/10.4161/cc.25691

Ponder, R. G., Fonville, N. C., & Rosenberg, S. M. (2005). A Switch from High-Fidelity to Error-Prone DNA Double-Strand Break Repair Underlies Stress-Induced Mutation. *Molecular Cell*, *19*(6), 791-804. https://doi.org/10.1016/j.molcel.2005.07.025

Poole, K. (2012). Bacterial stress responses as determinants of antimicrobial resistance. *Journal of Antimicrobial Chemotherapy*, *67*(9), 2069-2089. https://doi.org/10.1093/jac/dks196

Pribis, J. P., García-Villada, L., Zhai, Y., Lewin-Epstein, O., Wang, A. Z., Liu, J., Xia, J., Mei, Q., Fitzgerald, D. M., Bos, J., Austin, R. H., Herman, C., Bates, D., Hadany, L., Hastings, P. J., & Rosenberg, S. M. (2019). Gamblers: An Antibiotic-Induced Evolvable Cell Subpopulation Differentiated by Reactive-Oxygen-Induced General Stress Response. *Molecular Cell*, *74*(4), 785-800.e787. https://doi.org/10.1016/j.molcel.2019.02.037

Qiu, Z., & Goodman, M. F. (1997). The *Escherichia coli polB* Locus Is Identical to *dinA*, the Structural Gene for DNA Polymerase II: Characterization of Pol II purified from a *polB* mutant. *Journal of Biological Chemistry*, *272*(13), 8611-8617. https://doi.org/10.1074/jbc.272.13.8611

Ragheb, M. N., Thomason, M. K., Hsu, C., Nugent, P., Gage, J., Samadpour, A. N., Kariisa, A., Merrikh, C. N., Miller, S. I., Sherman, D. R., & Merrikh, H. (2019). Inhibiting the

Evolution of Antibiotic Resistance. *Molecular Cell*, *73*(1), 157-165.e155. https://doi.org/10.1016/j.molcel.2018.10.015

Ram, Y., Dellus-Gur, E., Bibi, M., Karkare, K., Obolski, U., Feldman, M. W., Cooper, T. F., Berman, J., & Hadany, L. (2019). Predicting microbial growth in a mixed culture from growth curve data. *Proceedings of the National Academy of Sciences*, *116*(29), 14698-14707. https://doi.org/10.1073/pnas.1902217116

Ram, Y., & Hadany, L. (2012). The Evolution of Stress-Induced Hypermutation in Asexual Populations. *Evolution*, *66*(7), 2315-2328. https://doi.org/10.1111/j.1558-5646.2012.01576.x

Ram, Y., & Hadany, L. (2014). Stress-induced mutagenesis and complex adaptation. *Proceedings of the Royal Society B: Biological Sciences*, *281*(1792), 20141025. https://doi.org/10.1098/rspb.2014.1025

Ramsay, J. O., Graves, S., & Hooker, G. (2022). *fda: Functional Data Analysis*. In R package version 6.0.5. https://CRAN.R-project.org/package=fda

Rattray, A., & Strathern, J. (2003). Error-prone DNA Polymerases: When Making a Mistake is the Only Way to Get Ahead. *Annual review of genetics*, *37*, 31-66. https://doi.org/10.1146/annurev.genet.37.042203.132748

Revitt-Mills, S. A., & Robinson, A. (2020). Antibiotic-Induced Mutagenesis: Under the Microscope [Review]. *Frontiers in Microbiology*, *11*. https://doi.org/10.3389/fmicb.2020.585175

Rosenberg, S. M., Shee, C., Frisch, R. L., & Hastings, P. J. (2012). Stress-induced mutation via DNA breaks in *Escherichia coli*: A molecular mechanism with implications for evolution and medicine. *BioEssays*, *34*(10), 885-892. https://doi.org/10.1002/bies.201200050

Saint-Ruf, C., Pesut, J., Sopta, M., & Matic, I. (2007). Causes and Consequences of DNA Repair Activity Modulation During Stationary Phase in *Escherichia coli*. *Critical Reviews in Biochemistry and Molecular Biology*, *42*(4), 259-270. https://doi.org/10.1080/10409230701495599

Sarkar, D. (2008). *Lattice: Multivariate Data Visualization with R*. Springer. http://lmdvr.r-forge.r-project.org

Sharan, S. K., Thomason, L. C., Kuznetsov, S. G., & Court, D. L. (2009). Recombineering: a homologous recombination-based method of genetic engineering. *Nature protocols*, *4*(2), 206-223. https://doi.org/10.1038/nprot.2008.227

Shaw, F. H., & Baer, C. F. (2011). Fitness-dependent mutation rates in finite populations. *Journal of Evolutionary Biology*, *24*(8), 1677-1684. https://doi.org/10.1111/j.1420-9101.2011.02320.x

Shee, C., Gibson, J. L., Darrow, M. C., Gonzalez, C., & Rosenberg, S. M. (2011). Impact of a stress-inducible switch to mutagenic repair of DNA breaks on mutation in *Escherichia coli*. *Proceedings of the National Academy of Sciences*, *108*(33), 13659-13664. https://doi.org/10.1073/pnas.1104681108

Shee, C., Hastings, P., & Rosenberg, S. M. (2013). Mutagenesis associated with repair of DNA double-strand breaks under stress. In *Stress-induced mutagenesis* (pp. 21-39). Springer. https://doi.org/10.1007/978-1-4614-6280-4_2

Shee, C., Ponder, R., Gibson, J. L., & Rosenberg, S. M. (2011). What limits the efficiency of double-strand break-dependent stress-induced mutation in *Escherichia coli*? *Journal of molecular microbiology and biotechnology*, *21*(1-2), 8-19. https://doi.org/10.1159/000335354

Shinagawa, H. (1996). SOS response as an adaptive response to DNA damage in prokaryotes. *Exs*, *77*, 221-235. https://doi.org/10.1007/978-3-0348-9088-5_14

Smith, B. T., & Walker, G. C. (1998). Mutagenesis and more: *umuDC* and the *Escherichia coli* SOS response. *Genetics*, *148*(4), 1599-1610. https://doi.org/10.1093/genetics/148.4.1599

Strauss, B. S., Roberts, R., Francis, L., & Pouryazdanparast, P. (2000). Role of the *dinB* Gene Product in Spontaneous Mutation in *Escherichia coli* with an Impaired Replicative Polymerase. *Journal of Bacteriology*, *182*(23), 6742-6750. https://doi.org/10.1128/JB.182.23.6742-6750.2000

Suresh Kumar, G., Lipman, R., Cummings, J., & Tomasz, M. (1997). Mitomycin C-DNA adducts generated by DT-diaphorase. Revised mechanism of the enzymatic reductive activation of mitomycin C. *Biochemistry*, *36*(46), 14128-14136. https://doi.org/10.1021/bi971394i

Sutton, M. D., Smith, B. T., Godoy, V. G., & Walker, G. C. (2000). The SOS Response: Recent Insights into *umuDC*-Dependent Mutagenesis and DNA Damage Tolerance. *Annual review of genetics*, *34*(1), 479-497. https://doi.org/10.1146/annurev.genet.34.1.479

Swings, T., Van den Bergh, B., Wuyts, S., Oeyen, E., Voordeckers, K., Verstrepen, K. J., Fauvart, M., Verstraeten, N., & Michiels, J. (2017). Adaptive tuning of mutation rates allows fast response to lethal stress in *Escherichia coli*. *eLife*, *6*, e22939. https://doi.org/10.7554/eLife.22939

Taddei, F., Matic, I., & Radman, M. (1995). cAMP-dependent SOS induction and mutagenesis in resting bacterial populations. *Proceedings of the National Academy of Sciences of the United States of America*, *92*(25), 11736-11740. https://doi.org/10.1073/pnas.92.25.11736

Tang, M., Pham, P., Shen, X., Taylor, J.-S., O'Donnell, M., Woodgate, R., & Goodman, M. F. (2000). Roles of *E. coli* DNA polymerases IV and V in lesion-targeted and untargeted SOS mutagenesis. *Nature*, *404*(6781), 1014-1018. https://doi.org/10.1038/35010020

Tashjian, T. F., Danilowicz, C., Molza, A. E., Nguyen, B. H., Prévost, C., Prentiss, M., & Godoy, V. G. (2019). Residues in the fingers domain of the translesion DNA polymerase *DinB* enable its unique participation in error-prone double-strand break repair. *J Biol Chem*, *294*(19), 7588-7600. https://doi.org/10.1074/jbc.RA118.006233

Tenaillon, O., Taddei, F., Radman, M., & Matic, I. (2001). Second-order selection in bacterial evolution: selection acting on mutation and recombination rates in the course of adaptation. *Research in Microbiology*, *152*(1), 11-16. https://doi.org/10.1016/S0923-2508(00)01163-3

Torres-Barceló, C., Kojadinovic, M., Moxon, R., & MacLean, R. C. (2015). The SOS response increases bacterial fitness, but not evolvability, under a sublethal dose of antibiotic. *Proc Biol Sci*, *282*(1816), 20150885. https://doi.org/10.1098/rspb.2015.0885

Trusca, D., Scott, S., Thompson, C., & Bramhill, D. (1998). Bacterial SOS checkpoint protein SulA inhibits polymerization of purified FtsZ cell division protein. *J Bacteriol*, *180*(15), 3946-3953. https://doi.org/10.1128/jb.180.15.3946-3953.1998

Tsui, H. C., Feng, G., & Winkler, M. E. (1997). Negative regulation of *mutS* and *mutH* repair gene expression by the Hfq and RpoS global regulators of *Escherichia coli K-12*. *J Bacteriol*, *179*(23), 7476-7487. https://doi.org/10.1128/jb.179.23.7476-7487.1997

Urry, L. A., Meyers, N., Cain, M. L., Wasserman, S. A., Minorsky, P. V., Reece, J. B., & Campbell, N. A. (2017). *Campbell Biology* (11th ed.). Pearson Australia.

Ushey, K., Allaire, J., Wickham, H., & Ritchie, G. (2022). *rstudioapi: Safely Access the RStudio API*. In R package version 0.14. https://CRAN.R-project.org/package=rstudioapi

Vahdati, A. R., Sprouffske, K., & Wagner, A. (2017). Effect of population size and mutation rate on the evolution of RNA sequences on an adaptive landscape determined by RNA folding. *International journal of biological sciences*, *13*(9), 1138.

Van, P., Jiang, W., Gottardo, R., & Finak, G. (2018). ggCyto: next generation open-source visualization software for cytometry. *Bioinformatics*, *34*(22), 3951-3953. https://doi.org/10.1093/bioinformatics/bty441

Vincent, M. S., & Uphoff, S. (2020). Bacterial phenotypic heterogeneity in DNA repair and mutagenesis. *Biochem Soc Trans*, *48*(2), 451-462. https://doi.org/10.1042/bst20190364

Wagner, J., Gruz, P., Kim, S.-R., Yamada, M., Matsui, K., Fuchs, R. P. P., & Nohmi, T. (1999). The *dinB* Gene Encodes a Novel *E. coli* DNA Polymerase, DNA Pol IV, Involved in Mutagenesis. *Molecular Cell*, *4*(2), 281-286. https://doi.org/10.1016/S1097-2765(00)80376-7

Wagner, J., & Nohmi, T. (2000). *Escherichia coli* DNA polymerase IV mutator activity: genetic requirements and mutational specificity. *Journal of Bacteriology*, *182*(16), 4587-4595. https://doi.org/10.1128/JB.182.16.4587-4595.2000

Wannier, T. M., Ciaccia, P. N., Ellington, A. D., Filsinger, G. T., Isaacs, F. J., Javanmardi, K., Jones, M. A., Kunjapur, A. M., Nyerges, A., Pal, C., Schubert, M. G., & Church, G. M. (2021). Recombineering and MAGE. *Nature Reviews Methods Primers*, *1*(1), 7. https://doi.org/10.1038/s43586-020-00006-x

Weber, H., Polen, T., Heuveling, J., Wendisch, V. F., & Hengge, R. (2005). Genome-wide analysis of the general stress response network in *Escherichia coli*: sigmaS-dependent genes, promoters, and sigma factor selectivity. *Journal of Bacteriology*, *187*(5), 1591-1603. https://doi.org/10.1128/JB.187.5.1591-1603.2005

Wickham, H., François, R., Henry, L., & Müller, K. (2022). *dplyr: A Grammar of Data Manipulation*. In R package version 1.0.10. https://CRAN.R-project.org/package=dplyr

Wilke, C. O. (2004). The Speed of Adaptation in Large Asexual Populations. *Genetics*, *167*(4), 2045-2053. https://doi.org/10.1534/genetics.104.027136

Williams, A. B., & Foster, P. L. (2012). Stress-Induced Mutagenesis. *EcoSal Plus*, *5*(1), 10.1128/ecosalplus.1127.1122.1123. https://doi.org/10.1128/ecosalplus.7.2.3

Woodgate, R., & Ennis, D. G. (1991). Levels of chromosomally encoded Umu proteins and requirements for in vivo *UmuD* cleavage. *Molecular and General Genetics MGG*, *229*(1), 10-16. https://doi.org/10.1007/bf00264207

Xie, Y., Allaire, J. J., & Grolemund, G. (2018). *R Markdown: The Definitive Guide*. Chapman and Hall/CRC. https://bookdown.org/yihui/rmarkdown

Yeiser, B., Pepper, E. D., Goodman, M. F., & Finkel, S. E. (2002). SOS-induced DNA polymerases enhance long-term survival and evolutionary fitness. *Proceedings of the National Academy of Sciences*, *99*(13), 8737-8741. https://doi.org/10.1073/pnas.092269199

Zaslaver, A., Bren, A., Ronen, M., Itzkovitz, S., Kikoin, I., Shavit, S., Liebermeister, W., Surette, M. G., & Alon, U. (2006). A comprehensive library of fluorescent transcriptional reporters for *Escherichia coli*. *Nat Methods*, *3*(8), 623-628. https://doi.org/10.1038/nmeth895

Zhang, Z., Schwartz, S., Wagner, L., & Miller, W. (2000). A greedy algorithm for aligning DNA sequences. *J Comput Biol*, *7*(1-2), 203-214. https://doi.org/10.1089/10665270050081478

Zhu, L., Cai, Z., Zhang, Y., & Li, Y. (2014). Engineering stress tolerance of *Escherichia coli* by stress-induced mutagenesis (SIM)-based adaptive evolution. *Biotechnology Journal*, *9*(1), 120-127. https://doi.org/10.1002/biot.201300277

6. APPENDIX 1: Plate design of 96-well deep well plates in the long-term evolution experiment

Table 6-1: Layout of the four 96-well deep well plates for the evolution experiment

Plate 1 [a]												
	1	2	3	4	5	6	7	8	9	10	11	12
A												
B												
C												
D												
E												
F												
G												
H												
Plate 2 [a]												
	1	2	3	4	5	6	7	8	9	10	11	12
A												
B												
C												
D												
E												
F												
G												
H												
Plate 3 [b]												
	1	2	3	4	5	6	7	8	9	10	11	12
A												
B												
C												
D												
E												
F												
G												
H												
Plate 4 [b]												
	1	2	3	4	5	6	7	8	9	10	11	12
A												
B												
C												
D												
E												
F												
G												
H												

[a] Plate 1 and 2. Light blue: REL606 $SIM^{-}MMC^{+}$; dark blue: REL606 $SIM^{-}MMC^{-}$; light green: MG1665 $SIM^{-}MMC^{+}$; dark green: MG1665 $SIM^{-}MMC^{-}$.

[b] Plate 3 and 4. Light orange: REL606 $SIM^{+}MMC^{+}$; dark orange: REL606 $SIM^{+}MMC^{-}$; light yellow: MG1655 $SIM^{+}MMC^{+}$; dark yellow: MG1655 $SIM^{+}MMC^{-}$. Both have white: DM250 only (negative control).

7. APPENDIX 2: DNA sequencing results

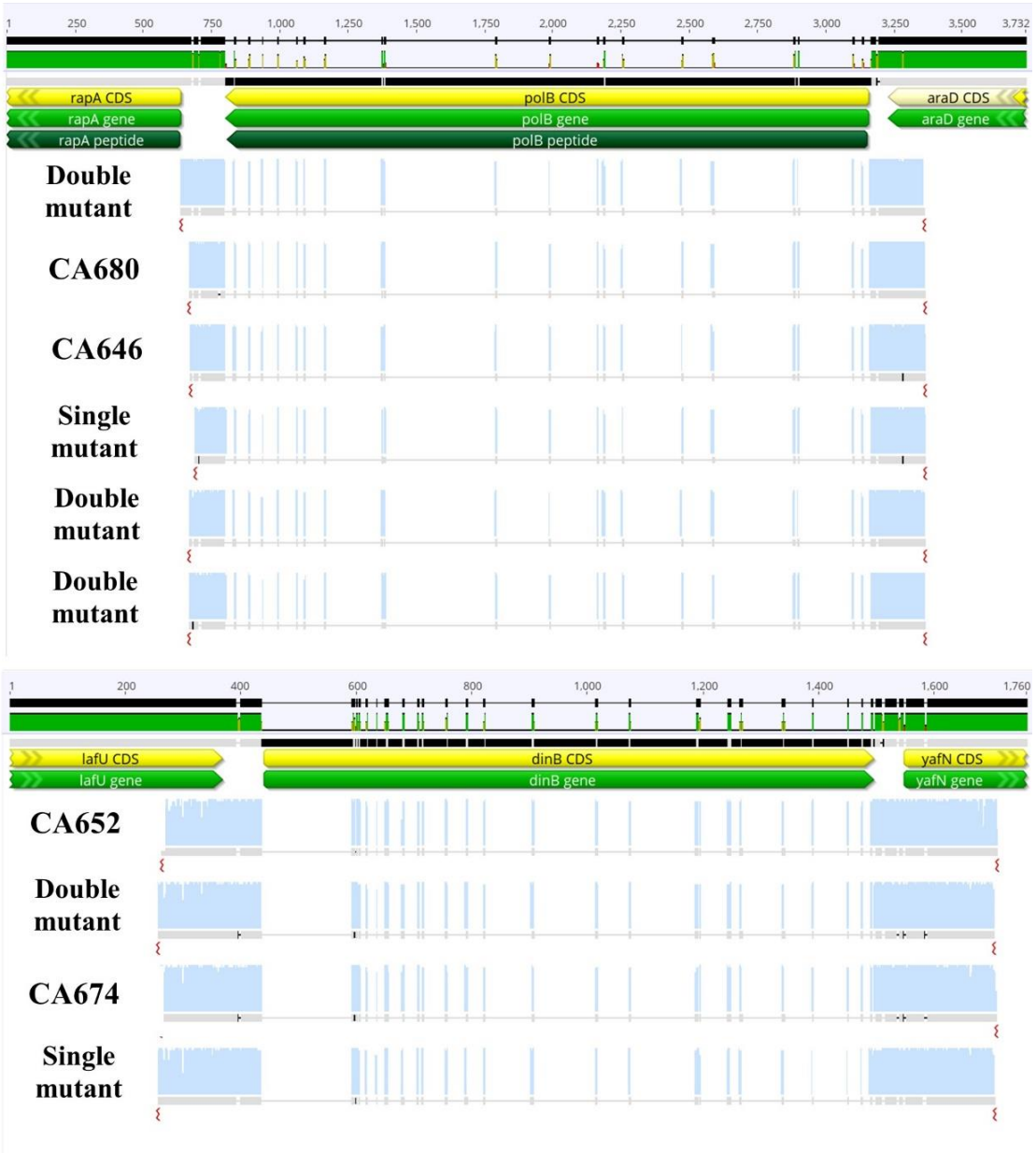

Figure 7-1: Sequencing results of single and double mutants using Geneious.
Top: Single and double mutants for *polB* gene. **Bottom:** Single and double mutants for *dinB* gene.

8. APPENDIX 3: SOS reporter assay preliminary results

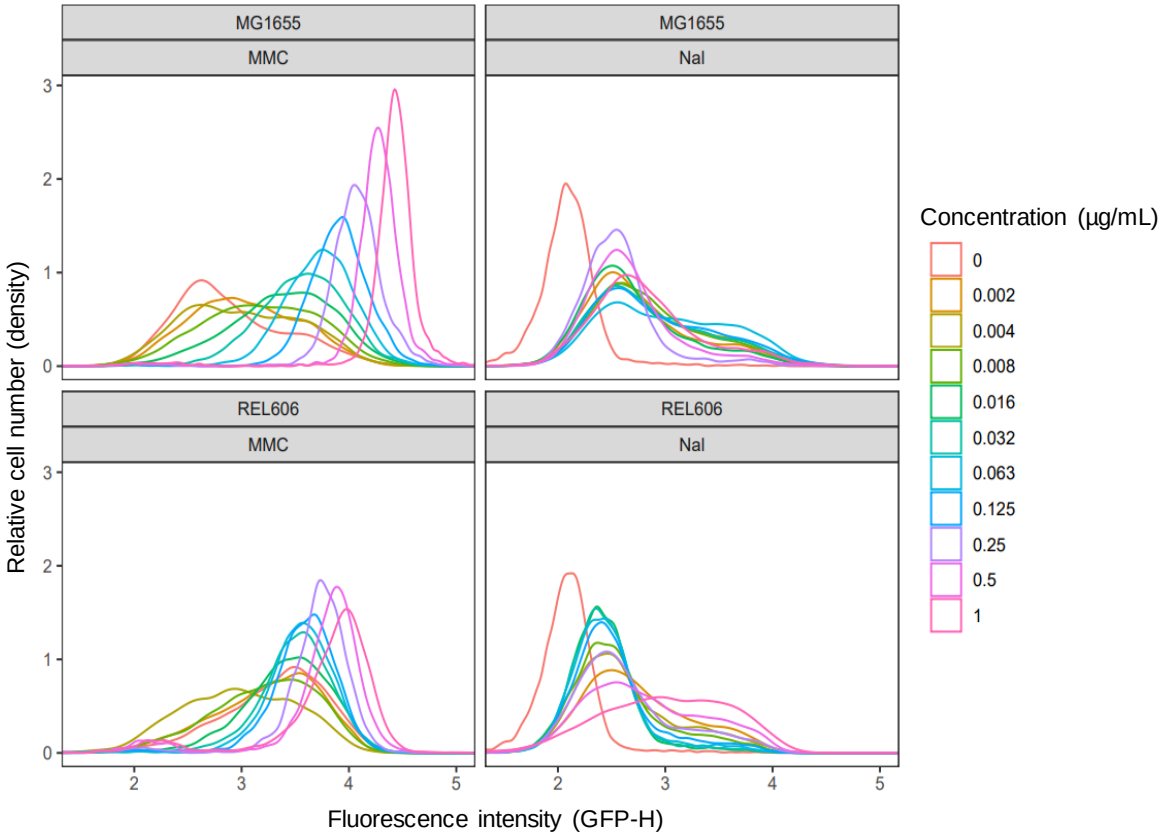

Figure 8-1: Density plots summarizing the effect of mitomycin C (MMC) and nalidixic acid (Nal) inducer concentrations on SOS induction.
Figure shows the first prelimanary experiment with a wide range of stressor concentrations. Each histogram represents two replicates for each combination of strain and stressor concentration. Concentration range was overly broad and too high to distinguish subpopulations with SOS induction.

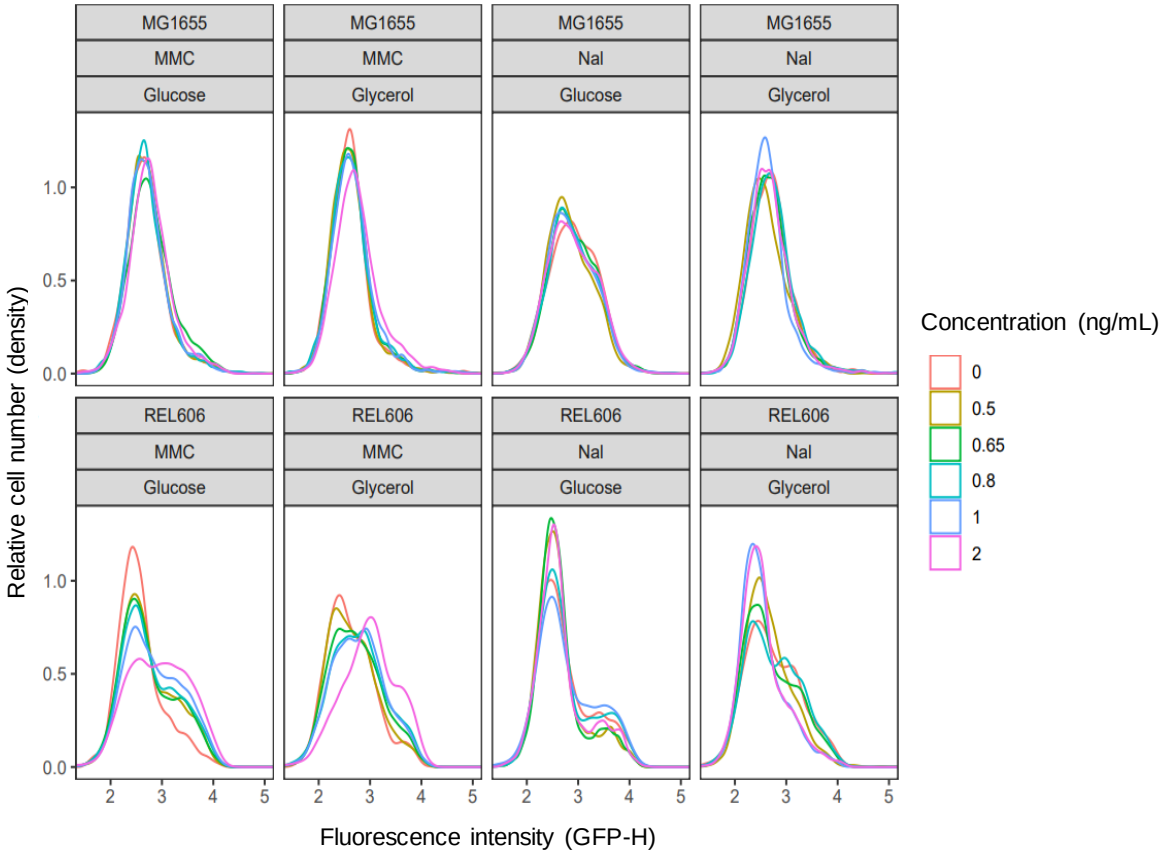

Figure 8-2: Density plots summarizing the effect of mitomycin C (MMC) and nalidixic acid (Nal) inducer concentrations in different growth conditions on SOS induction.
Figure shows the second prelimanary experiment with a narrower and lower range of stressor concentrations. Each histogram represents two replicates for each combination of strain, stressor, and media concentration. The concentrations of 0.5, 0.65, and 0.8 ng/mL were found to be the most effective in inducing the SOS response in REL606 due to having subpopulations displaying high GFP expression.

9. APPENDIX 4: Data for fluctuation test and competition assay and statistical analyses

Table 9-1: Mutation rates of double mutant and wild-type strains

Strain	Environment	Mutation Rate	95% Confidence Interval (CI)	
			Lower Bound	Upper Bound
REL606 SIM^-	MMC	1.13×10^{-8}	7.16×10^{-9}	1.54×10^{-8}
REL606 SIM^-	NI	3.42×10^{-8}	1.90×10^{-9}	4.94×10^{-9}
MG1655 SIM^-	MMC	1.15×10^{-8}	7.12×10^{-9}	1.59×10^{-8}
MG1655 SIM^-	NI	4.85×10^{-9}	3.02×10^{-9}	6.67×10^{-9}
REL606 SIM^+	MMC	1.50×10^{-8}	1.02×10^{-8}	1.98×10^{-8}
REL606 SIM^+	NI	6.45×10^{-9}	4.08×10^{-9}	8.83×10^{-9}
MG1655 SIM^+	MMC	1.96×10^{-8}	1.35×10^{-8}	2.56×10^{-8}
MG1655 SIM^+	NI	8.83×10^{-9}	5.72×10^{-9}	1.19×10^{-8}

Table 9-2: Mean fitness of SIM^- and SIM-evolved and ancestral strains competitions relative to the reference strain

Evolved populations competition				
Strain	**Environment**	**Mean Fitness**	**95% Confidence Interval (CI)**	
			Lower Bound	**Upper Bound**
REL606 SIM^-	MMC	0.863	0.839	0.887
REL606 SIM^+	MMC	0.880	0.853	0.908
REL606 SIM^-	NI	0.837	0.811	0.862
REL606 SIM^+	NI	0.863	0.845	0.882
Ancestral populations competition				
REL606 SIM^-	MMC	1.133	1.101	1.165
REL606 SIM^+	MMC	1.000	0.958	1.042
REL606 SIM^-	NI	1.150	1.130	1.170
REL606 SIM^+	NI	1.000	0.981	1.019

Table 9-3: Results of two-way ANOVA for evolved and ancestral competitions

Evolved competitions					
Source of Variation	**Degrees of Freedom (DF)**	**Sum of Squares (SS)**	**Mean Square (MS)**	**F**	***p*-value**
Strain	1	0.009	0.009	3.932	0.051
Environment	1	0.008	0.008	3.481	0.066
Interaction	1	0	0	0.161	0.690
Residuals	71	0.172	0.002		
Total	74	0.189			
Ancestral competitions					
Source of Variation	**Degrees of Freedom (DF)**	**Sum of Squares (SS)**	**Mean Square (MS)**	**F**	***p*-value**
Strain	1	0.174	0.174	85.640	< 0.001
Environment	1	0.011	0.011	5.202	0.029
Interaction	1	0	0	0.302	0.586
Residuals	35	0.071	0		
Total	38	0.256			

Table 9-4: Results of Tukey HSD post hoc for multiple comparisons of strain and environment in evolved and ancestral competitions

Evolved competitions					
A	**B**	**Mean difference (A-B)**	**95% Confidence Interval**		***p*-value**
			Lower Bound	**Upper Bound**	
$MMC^{+}SIM^{-}$	$MMC^{+}SIM^{+}$	-0.017	-0.062	0.027	0.727
$MMC^{-}SIM^{-}$	$MMC^{+}SIM^{-}$	-0.026	-0.069	0.017	0.378
$MMC^{-}SIM^{+}$	$MMC^{+}SIM^{+}$	-0.017	-0.059	0.025	0.714
$MMC^{-}SIM^{-}$	$MMC^{+}SIM^{+}$	-0.044	-0.087	-0.001	0.043
$MMC^{-}SIM^{-}$	$MMC^{-}SIM^{+}$	-0.027	-0.067	0.014	0.313
$MMC^{+}SIM^{-}$	$MMC^{-}SIM^{+}$	-0.001	-0.043	0.042	1.000
Ancestral competitions					
$MMC^{+}SIM^{-}$	$MMC^{+}SIM^{+}$	0.133	0.081	0.185	< 0.001
$MMC^{-}SIM^{-}$	$MMC^{+}SIM^{-}$	0.017	-0.033	0.067	0.795
$MMC^{-}SIM^{+}$	$MMC^{+}SIM^{+}$	< 0.001	-0.067	0.067	1.000
$MMC^{-}SIM^{-}$	$MMC^{+}SIM^{+}$	0.150	0.097	0.201	< 0.001
$MMC^{-}SIM^{-}$	$MMC^{-}SIM^{+}$	0.150	0.085	0.214	< 0.001
$MMC^{+}SIM^{-}$	$MMC^{-}SIM^{+}$	0.133	0.068	0.197	< 0.001